AUGUST 2023 M.Sc. in Mechanical Engineering REDWAN MOHAMMED MAMU

REPUBLIC OF TÜRKİYE
GAZİANTEP UNIVERSITY
GRADUATE SCHOOL OF NATURAL & APPLIED SCIENCES

VIBRATION ANALYSIS OF NANOBEAM IN THERMAL ENVIRONMENT

M.Sc. THESIS
IN
MECHANICAL ENGINEERING

BY
REDWAN MOHAMMED MAMU
AUGUST 2023

VIBRATION ANALYSIS OF NANOBEAM IN THERMAL ENVIRONMENT

M.Sc. Thesis

in

Mechanical Engineering

Gaziantep University

Supervisor

Assoc.Prof. Dr. Necla KARA TOĞUN

by

Redwan Mohammed MAMU

August 2023

I hereby declare that all information in this document has been obtained and presented in accordance with academic rules and ethical conduct. I also declare that, as required by these rules and conduct, I have fully cited and referenced all material and results that are not original to this work.

Redwan Mohammed MAMU

ABSTRACT

VIBRATION ANALYSIS OF NANOBEAM IN THERMAL ENVIRONMENT

MAMU, Redwan Mohammed
M.Sc. in Mechanical Engineering
Supervisor: Assoc.Prof. Dr. Necla KARA TOĞUN
August 2023

94 pages

Nanostructures are used widely in nanotechnology and nanodevice in recent years and this thesis paper presents the implementation of perturbation method for the vibration analysis of simple and fixed supported Euler-Bernoulli nanobeams resting on Winkler-Pasternak and nonlinear foundation in thermal environment. Considering the thermal loading, the equations of motion of the Euler-Bernoulli nanobeam are obtained using modified couple stress theory and nonlocal elasticity theory. The effect of thermal loadings on the free vibration of the Euler-Bernoulli nanobeam is presented. Hamilton's principle is employed for obtaining differential equation of motion of nanobeam in cooperation with suitable boundary conditions. An approximate solution of the presented system is developed considering the method of multiple scale, which is one of the perturbation techniques. The effects of temperature, Winkler and Pasternak parameters, nonlinear foundation parameter as well as effects of the simple-simple and clamped-clamped boundary conditions on the vibrations, are determined and presented numerically and graphically.

Key Words: Euler-Bernoulli Nanobeam, perturbation method, vibration, Temperature, Winkler-Pasternak foundation, nonlinear foundation, modified couple stress theory, Nonlocal Elasticity Theory

ÖZET

SICAK ORTAMDAKI NANOKIRIŞ'İN TİTREŞİM ANALİZİ

MAMU, Redwan Mohammed
Yüksek Lisans Tezi, Makine Mühendisliği
Danışman: Assoc.Prof. Dr. Necla KARA TOĞUN
Ağustos 2023
94 sayfa

Nanoyapılar, son yıllarda nanoteknoloji ve nanocihazlarda yaygın olarak kullanılmaktadır ve bu tezi, Winkler-Pasternak ve nonlinear temel üzerine oturan basit ve sabit destekli Euler-Bernoulli nanokirislerin termal ortamdaki titreşim analizi için pertürbasyon yönteminin uygulanmasını sunmaktadır. Termal yük dikkate alındığında, Euler-Bernoulli nanokirisin hareket denklemleri, modified couple stres ve nonlocal elasticity teorisi kullanılarak elde edildi. Termal yüklerin Euler-Bernoulli nanokirisin serbest titreşimi üzerindeki etkisi sunulmuştur. Hamilton prensibi, uygun sınır koşulları ile işbirliği içinde nano kirişin diferansiyel hareket denklemini elde etmek için kullanıldi. Sunulan sistemin yaklaşık çözümü, pertürbasyon tekniklerinden biri olan multiple scale yöntemi dikkate alınarak geliştirilmiştir. Sıcaklığın, Winkler ve Pasternak parametrelerinin, nonlinear temel parametresinin ve basit-basit ve ankastre-ankastre sınır koşullarının titreşimlere etkileri belirlenerek sayısal ve grafiksel olarak sunulmuştur.

Anahtar Kelimeler: Euler-Bernoulli Nanokiriş, pertürbasyon yöntemi, titreşim,Sıcaklık, Winkler-Pasternak temeli, Nonlinear Temeli, Modified Couple Stres Theori, Nonlocal Elasticity Theori

''To my dear family, with love and gratitude''

ACKNOWLEDGEMENTS

I would like to thank my supervisor, Dr. Necla Kara Toğun for her guidance and support throughout the study. I am thankful for her encouragement and motivation.

I would like to express my love and appreciation to my family for their support and best wishes.

Additionally, I would like to express my gratitude to Gaziantep University Scientific Research Project Unit, which supported my thesis financially through the MF.YLT.22.23 Project.

TABLE OF CONTENTS

Page

ABSTRACT .... **i**

ÖZET .... **v**

ACKNOWLEDGEMENTS .... **viii**

TABLE OF CONTENTS .... **ix**

LIST OF TABLES .... **xii**

LIST OF FIGURES .... **xiii**

LIST OF SYMBOLS .... **xviii**

CHAPTER 1 INTRODUCTION **1**

1.1 Nanomaterials 1

1.2 Application area of Nanomaterials 2

1.3 Gaps 5

1.4 Aims and Objective 5

CHAPTER 2 LITRETURE REVIEW **6**

CHAPTER 3 THEORY AND FORMULATION **11**

3.1 Modified Couple Stress Theory 11

3.1.1 Strain Energy 14

3.1.2 Kinetic Energy 15

3.1.3 Thermal Energy 15

3.1.4 Work done 15

3.1.5 Axial Force 16

3.1.6 Governing Equation and Boundary Conditions 16

3.2 Nonlocal Elasticity Theory 18

3.2.1 Strain Energy 20

3.2.2 Kinetic Energy 20

3.2.3 Thermal Energy 20

3.2.4 Governing Equation and Boundary Conditions 22

CHAPTER 4 PERTURBATION METHOD **24**

4.1 Method of Multiple Scale 24

4.1.1 Modified Couple Stress Theory 24
4.1.1.1 Linear Problem 27
4.1.1.2 Nonlinear Problem 29
4.2.1 Nonlocal Elasticity Theory 35
4.2.1.1 Linear Problem 36
4.2.1.2 Nonlinear Problem 38
CHAPTER 5 RESULT AND DISCUSSION 44
5.1 Numercal Result using Modified Couple stress Theory 44
5.2 Numerical result using Nonlocal Elasticity Theory 62
5.3 Validation Study 83
CHAPTER 6 CONCLUSION AND RECOMMENDATION 85
6.1 Conclusion and Recommendation for future work 85
REFERENCES 87
CURRICULUM VITAE 93

LIST OF TABLES

Page

Table 5.1 The first three frequencies for Simple-Simple nanobeams for different Temperature, Winkler and Pasternak parameter, nonlinear foundation parameter and material length scale parameter................................ 44

Table 5.2 The first three frequencies for Clamped-Clamped nanobeams for different Temperature, Winkler and Pasternak parameter,nonlinear foundation parameter and material length scale parameter............... 46

Table 5.3 The nonlinear correction term of the 1st mode SS nanobeam with different h/l, T, Kp and kw values when Knl=10,100 and 200.......... 47

Table 5.4 The nonlinear correction term of the 1st mode C-C nanobeam with different h/l, T, Kp and Kw values when Knl=10,100 and 200......... 48

Table 5.5 Effect of Temperature on C-C Boundary condition nanobeams on nonlinear foundation based on nonlocal theory................................. 62

Table 5.6 Effect of Temperature on S-S Boundary condition nanobeams on nonlinear foundation based on nonlocal theory................................. 63

Table 5.7 The nonlinear correction term of the first three frequencies C-C nanobeam with different γ, T, Knl, Kp and kw values 65

Table 5.8 The nonlinear correction term of the first three frequencies S-S nanobeam with different γ, T, Knl, Kp and kw values 66

Table 5.9 Comparison of the nonlinear frequency ratios obtained by the classical theory for various values of dimensionless amplitude for SS and CC micro beam. 83

Table 5.10 Comparison of the nondimensional first mode natural frequencies of a beam (SS) with ν=0.38, K_L=K_P= K_{NL}=0.. 83

Table 5.11 Comparison of the nondimensional first mode natural frequencies of a beam with ν=0.38, l/h=1, K_P=5, K_{NL}=10.. 84

Table 5.12 Model validation: estimates of the fundamental natural frequency for a beam with l/h=100, K_P=0, K_w=0, K_{NL} =0 and T=0....................... 84

LIST OF FIGURES

Page*

Figure 1.1 Insect Sized Robot 3

Figure 1.2 Application of Nanomaterial's in Cars 3

Figure 1.3 Applications of Nano composites in Aircraft 4

Figure 3.1 Boundary conditions for different beam supports 16

Figure 3.2 Boundary condition for different nonlocal nanobeam Support 19

Figure 5.1 Frequency-response curves of S-S nanobeams for different Low Temperature values T=0k, T=100k and T=200k , the first mode and (h/l=1, $Knl = 10, Kp = 5 \;\; and \;\; Kw = 10$) 49

Figure 5.2 Amplitude and Nonlinear natural frequency change of S-S nanobeams for different Low Temperature values when h/l=1, $Knl = 10, Kp = 5 \;\; and \;\; Kw = 10$ 49

Figure 5.3 Frequency-response curves of SS nanobeams for different High Temperature values T=200k, T=400k and T=600k , the first mode and (h/l=1, $Knl = 10, Kp = 5 \;\; and \;\; Kw = 10$) 50

Figure 5.4 Amplitude and Nonlinear natural frequency change of S-S nanobeams for different High Temperature values when h/l=1, $Knl = 10, Kp = 5 \;\; and \;\; Kw = 10$ 50

Figure 5.5 Frequency-response curves of CC nanobeams for different Low Temperature values T=0k, T=100k and T=200k, the first mode and (h/l=1, $Knl = 10, Kp = 5 \;\; and \;\; Kw = 10$) 51

Figure 5.6 Amplitude and Nonlinear natural frequency change of C-C nanobeams for different Low Temperature values, the first mode and (h/l=1, $Knl = 10, Kp = 5 \;\; and \;\; Kw = 10$) 51

Figure 5.7 Frequency-response curves of C-C nanobeams for different High Temperature values T=200k, T=400k and T=600k, the first mode and (h/l=1, $Knl = 10, Kp = 5 \;\; and \;\; Kw = 10$) 52

Figure 5.8 Amplitude and Nonlinear natural frequency change of C-C nanobeams for different High Temperature values, the first mode and (h/l=1, $Knl = 10$, $Kp = 5$ and $Kw = 10$) 52

Figure 5.9 Frequency-response curves of S-S nanobeams for different Winkler parameters Kw=10, Kw=100 and Kw=200, the first mode and (h/l=1, $Knl = 10$, $Kp = 5$ and $T = 0K$).. 53

Figure 5.10 Amplitude and Nonlinear natural frequency change of S-S nanobeams for different Winkler parameter Kw=0, Kw=100 and Kw=200, the first mode and (h/l=1, $Knl = 10$, $Kp = 5$ and $T = 0K$) 53

Figure 5.11 Frequency-response curves of C-C nanobeams for different Winkler parameters Kw=10, Kw=100 and Kw=200, the first mode and (h/l=1, $Knl = 10$, $Kp = 5$ and $T = 0K$) 54

Figure 5.12 Amplitude and Nonlinear natural frequency change of C-C nanobeams for different Winkler parameter Kw=0, Kw=100 and Kw=200, the first mode and (h/l=1, $Knl = 10$, $Kp = 5$ and $T = 0K$) 54

Figure 5.13 Frequency-response curves of S-S nanobeams for different Pasternak parameters Kp=5, Kp=50 and Kp=100, the first mode and (h/l=1, $Knl = 10$, $Kw = 10$ and $T = 0K$ 55

Figure 5.14 Amplitude and Nonlinear natural frequency change of S-S nanobeams for different Pasternak parameters Kp=5, Kp=50 and Kp=100, the first mode and (h/l=1, $Knl = 10$, $Kw = 10$ and $T = 0K$) 55

Figure 5.15 Frequency-response curves of C-C nanobeams for different Pasternak parameters Kp=5, Kp=50 and Kp=100, the first mode and (h/l=1, $Knl = 10$, $Kw = 10$ and $T = 0K$) 56

Figure 5.16 Amplitude and Nonlinear natural frequency change of C-C nanobeams for different Pasternak parameters Kp=5, Kp=50 and Kp=100, the first mode and (h/l=1, $Knl = 10$, $Kw = 10$ and $T = 0K$) 56

Figure 5.17 Frequency-response curves of S-S nanobeams for different Nonlinear foundation parameters Knl=10, Knl=100 and Knl=200, the first mode and (h/l=1, $Kp = 5$, $Kw = 10$ and $T = 0K$) 57

Figure 5.18 Amplitude and Nonlinear natural frequency change of S-S nanobeams for different nonlinear foundation parameters (Knl=10, Knl=100 and

Kw=200), the first mode and h/l=1, $Kw = 10$, $Kp = 5$ and $T = 0K$) 57

Figure 5.19 Frequency-response curves of C-C nanobeams for different Nonlinear foundation parameters Knl=10, Knl=100 and Knl=200, the first mode and (h/l=1, $Kp = 5$, $Kw = 10$ and $T = 0K$)..................................... 58

Figure 5.20 Amplitude and Nonlinear natural frequency change of C-C nanobeams for different nonlinear foundation parameters Knl=10, Knl=100 and Kw=200, the first mode and (h/l=1, $Kw = 10$, $Kp = 5$ and $T = 0K$) 58

Figure 5.21 Frequency-response curves of S-S nanobeams for different material length scale parameter h/l=1 and h/l=2 and h/l=3, the first mode and (Knl= 10, $Kp = 5$, $Kw = 10$ and $T = 0K$) 59

Figure 5.22 Amplitude and Nonlinear natural frequency change of S-S nanobeams for different material length scale parameter h/l=1, h/l=3 and h/l=5, the first mode and (Knl= 10, $Kw = 10$, $Kp = 5$ and $T = 0K$) 59

Figure 5.23 Frequency-response curves of C-C nanobeams for different material length scale parameter h/l=1 and h/l=3 and h/l=5, the first mode and (Knl= 10, $Kp = 5$, $Kw = 10$ and $T = OK$) 60

Figure 5.24 Amplitude and Nonlinear natural frequency change of C-C nanobeams for different material length scale parameter h/l=1, h/l=3 and h/l=5, the first mode and (Knl= 10, $Kw = 10$, $Kp = 5$ and $T = 0K$)............... 60

Figure 5.25 1st mode ($\omega 1$), 2nd mode ($\omega 2$) and 3rd mode ($\omega 3$) frequency-response curves of S-S nanobeams for (h/l=1, Knl= 10, $Kp = 5$, $Kw = 10$ and $T = 0K$) 61

Figure 5.26 1st mode ($\omega 1$), 2nd mode ($\omega 2$) and 3rd mode ($\omega 3$) frequency-response curves of C-C nanobeams for (h/l=1, Knl= 10, $Kp = 5$, $Kw = 10$ and $T = 0K$) 61

Figure 5.27 Frequency-response curves of S-S nanobeams for different Low Temperature values T=0K, T=100K and T=200K , the first mode and ($\boldsymbol{\gamma}$=0.1, $Knl = 10$, $Kp = 5$ and $Kw = 10$) 67

Figure 5.28 Amplitude and Nonlinear natural frequency change of SS nanobeams for different Low Temperature values when $\boldsymbol{\gamma}$=0.1, Knl = 10, Kp = 5 and Kw = 10 68
Figure 5.29 Frequency-response curves of SS nanobeams for different High Temperature values T=200K, T=400K and T=600K , the first mode and ($\boldsymbol{\gamma}$=0.1, Knl = 10, Kp = 5 and Kw = 10) 68
Figure 5.30 Amplitude and Nonlinear natural frequency change of S-S nanobeams for different High Temperature values when $\boldsymbol{\gamma}$=0.1, Knl = 10, Kp = 5 and Kw = 10 69
Figure 5.31 Frequency-response curves of C-C nanobeams for different Low Temperature values T=0K, T=100K and T=200K , the first mode and ($\boldsymbol{\gamma}$=0.1, Knl = 10, Kp = 5 and Kw = 10) 69
Figure 5.32 Amplitude and Nonlinear natural frequency change of C-C nanobeams for different Low Temperature values, the first mode and ($\boldsymbol{\gamma}$=0.1, Knl = 10, Kp = 5 and Kw = 10) 70
Figure 5.33 Frequency-response curves of C-C nanobeams for different High Temperature values T=200K, T=400K and T=600K, the first mode and ($\boldsymbol{\gamma}$=0.1, Knl = 10, Kp = 5 and Kw = 10) 70
Figure 5.34 Amplitude and Nonlinear natural frequency change of C-C nanobeams for different High Temperature values, the first mode and ($\boldsymbol{\gamma}$=0.1, Knl = 10, Kp = 5 and Kw = 10) 71
Figure 5.35 Frequency-response curves of S-S nanobeams for different Winkler parameters Kw=10, Kw=100 and Kw=200, the first mode and ($\boldsymbol{\gamma}$=0.1, Knl = 10, Kp = 5 and T = 0K) 71
Figure 5.36 Amplitude and Nonlinear natural frequency change of S-S nanobeams for different Winkler parameter Kw=0, Kw=100 and Kw=200, the first mode and ($\boldsymbol{\gamma}$=0.1, Knl = 10, Kp = 5 and T = 0K) 72
Figure 5.37 Frequency-response curves of C-C nanobeams for different Winkler parameters Kw=10, Kw=100 and Kw=200, the first mode and ($\boldsymbol{\gamma}$=0.1, Knl = 10, Kp = 5 and T = 0K) 72
Figure 5.38 Amplitude and Nonlinear natural frequency change of C-C nanobeams for different Winkler parameter Kw=0, Kw=100 and Kw=200, the first mode and ($\boldsymbol{\gamma}$=0.1, Knl = 10, Kp = 5 and T = 0K) 73

Figure 5.39 Frequency-response curves of S-S nanobeams for different Pasternak parameters Kp=5, Kp=50 and Kp=100, the first mode and (γ=0.1, Knl = 10, Kw = 10 and T = 0K) 73

Figure 5.40 Amplitude and Nonlinear natural frequency change of S-S nanobeams for different Pasternak parameters Kp=5, Kp=50 and Kp=100, the first mode and (γ=0.1, Knl = 10, Kw = 10 and T = 0K) 74

Figure 5.41 Frequency-response curves of C-C nanobeams for different Pasternak parameters Kp=5, Kp=50 and Kp=100, the first mode and (γ=0.1, Knl = 10, Kw = 10 and T = 0K) 74

Figure 5.42 Amplitude and Nonlinear natural frequency change of C-C nanobeams for different Pasternak parameters Kp=5, Kp=50 and Kp=100, the first mode and (γ=0.1, Knl = 10, Kw = 10 and T = 0K) 75

Figure 5.43 Frequency-response curves of S-S nanobeams for different Nonlinear foundation parameters Knl=10, Knl=100 and Knl=200, the first mode and (γ=0.1, Kp = 5, Kw = 10 and T = 0K) 75

Figure 5.44 Amplitude and Nonlinear natural frequency change of S-S nanobeams for different nonlinear foundation parameters Knl=10, Knl=100 and Kw=200, the first mode and (γ=0.1, Kw = 10, Kp = 5 and T = 0K) 76

Figure 5.45 Frequency-response curves of C-C nanobeams for different Nonlinear foundation parameters Knl=10, Knl=100 and Knl=200, the first mode and (γ=0.1, Kp = 5, Kw = 10 and T = 0K) 76

Figure 5.46 Amplitude and Nonlinear natural frequency change of C-C nanobeams for different nonlinear foundation parameters Knl=10, Knl=100 and Kw=200, the first mode and (γ=0.1, Kw = 10, Kp = 5 and T = 0K) 77

Figure 5.47 Frequency-response curves of S-S nanobeams for different Nonlocal parameters γ=0 and γ=0.2 and γ=0.4, the first mode and (Knl= 10, Kp = 5, Kw = 10 and T = 0K) 77

Figure 5.48 Amplitude and Nonlinear natural frequency change of S-S nanobeams for different nonlocal parameters γ=0, γ=0.2 and γ=0.4, the first mode and (Knl= 10, Kw = 10, Kp = 5 and T = 0K) 78

Figure 5.49 Frequency-response curves of C-C nanobeams for different Nonlocal parameters $\boldsymbol{\gamma}$=0 and $\boldsymbol{\gamma}$=0.2 and $\boldsymbol{\gamma}$=0.4, the first mode and (Knl= 10, Kp = 5, Kw = 10 and T = 0K) 78

Figure 5.50 Amplitude and Nonlinear natural frequency change of C-C nanobeams for different nonlocal parameters $\boldsymbol{\gamma}$=0, $\boldsymbol{\gamma}$=0.2 and $\boldsymbol{\gamma}$=0.4, the first mode and (Knl= 10, Kw = 10, Kp = 5 and T = 0K) 79

Figure 5.51 1st mode ($\omega1$), 2nd mode ($\omega2$) and 3rd mode ($\omega3$) frequency-response curves of S-S nanobeams for ($\boldsymbol{\gamma}$=0.1, Knl= 10, Kp = 5, Kw = 10 and T = K) 79

Figure 5.52 1st mode ($\omega1$), 2nd mode ($\omega2$) and 3rd mode ($\omega3$) frequency-response curves of C-C nanobeams for ($\boldsymbol{\gamma}$=0.1, Knl= 10, Kp = 5, Kw = 10 and T = 0K) 80

LIST OF SYMBOLS

A	Amplitude
A	Area
N	Axial Normal Force
B	Base
$\boldsymbol{\varepsilon_b}$	Bending Strain
f	Body Force
c	Body Couple
$\boldsymbol{\alpha}$	Coefficient of thermal expansion
$\boldsymbol{A(T_1)}$	Complex Amplitude
cc	Complex Conjugate
$\boldsymbol{e_0}$	Constant
$\boldsymbol{Y_{xy}}$	Couple Moment
$\boldsymbol{A'}$	Derivative of Amplitude
m	Deviatoric Couple stress tensor
$\boldsymbol{D_n}$	Differential Parameter
u	Displacement vector
$\boldsymbol{C_0}$	Elastic Stiffness Matrix
$\boldsymbol{\Omega}$	Excitation Frequency
$\boldsymbol{\varepsilon_{xx}}$	Extensional Strain
$\boldsymbol{W^{ext}}$	External Work done
H	Height
$\boldsymbol{a}$	Internal Characteristic Length
T	Kinetic Energy
L	Lagrange Function
$\boldsymbol{\lambda}$, **μ**	Lame’s constants
$\boldsymbol{\nabla^2}$	Laplacian Operator
$\boldsymbol{\tau_{ij}}$	Local Stress tensor
l	Material Length

$\boldsymbol{\omega}$	Natural Frequency
$\boldsymbol{K_{NL}}$	Nonlinear elastic medium
$\boldsymbol{\sigma_{ij}}$	Nonlocal Stress
$\boldsymbol{K_P}$	Pasternak parameter
$\boldsymbol{\theta}$	Phase
$\boldsymbol{\upsilon}$	Poisson's ratio
U	Potential Energy
r	Radius of Gyration
M	Resultant Moment
Ψ	Rotation angle
ϴ	Rotation vector
μ	Shear modulus
σ	Stress tensor
Ɛ	Strain tensor
S	Surface Couple

CHAPTER 1
INTRODUCTION

1.1 Nanomaterials

In recent years, advancement of modern technologies, micro electro-mechanical and Nano-electromechanical systems (MEMS/NEMS) consisting of features such as lightweight, small size, high sensitivity, fast response, low energy dissipation, and increasing durability have been found to have wide range of applications [17]. This technological advancement in many engineering fields has facilitated the application of nanostructures because of their extraordinary electrical, thermal and mechanical properties. Nanostructures with temperature dependent properties have been used in Nano-electromechanical systems (NEMS). Thus, introducing an accurate mathematical model of nanobeams with temperature-dependent properties is a major and important topic for the design of NEMS. This observation is very important in the industry, especially in the design of precision devices and machines. Nanostructures are capable of making significant difference in people's lives and study on nanobeams, which are an important element of nanostructures, are necessary. Due to widespread utilization of this peerless category of materials at micro and nano scales, during past few years, many experimental tests have been done and a lot of experimental papers have been published on this topic to get the most compatible theory to analyze their behavior. [2-11]

The performance of such systems largely depends on a characteristic, termed as the quality factor. The quality factor is defined as the ratio of stored energy in the system and dissipated energy by the system per cycle of vibration. A high-quality factor indicates a lower rate of energy dissipation in the vibrating systems. This implies that we need to design systems with high-quality factor so that the systems can vibrate for a longer time [17].

The static and dynamic behavior of nanobeams has received considerable attention. Classical elasticity and plasticity cannot be used to interpret the size effect observed in numerous tests at micron and nanometer scales because of their lack in an internal material length scale parameter. However, higher-order (non-local) continuum theories contain material length scale parameters and are capable of explaining microstructure related size (and other) effects. Couple stress theories represent one class of such higher-order theories [3].

The classical couple stress elasticity theory contains four material constants (two classical and two additional) for isotropic elastic materials. The two additional constants are related to the underlying microstructure of the material and are inherently difficult to determine, opening a door for a development of higher order theories like modified couple stress theory. Compared to the classical theory, the modified theory has two advantages: the couple stress tensor being symmetric, and only one internal length scale parameter involved. These features make the modified couple stress theory easier to use.

1.2 Application areas of Nanomaterial's

Nanotechnology is an evolving technology, and we can see more applications in nanotechnology. Nowadays, it is clear that it will spread much wider in the future. Nanotechnology is a golden key for technology, as technology developments continue and human needs is now being ensured by smaller materials and tools [25]. Nanomaterial's attracted great concentration due to numerous applications in science and engineering areas such as mechanical, automobile, aviation and space research, defense sector, environment and energy, wireless networks(communication), biomedical sectors, electronics (Nano rods), material and manufacturing industry, optics, several engineering structures and etc. Hence, detailed investigation of the mechanical behavior of nanostructures including bending, buckling and vibration are necessary to increase their reliability and obtain the proper design of small-scale systems. Among the few applications of nanomaterial's, scientists have developed a new insect-sized robot that can scurry across the floor at nearly the speed of a darting cockroach and withstand the weight of a human. Small, durable robots like these could be advantageous in search and rescue missions, squeezing and squishing into places where dogs or humans cannot fit, or where it may be too dangerous for them to go, researchers said. [43]

Figure 1.1. Insect sized Robot (devdiscourse.com, Oct 2022)

Vehicles of the future are anticipated to be nothing like how it is today. Many disruptive trends including nanotechnology are sweeping the automotive industry by storm. At a time when the reduction of fuel consumption, environmental impact, safety, driver information, comfort, and alternatives to toxic or expensive materials are taken into account, nanotechnology appears to transform car manufacturing [44]. The weight of vehicles can be reduced by using lightweight materials in the making of exterior and structural chassis. In such a scenario, Nano-manipulation of materials can help in developing durable and lightweight chassis and panels than the existing ones. Besides, nanotechnology in cars has also helped produce self-repair and reformable plastic panels [45].

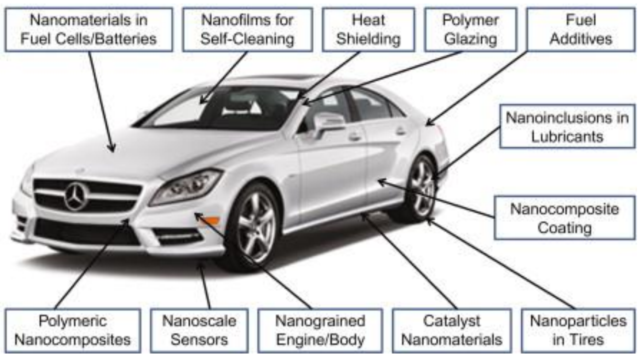

Figure 1.2. Application of Nanomaterial's in Cars

Potential of nanotechnology in the aerospace industry cannot is immense. Nanotechnology is a crucial tool that can be used to engineer vehicles with the necessary properties to endure the harsh conditions of space. Nanotechnology, an ever-evolving discipline, finds several uses within the aerospace industry. Now, nanotechnology, more precisely nanomaterial has created almost perfect material. As an example, improvised steel enhances performance and passenger safety while saving notable money. These materials exhibit considerably enhanced properties matched to their counterparts with micro scale or larger grain structures. Nanomaterial's are engineered particles made to have remarkably small dimensions to take advantage of unique physical and chemical properties that exist at the Nano scale [46].

Figure 1.3. Applications of Nano composites in Aircraft

With dimensions between approximately 1 and 100 nanometers – about the size of a virus -nanomaterial's have unusual physical, chemical and biological properties that can differ significantly from the properties of bulk materials, including single atoms or molecules. These differences enable the aerospace industry to do several things including engineering aircraft structures that are flexible and adaptive, developing innovative energy generation and storage systems for air travel and manufacturing sensors that monitor virtually every element of air travel [46].

1.3 Gaps

When nanostructures structures are exposed to thermal environment, thermal stress is created in the structures. As the thermal stress reach to certain level, the nanostructures may lose their stability and undergo thermal buckling. Considering the exposure of many nanostructures to thermal environments, it is highly necessary to investigate their behavior in such environments [15]. To be able to design a nanostructure it is very vital to know more about the mechanical and physical behaviors they show. The Literature Review shows that many researchers have conducted investigation on bending, buckling and vibration analysis of nanobeam based on modified couple stress theory and nonlocal elasticity theory but less attention was given about the behavior of nanobeam in thermal environment via these theories. To the best of author's knowledge, the effect of the temperature on the vibration of the nanobeam resting on Winkler-Pasternak and nonlinear foundation via modified couple stress theory and nonlocal elasticity theory using multiple scale perturbation technique has not been done. To fill this gap, the vibrational analysis of nanobeam considering the temperature is presented in this paper.

1.4 Aims and Objective

In view of above gaps, our aim in this research is develop numerical methods that best suits to solve the vibration analysis of nanobeam in thermal environment. Hence, this work presents vibration analysis of Euler-Bernoulli nanobeam resting on Winkler-Pasternak and nonlinear foundation considering a thermal effect. Size dependency of the nanobeam is described via modified couple stress theory and Nonlocal Elasticity theory. The governing equations are obtained by Hamilton principle and solved by using multiple scale perturbation method. It includes the study of the influence of thermal characteristics of a nanobeam on the vibration analysis. The results obtained by using modified couple stress theory and nonlocal elasticity theory about vibration analysis of nanobeam in thermal environment is analyzed. The material is considered linear and the cross-section properties are assumed constant. In this analysis, the influence of temperature performing both theories, the nonlocal parameter, and the modified couple stress material length parameter on the considered physical quantities are examined and discussed in detail. The obtained results in this work may be used in guiding experiments and application of nanomaterials under thermal environment.

CHAPTER 2
LITRETURE REVIEW

Many researchers have considered the mechanical behavior of nanostructures. The following literature review covers previous researches done on the investigation of vibration analysis of nanobeam under different effects, especially thermal. Ahmed and Marin [5] derived a new thermoelastic model for Euler-Bernoulli nanobeam whose properties are temperature dependent using state-space method by employing a modified couple stress theory and found out that there is a clear effect on thermal and mechanical properties. Majid and Nevvab analyzed thermal vibration of rotary functionally graded Timoshenko microbeam based on modified couple stress theory considering temperature change in four types of temperature distribution on thermal environment [6]. Rahmani et al. [7] developed a comprehensive wave propagation analysis of a magneto-electro-thermo-elastic nanobeam resting on visco-elastic medium via Eringen's non-local and modified couple stress theories and compared the results. The result showed significant difference between the theories.

Vibration analysis of piezoelectric nanobeam resting on Winkler-Pasternak foundation via quadrature technique was done by O. Ragb et al. [8]. The study showed the influence of foundation parametersand temperature change on natural frequencies and mode shapes of the problem. A. Rahmani et al. [9] investigated wave propagation of rotating viscoelastic nanobeams with temperature effect by employing non-local Eringen's theory along with modified couple stress theory, where Reddy Beam theory is adopted to develop motion equations for the nanobeam. A comprehensive vibrational analysis of rotating nanobeams on visco-elastic foundations with thermal effect based on modified couple stress and Eringen's non-local elasticity theories was also done by A. Rahmani et al. [12].

Thermoelastic interactions in isotropic nanobeams subjected to ramp type heating was studied via the modified couple stress and generalized thermoelastic theories by

Abouelregal and Mohammed[10]. Another study presented the thermoelastic dynamic response of a nanobeam subjected to a ramp up heating with both size-dependent and memory-dependent effects using modified couple stress theory by Z. Qi et al. [11]. Thermal and size effects on the buckling behavior of a nanobeam symmetrically located between two electrodes was investigated based on modified couple stress theory by Dashtaki et al. [13]. Thermoelastic rotating nanobeams under periodic pulse heating by applying non-local modified couple stress theory and generalized thermoelastic theory was introduced by Yahya et al.[16]

Post-buckling of functionally graded (FG) nanobeams based on modified couple stress theory was investigated by Khorshidi et al. [14]. B. Alibeigi et al. [15] presented the buckling response of nanobeams on the basis of Euler-Bernoulli beam model with the Von-Karman geometrical non-linearity using modified couple stress theory under various types of thermal loading, electrical and magnetic fields. H. Kumar et al. [17] introduced the response of deflection and thermal moment of Timoshenko microbeam via modified couple stress theory and dual-phase-lag heat conduction model. A. Attia et al. [18] investigated the non-linear vibration characteristics of pre- and post- buckled non-uniform bi-directional functionally graded microbeams subjected to nonlinear thermal loading based on modified couple stress Reddy beam theory. Vibration analysis of thermoelastic microbeams due to temperature pulse heating by M.A. Kutbi et al. [21] based on modified couple stress theory.

Thermo-mechanical vibration analysis of functionally graded nanoscale beams with porosities was done by F. Ebrahimi et al. [19] using modified couple stress theory. A. Bobaei et al. [20] temperature-dependent free vibration analysis of functionally graded micro-beams based on modified couple stress theory. O. Rahmani et al. [22] carried out investigation on vibration analysis of deep curved FG nanobeams based on modified couple stress theory. Modified couple stress was utilized by M. Sobhy and AM Zenkour to investigate the bending of viscoelastic nanobeams laying on visco-Pasternak elastic foundation based on new shear and deformation beam theory [23]. MH Jalali et al. [24] investigated free vibration of functionally graded (FG) microbeams in thermal environment based on modified couple stress theory.

MÖ Yaylı et al. [25] examined the bending analysis of a nanobeam with modified couple stress theory and weighted residual method. X.L. Jia et al [26] presented thermal, mechanical and electrical behavior of functionally graded micro-beams based on modified couple stress theory. N. Shafiei et.al [27] investigated vibration analysis of rotary tapered axially functionally graded Timoshenko nanobeam in thermal environment via non-local theory, where the solution method is considered using generalized differential quadrature element method. M. A. Attia et.al. [28] presented a size-dependent, nonlinear beam model for bending, buckling and free vibrations of electrically actuated viscoelastic clamped–clamped microbeams based on modified couple stress theory. Nonlinear vibration of nanobeams embedded in the linear and non-linear elastic materials under magnetic and temperature effects using a non-local Euler-Bernoulli beam model is investigated by SS Abdullah et.al. [29]. A size dependent three-dimensional dynamic model of rotating functionally graded microbeams based on Euler-Bernoulli beam model via modified couple stress theory was developed by J. Fang et.al [30]. A. Khorshidi et.al. [31] examined the post-buckling of viscoelastic micro and nanobeams embedded in visco-Pasternak foundations based on modified couple stress theory. Karami et.al. [32] studied flexural and longitudinal wave behaviors of nanobeams made of nano porous-graded materials surrounded by Winkler-Pasternak foundation subjected to the longitudinal magnetic field and exposed to hygrothermal environment.

Das et.al. [33] presented geometrical nonlinear forced vibration analysis of higher order shear-deformable functionally graded microbeam, where the beam is supported on a three-parameter Winkler–Pasternak-type nonlinear elastic foundation and subjected to a harmonically varying distributed load based on modified couple stress theory. Bekir Akgöz and Ömer Civalek [34] examined thermos-elastic vibrational behavior of thick microbeams embedded in Winkler-Pasternak foundation via modified couple stress and other various beam theories. H Liu et.al. [35] presented vibration analysis of nanobeams embedded in visco-Pasternak foundation in magnetic and electrical environment based on the non-local Timoshenko beam theory in conjunction with the Kelvin-Voigt viscoelastic model.M.E Nasr et.al. [36] introduced the thermoelastic vibration of nonlocal nanobeams resting on Winkler-Pasternak foundation based on the generalized dual phase-lag heat conduction and nonlocal beam theories. S.K. et al. [37] investigated the vibration characteristics of a nanobeam embedded in a Winkler-Pasternak elastic foundation adopting wavelet-based two relatively recent techniques, namely the Haar wavelet method(HWM) and the Higher order Haar wavelet method(HOHWM). M. Zarepour and S. A. Hosseini [38] presented nonlinear free vibration of a nanobeam under electrothermal-mechanical loading with elastic medium and various boundary conditions via Eringen's theory. Esen et al. [40] investigated a vibrational behavior of functionally graded (FG) cracked microbeam rested on elastic foundation and exposed to thermal and magnetic fields where Euler-Bernoulli beam theory is used for kinematic assumption and non-local elasticity theory for size-dependency effects.

C. Xiao et al. [41] examined the nonlinear vibration analysis of the nanobeams subjected to magneto-electro-thermal loading based on a novel higher-order shear deformation theory (HSDT and analytical solutions are obtained based on the method of multiple scales (MMS) and perturbation technique. N. Toğun et al. [41] employed non-local Euler-Bernoulli beam theory on the nonlinear free and forced vibration analysis of a nanobeam resting on an elastic foundation of the Pasternak type where the linear part of the problem is solved by using the first equation of the perturbation series to obtain the natural frequencies.

Thermoelastic vibration analysis of Euler–Bernoulli nanobeams was investigated using the theory of non-local elasticity proposed by Eringen to study the effect of temperature change[51]. Ebrahimi et al[52] investigated the influence of temperature on buckling and free vibration of functionally graded (FG) size-dependent Timoshenko nanobeams subjected to in-plane thermal loading for the first time using a Navier type solution. Eringen's nonlocal elasticity theory is used to account for the small scale effect. The nonlocal equations of motion are derived from Timoshenko beam theory using Hamilton's principle and are solved analytically.

The combined effect of moisture and temperature on the free vibration characteristics of functionally graded (FG) nanobeams resting on elastic foundations is investigated[53]. The size-dependent description of the nanobeam is done using Eringen's nonlocal elasticity theory. The vibration characteristics of magneto-electro-thermo-elastic functionally graded nanobeams are explored using third order shear deformation theory[54]. Eringen's nonlocal elasticity theory is used to capture small size effects. The nonlocal governing equations are generated using the Hamilton's principle and then solved analytically to yield the natural frequencies of the nanobeams. Ebrahimi et.al [55] based on nonlocal strain gradient elasticity theory and the Euler-Bernoulli beam model, examined the surface and temperature impacts on the vibration characteristics of viscoelastic functionally graded (FG) nanobeams embedded in a viscoelastic foundation. Ismail Esen et.al [56] investigated a vibrational behaviour of functionally graded (FG) cracked microbeam rested on elastic foundation that is exposed to thermal and magnetic fields.

Ebrahimi et.al [57] examined the thermal effect on free vibration characteristics of functionally graded (FG) size-dependent nanobeams subjected to an in-plane thermal loading based on nonlocal elasticity theory of Eringen. The nonlocal equations of motion are derived through Hamilton's principle and they are solved applying differential transform method (DTM).

Mohammadi, M et.al [58] investigated the vibration behavior of the rotating viscoelastic nanobeam embedded in the visco-Pasternak foundation. The governing equation is extracted by using the surface elasticity and the nonlocal elasticity theory. The influence of the humidity on the vibration frequencies of the viscoelastic nanobeam in thermal environment is examined. Hamza-Cherif et.al [59] investigated the vibration analysis of a single-walled carbon nanotube embedded in an elastic medium under thermal effect based on nonlocal Euler- Bernoulli beam model using differential Transform Method (DTM).

CHAPTER 3
THEORY AND FORMULATION

3.1 Modified Couple Stress Theory

According to the modified couple stress theory of Yang et al [1], the strain energy is a function of both strain (conjugated with stress) and curvature (conjugated with couple stress). It then follows that the strain energy U in a deformed isotropic linear elastic material occupying region **Ω** is given by

$$U = \frac{1}{2}\iiint_{\Omega}(\sigma:\varepsilon + m:\chi)dv \tag{3.1}$$

$$U = \iiint \sigma_{xx}\mathcal{E}_{xx}dAdx + \iiint m\chi dAdx \tag{3.2}$$

Where σ and Ɛ are the stress tensor and strain tensor, respectively.Whereas, m is the deviatoric part of the couple stress tensor and χ is the symmetric curvature tensor. These tensors are expressed as:

$$\mathcal{E} = \frac{1}{2}((\nabla u) + (\nabla u)^T) = \frac{1}{2}\left(u_{i,j} + u_{j.i}\right) \tag{3.3}$$

$$\chi = \frac{1}{2}((\nabla \Theta) + (\nabla \Theta)^T) = \frac{1}{2}\left(\Theta_{i,j} + \Theta_{j,i}\right) \tag{3.4}$$

$$\sigma = \lambda tr(\mathcal{E})I + 2\mu\mathcal{E} \tag{3.5}$$

$$m = 2l^2\mu\chi \tag{3.6}$$

Where $\boldsymbol{\lambda}$ and $\boldsymbol{\mu}$ being Lame's constants, and l a material length scale parameter, which is physically a property characterizing the effect of couple stress. u and Θ are the displacement vector and rotation vector respectively.

$$\Theta = \frac{1}{2} curl\mathbf{u} \qquad (3.7)$$

The work done by external forces are given as [3]

$$W = \frac{1}{2}\iiint_{\Omega}(f.u + c.\theta)dv + \frac{1}{2}\iiint_{\delta\Omega}(t.u + c.\theta)da \qquad (3.8)$$

Where f, c, t and s are body force, body couple, traction and surface couple respectively, and $\delta\Omega$ is the surface of **Ω**.

$$\lambda = \frac{Ev}{(1+v)(1-2v)} \qquad (3.9)$$

$$\mu = \frac{E}{2(1+v)} \qquad (3.10)$$

$$\eta = \frac{1-v}{(1+v)(1-2v)} \qquad (3.11)$$

$$\zeta = \frac{1}{1-2v} \qquad (3.12)$$

Where v is Poisson's ratio, **μ** is shear modulus and E is young's modulus.

Kronecker delta $\delta_{ij} = 1$ for i = j otherwise 0

Euler-Bernoulli beam is represented by

$$u = -z\Psi(x) \qquad v = 0 \qquad w = w(x) \qquad (3.13)$$

Where u, v, and w are x, y, z components of the displacement vector u respectively and Ψ is the rotation angle of the centroidal axis of the beam and given approximtely as below for small deformation.

$$\Psi \approx \frac{\mathrm{dw(x)}}{\mathrm{dx}} \qquad (3.14)$$

Equation (3.3), (3.13) and (3.14) gives

$$\mathcal{E}_{xx} = -z\frac{d^2w(x)}{dx^2} \quad where\ \mathcal{E}_{yy} = \mathcal{E}_{zz} = \mathcal{E}_{xy} = \mathcal{E}_{yz} = \mathcal{E}_{zx} = 0 \qquad (3.15)$$

and Equation (3.7), (3.13) and (3.14) gives

$$\Theta_y = -\frac{dw(x)}{dx} \quad \text{where } \Theta_x = \Theta_z = 0 \tag{3.16}$$

Equation (3.4) and (3.14)

$$\chi_{xy} = -\frac{1}{2}\frac{d^2w(x)}{dx^2} \quad \text{where} \quad \chi_{xx} = \chi_{yy} = \chi_{zz} = \chi_{yz} = \chi_{zx} = 0 \tag{3.17}$$

Inserting equation (3.15) into (3.5) gives

$$\sigma_{xx} = \frac{Ev}{(1+v)(1-2v)}(-z\frac{d^2w(x)}{dx^2})(1) + 2\frac{E}{2(1+v)}(-z\frac{d^2w(x)}{dx^2})$$

$$\sigma_{xx} = \frac{E(1-v)}{(1+v)(1-2v)}\left(-z\frac{d^2w(x)}{dx^2}\right) \tag{3.18}$$

$$\sigma_{yy} = \sigma_{zz} = \frac{Ev}{(1+v)(1-2v)}\left(-z\frac{d^2w(x)}{dx^2}\right) \tag{3.19}$$

Where $\sigma_{xy} = \sigma_{yz} = \sigma_{zx} = 0$

For slender beam with large aspect ratio the poisons effect is secondary and maybe neglected. By setting v=0 as was done in classical beam theories σ_{xx} reduces to

$$\sigma_{xx} = -Ez\frac{d^2w(x)}{dx^2}) \tag{3.20}$$

By inserting equation (3.17) into (3.6)

$$m_{xy} = -\mu l^2\frac{d^2w(x)}{dx^2} \quad = 0 \tag{3.21}$$

$$where\ m_{xx} = m_{yy} = m_{zz} = m_{yz} = m_{zx}$$

Hamilton's principle is one of the most fundamental principles in vibration analysis. It leads to the basic equations of dynamics and elasticity. It’s based on the assumption that when a system moves from a state at a time t1 to a new state at the time t2, in a Newtonian route, then the actual route out of all the possible ones obeys stationary. This condition leads to Hamilton's principle.

The Hamilton principle:

$$\delta \int_{t1}^{t2} \mathrm{L}dt = 0 \tag{3.22}$$

$$\int_{t1}^{t2} (\delta \mathrm{T} - (\delta \mathrm{U} - \delta \mathrm{W}^{ext}))d_t^{\,*} = 0 \tag{3.23}$$

Where L is Lagrange function, T is the kinetic energy of the system; U is the potential energy of the system and W^{ext} is the external work done.

3.1.1 Strain Energy

Substituting equations (3.15), (3.17), (3.19) and (3.20) into equation (1) then leads to

$$\mathrm{U} = \frac{1}{2} \iiint (\sigma : \varepsilon + m : \chi) dv$$

$$\mathrm{U} = \iiint \sigma_{xx} \mathcal{E}_{xx} dAdx + \iiint m\chi dAdx$$

$$\mathrm{U} = -\frac{1}{2} \int \mathrm{M} \frac{d^2 w(x)}{dx^2} dx \; - \frac{1}{2} \int \mathrm{Y}_{xy} \frac{d^2 w(x)}{dx^2} dx \tag{3.24}$$

Where the Resultant moment M and the couple moment Y_{xy} is stated as

$$\mathrm{Y}_{xy} = \int_{\hat{A}} m_{xy} d\hat{A} \qquad \mathrm{M} = \int_{\hat{A}} z.\, \sigma_{xx} d\hat{A} \tag{3.25}$$

Combining the results gives

$$\mathrm{U} = -\frac{1}{2} \int \left(\mathrm{M} + \mathrm{Y}_{xy}\right) \frac{d^2 w(x)}{dx^2} dx \tag{3.26}$$

From equation (3.19), (3.20) and (3.22), it follows that

$$\mathrm{M} = -\mathrm{EI} \frac{d^2 w(x)}{dx^2}) \qquad \mathrm{Y}_{xy} = -\mu A l^2 \frac{d^2 w(x)}{dx^2} \tag{3.27}$$

Substituting equation (3.27) into (3.26), the strain energy becomes

$$U = \frac{1}{2}\int (EI + \mu Al^2)\frac{d^4w(x)}{dx^4}dx \tag{3.28}$$

$$U = \frac{1}{2}\int EI\frac{d^4w(x)}{dx^4}dx + \frac{1}{2}\int_0^L \mu Al^2\frac{d^4w(x)}{dx^4}dx \tag{3.29}$$

Where second moment of cross-sectional area is given as $I = \int_A Z^2\, dA$

3.1.2 Kinetic Energy

The Kinetic energy is written as [4]

$$T = \frac{1}{2}\rho A\int_0^L (\frac{dw}{dt})^2 dx \tag{3.30}$$

3.1.3 Thermal Energy

The Strain energy caused by thermal loading is evaluated by using [6]

$$\overline{N_t} = -\int_A E\alpha(\Delta T)dA \tag{3.31}$$

Where E and α are Young's modulus and thermal expansion

$$U^T = \frac{1}{2}\int_0^L \overline{N_t}\left(\frac{dw}{dx}\right)^2 dx \tag{3.32}$$

$$U^T = -\frac{1}{2}\int_0^L E\alpha A(\Delta T)\left(\frac{dw}{dx}\right)^2 dx \tag{3.33}$$

Where $\overline{N_t}$ is the applied thermal load. Also, θ , α and υ are the temperature change, the coefficient of thermal expansion in the direction of the x-axis and the Poisson's ratio, respectively.

3.1.3 Work done

In this paper, we have a linear layer (Winkler) and a shearing layer(Pasternak) for which their effects do not generate any non-linearity. A quadratic non-linear layer, which generates non-linearity in the equation is also added. The external work done by Winkler-Pasternak foundation is given as [12] and the non-linear foundation is given as [49]

$$\delta W^{ext-f} = -\int_0^L [K_w w^2 - K_p \left(\frac{dw}{dx}\right)^2 + K_{NL} w^4] dx \qquad (3.34)$$

Where K_w and K_p are Winkler and Pasternak coefficients due to elastic foundation respectively.

3.1.4 Axial Normal Force

The axial normal force N is given as

$$N = \frac{EA}{2L} [\int_0^L \left(\frac{\partial y^*}{\partial x^*}\right)^2 dx^*] \qquad (3.35)$$

3.2.5 Governing Equations and Boundary Condition

In this study, the two types of boundary conditions that are considered in this study are simple-simple and clamped-clamped boundary conditions. Hamilton's principle and the modified couple stress theory are used to derive the governing equations of motion and boundary condition of Euler-Bernoulli beam model nanobeam.

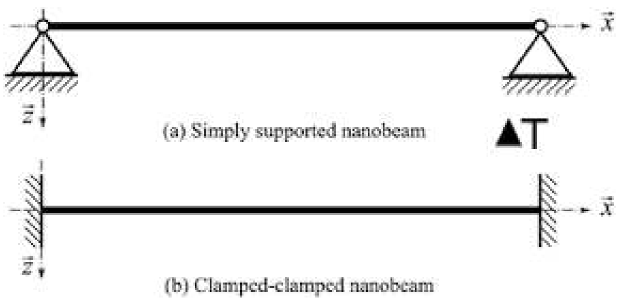

Figure 3.1. Boundary conditions for different beam supports

The equation of motion of the nanobeam is obtained using the Hamilton principle. In order to apply the Hamilton principle, we need to find the Lagrange of the nanobeam. The system's Lagrange is obtained by subtracting strain energy from its kinetic energy and work done. By substituting equation (3.29), (3.30), (3.33), (3.34) and (3.35) into equation (3.23) gives the following equation

$$£ = \frac{1}{2}\int_0^L \rho A\,(\frac{\partial y^*}{\partial t^*})^2 dx^* - \frac{1}{2}\int_0^L EI\left(\frac{\partial^2 y^*}{\partial x^{*2}}\right)^2 dx^* - \frac{1}{2}\frac{E}{2(1+\upsilon)}Al^2\int_0^L \left(\frac{\partial^2 y^*}{\partial x^{*2}}\right)^2 dx^*$$
$$+\frac{1}{2}\int_0^L \overline{N_t}^*\left(\frac{\partial y^*}{\partial x^*}\right)^2 dx^* - \frac{1}{2}\int_0^L N^*\left(\frac{\partial y^*}{\partial x^*}\right)^2 dx^*$$
$$-\int_0^L K_p{}^*\left(\frac{\partial y^*}{\partial x^*}\right)^2 dx^* + \int_0^L K_w{}^* y^{*2} dx^*$$
$$+\int_0^L K_{NL}{}^* y^{*4} dx^* \qquad (3.36)$$

Where y^* denotes the transverse displacement of the beam section between supports, l is the length of the beam,t^* is the time, $\boldsymbol{\rho}$A is the mass per unit length, N^* is the axial force, EA is longitudinal rigidity andEI is flexural rigidity. Expressions with asterisk are dimensional. Whereas, parameters with no asterisk are dimensionless and are defined below.

$x = \frac{x^*}{L}$, $y = \frac{y^*}{L}$, $\xi = \frac{h}{l}$, $t = \frac{t^*}{L^2}\sqrt{\frac{EI}{\rho A}}$, $\eta = \frac{6}{(1+\upsilon)\xi^2}$, $K_P = \frac{k_p{}^* L^2}{EI}$,

$K_w = \frac{k_w{}^* L^4}{EI}$, $N_t = \frac{\alpha A(\Delta T)L^2}{I}$, $K_{NL} = \frac{K_{NL}{}^* L^4 r^2}{EI}$

Where $r = \sqrt{\frac{I}{A}}$ is the radius of gyration of the cross-section.

$$\left(EI + \frac{E}{2(1+\upsilon)}Al^2\right)\frac{\partial^4 y^*}{\partial x^{*4}} + \rho A\frac{\partial^2 y^*}{\partial t^{*2}} + E\alpha A(\Delta T)\frac{\partial^2 y^*}{\partial x^{*2}} - K_p{}^*\frac{\partial^2 y^*}{\partial x^{*2}} + K_w{}^* y^*$$
$$+ K_{NL}{}^* y^{*3} = \frac{EA}{2L}[\int_0^L \left(\frac{\partial y^*}{\partial x^*}\right)^2 dx^*]\frac{\partial^2 y^*}{\partial x^{*2}} \qquad (3.37)$$

Taking EI on both sides and substituting the dimensionless parameters it becomes

$$\left(1 + \frac{Al^2}{2I(1+\upsilon)}\right)\frac{\partial^4 y}{\partial x^4} + \frac{\rho A}{EI}\frac{L^4\,\partial^2 y}{\partial(t^2 L^4 \frac{\rho A}{EI})} + \frac{E\alpha A(\Delta T)}{EI}\frac{L^4}{L^2}\frac{\partial^2 y}{\partial x^2} - \frac{k_p{}^*}{EI}\frac{L^4}{L^2}\frac{\partial^2 y}{\partial x^2} + \frac{k_w{}^* L^4 y}{EI}$$
$$+ \frac{K_{NL}{}^* L^4 r^2}{EI} = \frac{EAL^3}{2EIL}[\int_0^L \left(\frac{\partial y}{\partial x}\right)^2 dx]\frac{\partial^2 y}{\partial x^2} \qquad (3.38)$$

$$(1+\eta)\frac{\partial^4 y}{\partial x^4}+\frac{\partial^2 y}{\partial t^2}+N_t\frac{\partial^2 y}{\partial x^2}-K_p\frac{\partial^2 y}{\partial x^2}+K_w y+K_{NL}y^3$$
$$=\frac{1}{2}\int_0^L\left[\left(\frac{\partial y}{\partial x}\right)^2 dx\right]\frac{\partial^2 y}{\partial x^2} \qquad (3.39)$$

Classical Euler-Bernoulli beam equation can be obtained by applying the length scale parameter equal to zero ($l = 0$).The material length scale parameterl, which is regarding the nanostructure of the nanobeam. The corresponding boundary conditions at the beam-endsx $= 0$ and $x = 1$ are

S-S case **C-C case**

$y(0) = 0 \quad y(1) = 0 \qquad y(0) = 0 \quad y(1) = 0$

$y''(0) = 0 \quad y''(1) = 0 \qquad y'(0) = 0 \quad y'(1) = 0 \qquad (3.40)$

3.2 Nonlocal Elasticity Theory

The stress state at a place inside a body is treated as a function of strains at all points in the neighboring areas, according to the Eringen nonlocal elasticity model [51]. The nonlocal stress-tensor components ij at each position x in a homogeneous elastic solid can be expressed as

$$\sigma_{ij}(x)=\int_{\Omega}\alpha(x,x')\tau_{ij}x'dv \qquad (3.41)$$

Where $\tau_{ij}(x)$the component of the local stress tensor available at position x that is connected with the strain tensor components ε_{ij} as:

$$\varepsilon_{ij}=\frac{1}{2}\left(u_{i,j}+u_{j,i}\right) \qquad (3.42)$$

Where σ_{ij} and ε_{ij} are the nonlocal stress and strain tensors, respectively; τ_{ij} is the classical stress tensor, (x,x') is the kernel function representing the effect of strains at different locations x′ on the stress at a given position x, and V is the total body considered. We can see from the above equation that not only does the strain state at x have an effect on the stress, but the strain state at x′ can also have an effect on the stress state at x. Because it is difficult to apply constitutive relations with integral forms, partial differential expressions are applied, which is expressed as follows

$$[1-(e_o a)^2\nabla^2]\sigma = C_O : \varepsilon \quad (3.43)$$

where e_o is the constant and a is the internal characteristic length, ∇^2 is the Laplacian operator, $\boldsymbol{\varepsilon}$ is the strain vector, and C_O is the elastic stiffness matrix of classical elasticity. It should be noted that $e_o a$ is a scale coefficient that represents the effect of tiny scale on nanostructure mechanical characteristics.

The Hook's law for the nonlocal continuum theory can be described as the following one-dimensional form where E indicates elasticity modulus

$$\sigma_x (e_o a)^2 \frac{\partial^2 \sigma_x}{\partial x^2} = E\varepsilon_x \quad (3.44)$$

The vibration analysis of a nanobeam in a thermal environment based on a Winkler-Pasternak and non-linear foundation is described using Eringen's nonlocal elasticity theory. Winkler elastic spring constants (K_w), Pasternak parameter (K_p), and nonlinear elastic medium (K_{NL}) are all part of the elastic foundation. Boundary conditions such as simple-simple and clamped-clamped are explored. Hamilton's concept is used to generate governing equations.

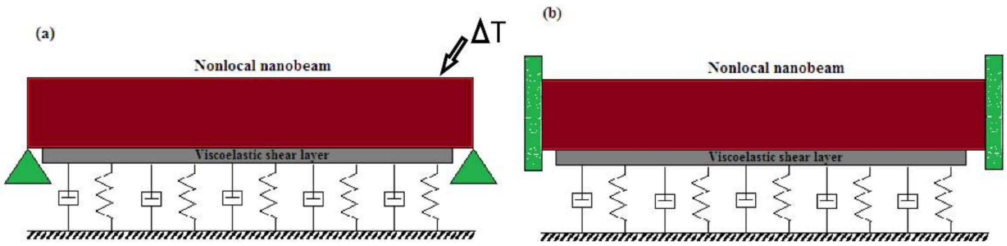

Figure 3.2. Boundary condition for different nonlocal nanobeam Support(S-S/C-C)

$$u_{(x)}(x,z,t) = u(x,t) - z\frac{\partial w}{\partial x}, \quad u_{(y)} = 0 \ , \qquad u_{(z)}(x,z,t) = w(x,t) \quad (3.45)$$

Where t denotes time and u and w denote the axial and transverse displacements of the mid-plane along the x and z axes, respectively. As a result, according to Euler-Bernoulli beam theory, all elements of the strain tensor save normal strain in the x-direction vanish. As a result, the only nonzero normal strain is:

$$\varepsilon_{non-Strain} = \varepsilon_{xx} + \varepsilon_b = \left(\frac{\partial u}{\partial x}\right) + \frac{1}{2}\left(\frac{\partial w}{\partial x}\right)^2 + \frac{\partial^2 w}{\partial x^2} \quad (3.46)$$

Where ε_{xx} *and* ε_b are extensional and bending strain respectively

The axial force and resultant bending moment of the beam model is

$$N = \int_A \sigma_x dA \quad M = \int_A z\sigma_x dA \tag{3.47}$$

The force-strain and moment-strain relation of the non-local beam theory is obtained from equation (3.46) and equation (3.47)

$$\mathrm{N} - (e_o a)^2 \left(\frac{\partial \mathrm{N}}{\partial \mathrm{x}}\right)^2 = EA\left[\left(\frac{\partial u}{\partial x}\right) + \frac{1}{2}\left(\frac{\partial w}{\partial x}\right)^2\right] \tag{3.48}$$

$$\mathrm{M} - (e_o a)^2 \left(\frac{\partial \mathrm{M}}{\partial \mathrm{x}}\right)^2 = -EI\frac{\partial^2 w}{\partial x^2} \tag{3.49}$$

Hamilton's principle:

$$\delta \int_{\mathrm{t1}}^{\mathrm{t2}} \mathrm{Ldt} = 0 \tag{3.50}$$

$$\delta \int_{\mathrm{t1}}^{\mathrm{t2}} (\mathrm{T} - (\mathrm{U} - \mathrm{Wext})\mathrm{dt} = 0 \tag{3.51}$$

Where L is Lagrange function

3.2.1 Strain Energy

$$U = \frac{1}{2}\rho A \int_0^L N\left[\left(\frac{\partial u}{\partial x}\right) + \frac{1}{2}\left(\frac{\partial w}{\partial x}\right)^2\right] + M\frac{\partial^2 w}{\partial x^2}dx \tag{3.52}$$

Where ρA is the mass per unit length

3.2.2 Kinetic Energy

The Kinetic energy is written as

$$T = \frac{1}{2}\rho A \int_0^L [\left(\frac{\partial u}{\partial t}\right)^2 + \left(\frac{\partial w}{\partial t}\right)^2]dx \tag{3.53}$$

3.2.3 Thermal Energy

The Strain energy caused by thermal loading is evaluated by using the following formula [6]

$$\overline{N_t} = -\int_A E\alpha(\Delta T)dA \tag{3.54}$$

Where E and α are Young's modulous and thermal expansion, respectively.

$$N^T = \frac{1}{2}\int_0^L \overline{N_t}\left(\frac{dw}{dx}\right)^2 dx \tag{3.55}$$

Substituting equation (3.54) into equation (3.55) gives

$$N^T = -\frac{1}{2}\int_0^L E\alpha A(\Delta T)\left(\frac{dw}{dx}\right)^2 dx \tag{3.56}$$

Where $\overline{N_t}$ is the applied thermal load. Also,θ , α and υ are the temperature change, the coefficient of thermal expansion in the direction of the x-axis and the Poisson's ratio, respectively.

Let $\text{h and t} = 1\text{nm}\ \text{b} = 2\text{h}, \text{L} = 20\text{nm}\ \text{E} = 30\ \text{Gpa}, \text{v} = 0.3, \rho = 1kg/m^3$

$\alpha_T = -1.6 * 10^{-6} 1/k$ For room or low Temperature T=0k, 100k and 200k

$\alpha_T = 1.1 * 10^{-6} 1/k$ For high temperature T=0k, 100k, 200k, 400k, and 600k

Calculating the area

$$A = bh = 2nm * 1nm = 2 * 10^{-18} \tag{3.57}$$

Inertia

$$I = \frac{bh^3}{12} = \frac{2 * 1}{12} = 0.166 * 10^{-36} \tag{3.58}$$

Temperature effect

$$N_{temp} = \frac{EA\alpha\Delta TL^2}{EI(1-2v)} \tag{3.59}$$

$$N_{temp} = \frac{2 * 10^{-18} * 400 * 10^{-18}}{0.166 * 10^{-36}(1-2(0.6))} \alpha \Delta T = 12000 \alpha \Delta T$$

For $\alpha_T = -1.6 * 10^{-6} 1/\text{k}$(low Temp), $N_{temp} = -0.0192 \Delta T$

For $\alpha_T = 1.1 * 10^{-6} 1/k$(High Temp) , $N_{temp} = 0.0132 \Delta T$

The work done and axial normal force has been discussed in the previous discussions.

Expressions of the nonlocal force and nonlocal moment then becomes

$$N = EA\left[\left(\frac{\partial u}{\partial x}\right) + \frac{1}{2}\left(\frac{\partial w}{\partial x}\right)^2\right] + (e_o a)^2 \frac{\partial^3 u}{\partial x \partial t^2} \tag{3.60}$$

$$M = -EI\frac{\partial^2 w}{\partial x^2} + (e_o a)^2[\rho A \frac{\partial^2 w}{\partial x^2} + N\frac{\partial^2 w}{\partial x^2} - K_w w - \overline{N_t}\frac{\partial^2 w}{\partial x^2} + K_p \frac{\partial^2 w}{\partial x^2} - K_{NL} w^3]$$

3.2.4 Governing Equations and Boundary Condition

The vibration of a nanobeam on a Winkler-Pasternak foundation in a heat environment is investigated in this paper. Simple-simple and clamped-clamped boundary conditions are the two types of boundary conditions investigated in this study. The governing equations of motion and boundary conditions of the Euler-Bernoulli beam model nanobeam are derived using Hamilton's principle and the Eringen's Nonlocal elasticity theory.

The Hamilton principle is used to calculate the nanobeams equation of motion. To apply the Hamilton principle, we must first determine the Lagrange of the nanobeam.

$$\begin{aligned}
£ = & \frac{1}{2}\int_0^L \rho A \left(\frac{\partial y^*}{\partial t^*}\right)^2 dx^* \\
& + \int_0^L [(e_o a)^2 \rho A \left(\frac{\partial y^*}{\partial t^*}\right)^2 - (e_o a)^2 N^* \left(\frac{\partial y^*}{\partial x^*}\right)^2 + (e_o a)^2 K_w{}^* \\
& - (e_o a)^2 K_p{}^* \left(\frac{\partial y^*}{\partial x^*}\right)^2 + (e_o a)^2 K_{NL}{}^* y^{*2} - EI \left(\frac{\partial^2 y^*}{\partial x^{*2}}\right)^2] \frac{\partial^2 y^*}{\partial x^{*2}} dx^* \\
& - \frac{1}{2}\int_0^L N^* \left(\frac{\partial y^*}{\partial x^*}\right)^2 dx^* - \int_0^L K_p{}^* \left(\frac{\partial y^*}{\partial x^*}\right)^2 dx^* + \int_0^L K_w{}^* y^{*2} dx^* \\
& + \int_0^L K_{NL}{}^* y^{*4} dx^*
\end{aligned} \tag{3.61}$$

Where y^* denotes the transverse displacement of the beam section between supports, l is the length of the beam, t^* is the time, $\boldsymbol{\rho}$A is the mass per unit length, N^* is the axial force, EA is longitudinal rigidity and EI is flexural rigidity. Expressions with asterisk are dimensional. Whereas, parameters with no asterisk are dimensionless and are defined below.

$$x = \frac{x^*}{L}\ ,\quad y = \frac{y^*}{L},\quad \xi = \frac{h}{l}\ ,\quad t = \frac{t^*}{L^2}\sqrt{\frac{EI}{\rho A}},\quad \eta = \frac{6}{(1+\upsilon)\xi^2},\ K_P = \frac{{k_p}^* L^2}{EI},$$

$$K_w = \frac{{k_w}^* L^4}{EI} N_t = \frac{\alpha A(\Delta T) L^2}{I}\ ,\quad A = bh\ ,\ I = \frac{1}{12} bh^3\quad K_{NL} = \frac{{K_{NL}}^* L^4 r^2}{EI}\quad \gamma = \frac{e_o a}{L}$$

Where $r = \sqrt{\frac{I}{A}}$ is the radius of gyration of the cross-section. Then adding the thermal term

$$(EI)\frac{\partial^4 y^*}{\partial x^{*4}} + \rho A \frac{\partial^2}{\partial t^{*2}}\left(y^* - (e_o a)^2 \frac{\partial^2 y^*}{\partial x^{*2}}\right) - {K_p}^*\left(\frac{\partial^2 y^*}{\partial x^{*2}} - (e_o a)^2 \frac{\partial^4 y^*}{\partial x^{*4}}\right) + {K_w}^*\left(y^* - (e_o a)^2 \left(\frac{\partial y^*}{\partial x^*}\right)^2\right) + {K_{NL}}^*\left(y^{*3} - 3(e_o a)^2\left(2y^*\left(\frac{\partial y^*}{\partial x^*}\right)^2 + y^{*2}\frac{\partial^4 y^*}{\partial x^{*4}}\right) + \overline{N_t}\left(\frac{\partial^2 y^*}{\partial x^{*2}} - (e_o a)^2 \frac{\partial^4 y^*}{\partial x^{*4}}\right) = \frac{EA}{2L}\left[\int_0^L \left(\frac{\partial y^*}{\partial x^*}\right)^2 dx^*\right]\left[\frac{\partial^2 y^*}{\partial x^{*2}} - (e_o a)^2 \frac{\partial^4 y^*}{\partial x^{*4}}\right] \qquad (3.62)$$

Taking EI on both sides and substituting the dimensionless parameters it becomes

$$\frac{\partial^4 y^*}{\partial x^{*4}} + \frac{\rho A}{EI}\frac{\partial^2}{\partial t^{*2}}\left(y^* - (e_o a)^2 \frac{\partial^2 y^*}{\partial x^{*2}}\right) - \frac{{K_p}^*}{EI}\left(\frac{\partial^2 y^*}{\partial x^{*2}} - (e_o a)^2 \frac{\partial^4 y^*}{\partial x^{*4}}\right) + \frac{{K_w}^*}{EI}\left(y^* - (e_o a)^2\left(\frac{\partial y^*}{\partial t^*}\right)^2\right) + \frac{{K_{NL}}^*}{EI}\left(y^{*3} - 3(e_o a)^2\left(2y^*\left(\frac{\partial y^*}{\partial x^*}\right)^2 + y^{*2}\frac{\partial^4 y^*}{\partial x^{*4}}\right) + \frac{\overline{N_t}}{EI}\left(\frac{\partial^2 y^*}{\partial x^{*2}} - (e_o a)^2 \frac{\partial^4 y^*}{\partial x^{*4}}\right) = \frac{EA}{2EIL}\left[\int_0^L \left(\frac{\partial y^*}{\partial x^*}\right)^2 dx^*\right]\left[\frac{\partial^2 y^*}{\partial x^{*2}} - (e_o a)^2 \frac{\partial^4 y^*}{\partial x^{*4}}\right] \qquad (3.63)$$

$$y^{iv} + \ddot{y} - \gamma^2 \ddot{y}^2 + N_t(y'' - \gamma^2 y^{iv}) - K_p(y'' - \gamma^2 y^{iv}) + K_w(y - \gamma^2 y'') + K_{NL}(y^3 - 3\gamma^2(2yy'^2 + y^2 y'') = \frac{1}{2}\int_0^L [y'^2 dx]\,[y'' - \gamma^2 y^{iv}] \qquad (3.64)$$

$$y(0) = 0 \qquad y(1) = 0 \qquad\qquad y(0) = 0 \quad y(1) = 0$$
$$y''(0) = 0 \qquad y''(1) = 0 \qquad\qquad y'(0) = 0 \quad y'(1) = 0$$

CHAPTER 4

PERTURBATION METHOD

Perturbation theory is a numerical method applied at the point where the analytic (implicit) solution of the interested equation cannot be solved. In this study, the method of multiple scales, one of the perturbation methods Nayfeh [39], will be used. In the case of variable amplitude problems in the equation concerned, the multi-scale method should be used. In this method, fast (T0=t) and slow (T1=εt) time scales should be defined

4.1 The Method of Multiple scale

The method of multiple scales (also called the multiple-scale analysis) comprises techniques used to construct uniformly valid approximations to the solutions of perturbation problems in which the solutions depend simultaneously on widely different scales. This is done by introducing fast-scale and slow-scale variables for an independent variable, and subsequently treating these variables, fast and slow, as if they are independent. A typical example is the modulation of an oscillatory solution over time-scales that are much greater than the period of the oscillations. On this paper, this perturbation method was used for the vibration analysis of nanobeam. Forcing and damping term is added to the dimensionless form of equation of motion.

4.1.1 Modified couple Stress Theory

$$(1+\eta)\frac{\partial^4\bar{y}}{\partial x^4}+\frac{\partial^2\bar{y}}{\partial t^2}+N_t\frac{\partial^2\bar{y}}{\partial x^2}-K_p\frac{\partial^2\bar{y}}{\partial x^2}+K_w\bar{y}+K_{NL}\bar{y}^3$$
$$=\frac{1}{2}\int_0^L\left[\left(\frac{\partial\bar{y}}{\partial x}\right)^2 dx\right]\frac{\partial^2\bar{y}}{\partial x^2}+\bar{F}cos\Omega t-2\bar{\mu}\frac{\partial\bar{y}}{\partial t} \qquad (4.1)$$

$$x=\frac{x^*}{L}\ ,\quad y=\frac{y^*}{L},\quad \xi=\frac{h}{l}\ ,\quad t=\frac{t^*}{L^2}\sqrt{\frac{EI}{\rho A}},\quad \eta=\frac{6}{(1+\upsilon)\xi^2},\ K_P=\frac{{k_p}^*L^2}{EI},$$

$$\mathrm{K_w} = \frac{\mathrm{k_w}^* L^4}{\mathrm{EI}} \mathrm{N_t} = \frac{\alpha \mathrm{A}(\Delta \mathrm{T}) L^2}{\mathrm{I}} \;,\;\; \mathrm{K_{NL}} = \frac{\mathrm{K_{NL}}^* \mathrm{L}^4 \mathrm{r}^2}{\mathrm{EI}} \mathrm{A} = \mathrm{bh}\,,\;\; \mathrm{I} = \frac{1}{12}\mathrm{bh}^3$$

Where $\bar{y} = \sqrt{\mathcal{E}}y \quad \bar{\mu} = \mathcal{E}\boldsymbol{\mu}\bar{F} = \mathcal{E}\sqrt{\mathcal{E}}F$ transformation is performed for the damping and forcing terms based on multiple scale method. So that they are counter effect of non-linearity.

$$(1+\eta)\frac{\partial^4 \sqrt{\mathcal{E}}y}{\partial x^4} + \frac{\partial^2 \sqrt{\mathcal{E}}y}{\partial t^2} + N_t \frac{\partial^2 \sqrt{\mathcal{E}}y}{\partial x^2} - \mathrm{K_p}\frac{\partial^2 \sqrt{\mathcal{E}}y}{\partial \mathrm{x}^2} + \mathrm{K_w}\sqrt{\mathcal{E}}y + \mathrm{K_{NL}}(\sqrt{\mathcal{E}}y)^3$$
$$= \frac{1}{2}\int_0^{\mathrm{L}} \left[\left(\frac{\partial \sqrt{\mathcal{E}}y}{\partial \mathrm{x}}\right)^2 dx\right] \frac{\partial^2 \sqrt{\mathcal{E}}y}{\partial \mathrm{x}^2} + \mathcal{E}\sqrt{\mathcal{E}}F\cos\Omega t - 2\mathcal{E}\boldsymbol{\mu}\frac{\partial \sqrt{\mathcal{E}}y}{\partial t} \qquad (4.2)$$

$$\sqrt{\mathcal{E}}\left[(1+\eta)\frac{\partial^4 y}{\partial x^4} + \frac{\partial^2 y}{\partial t^2} + N_t \frac{\partial^2 y}{\partial x^2} - \mathrm{K_p}\frac{\partial^2 y}{\partial \mathrm{x}^2} + \mathrm{K_w} y\right]$$
$$= \mathcal{E}\sqrt{\mathcal{E}}\left[\frac{1}{2}\int_0^{L} \left(\frac{\partial \sqrt{\mathcal{E}}y}{\partial \mathrm{x}}\right)^2 dx \frac{\partial^2 \sqrt{\mathcal{E}}y}{\partial \mathrm{x}^2} - \mathrm{K_{NL}}y^3 + F\cos\Omega t - 2\boldsymbol{\mu}\frac{\partial y}{\partial t}\right] (4.3)$$

$$\left[(1+\eta)\frac{\partial^4 y}{\partial x^4} + \frac{\partial^2 y}{\partial t^2} + N_t \frac{\partial^2 y}{\partial x^2} - \mathrm{K_p}\frac{\partial^2 y}{\partial \mathrm{x}^2} + \mathrm{K_w} y\right]$$
$$= \mathcal{E}\left[\frac{1}{2}\int_0^{L} \left(\frac{\partial y}{\partial \mathrm{x}}\right)^2 dx\right] \frac{\partial^2 y}{\partial \mathrm{x}^2} - \mathcal{E}\mathrm{K_{NL}}y^3 + \mathcal{E}F\cos\Omega t - 2\mathcal{E}\boldsymbol{\mu}\frac{\partial y}{\partial t} \qquad (4.4)$$

Analytical solution will be approximately obtained with the help of the multiple scale methods having an important perturbation technique. According to the following expansion

$$y(x,t;\epsilon) = \hat{u}(T_0, T_1, T_2, T_3, \ldots\ldots; \epsilon) \qquad (4.5)$$

Where T_n , are defined $\qquad T_0 = tT_1 = \epsilon t \; T_2 = \epsilon^2 t T_3 = \epsilon^3 t$........

We note that the T_n represent different time scales because ϵ is a small parameter. For example, if $= \frac{1}{60}$, variations on the scale T_0 can be observed on the second arm of a watch, variations on the scale T_1, can be observed on the minute arm of a watch, and variations on the scale T_2 can be observed on the hour arm of a watch. Thus, T_0 represents a fast scale, T_1 represents a slower scale, T_2 represents an even slower scale, and so on. Since the dependence of u on t and ϵ occurs on different scales, we imagine that we have a watch and attempt to observe the behavior of u on the different scales of the watch.

Thus, instead of determining u as a function of t, we determine u as a function of T_0, T_1, T_2,...

$$\frac{d}{dt} = \frac{dT_0}{dt}\frac{\partial}{\partial T_0} + \frac{dT_1}{dt}\frac{\partial}{\partial T_1} + \frac{dT_2}{dt}\frac{\partial}{\partial T_2} + \cdots \quad (4.6)$$

$$\frac{d}{dt} = \epsilon^0 D_0 + \epsilon^1 D_1 + \cdots \quad (4.7)$$

$$\frac{d^2}{dt^2} = \boldsymbol{\epsilon}^0 {D_0}^2 + 2\epsilon D_0 D_1 \quad (4.8)$$

Which ε is a small dimensionless parameter and D_n is the new differential operator, which is defined as:

$$D_n = \frac{\partial}{\partial T_n} \;, n = 0,1,2,3, \ldots \quad (4.9)$$

$$\left[(1+\eta)\frac{\partial^4 y}{\partial x^4} + \frac{\partial^2 y}{\partial t^2} + N_t\frac{\partial^2 y}{\partial x^2} - K_p\frac{\partial^2 y}{\partial x^2} + K_w y\right] = \mathcal{E}\left[\frac{1}{2}\int_0^L \left(\frac{\partial y}{\partial x}\right)^2 dx\right]\frac{\partial^2 y}{\partial x^2} - \mathcal{E}K_{NL}y^3 + \mathcal{E}Fcos\Omega t - 2\mathcal{E}\mu\frac{\partial y}{\partial t} \quad (4.10)$$

$$\left[(1+\eta)\left(\epsilon^0 {y_0}^{iv} + \epsilon^1 {y_1}^{iv}\right) + \left(\epsilon^0 {D_0}^2 + 2\epsilon D_0 D_1\right)(\epsilon^0 y_0' + \epsilon^1 y_1') + N_t(\epsilon^0 y_0'' + \epsilon^1 y_1'') - K_p(\epsilon^0 y_0'' + \epsilon^1 y_1'') + K_w y\right] = \epsilon\left[\frac{1}{2}\int_0^L (\epsilon^0 y_0' + \epsilon^1 y_1')^2 dx\right](\epsilon^0 y_0'' + \epsilon^1 y_1'') - \mathcal{E}K_{NL}y^3 + \epsilon Fcos\Omega t - 2\epsilon\mu(\epsilon^0 D_0 + \epsilon^1 D_1)(\epsilon^0 y_0 + \epsilon^1 y_1) \quad (4.11)$$

$$\left[(1+\eta){y_0}^{iv} + \epsilon(1+\eta){y_1}^{iv} + {D_0}^2 y_0 + \epsilon {D_0}^2 y_1 + 2\epsilon D_0 D_1 y_0 + 2\epsilon^2 D_0 D_1 y_1 + N_t y_0'' + \epsilon N_t y_1'' - K_p y_0'' - \epsilon K_p y_1'' + K_w y_0 + K_w y_1\right] = \epsilon\left[\left[\frac{1}{2}\int_0^L {y_0'}^2 + 2\epsilon y_0' y_1' + \epsilon^2 {y_1'}^2 dx\right](y_0'' + \epsilon y_1'') - K_{NL}y^3 + Fcos\Omega t - 2\mu D_0 y_0\right] + \epsilon^2(\ldots) \quad (4.12)$$

Categorizing the obtained result into their respective orders

Order (1):

$$(1+\eta){y_0}^{iv}+{D_0}^2 y_0+N_t {y_0}''-\mathrm{k_p}{y_0}''+\mathrm{k_w}y_0=0 \tag{4.13}$$

Order ($\boldsymbol{\epsilon}$)

$$\begin{aligned}(1+\eta){y_1}^{iv}+{D_0}^2 y_1+N_t {y_1}''-\mathrm{k_p}{y_1}''+\mathrm{k_w}y_1 \\ =-2D_0D_1y_0+\frac{1}{2}\int_0^{\mathrm{L}}\left[{y_0'}^2 dx\right]{y_0}''-\mathrm{K_{NL}}y^3+Fcos\Omega t \\ -2\mu D_0 y_0\end{aligned} \tag{4.14}$$

Fundamental expressions are obtained by solving the first order of expansion. For solvability condition the second order of expansion is used.

4.1.1.1 The Linear Problem

The first order of perturbation is linear, as given in Equation (4.13). In this section, solutions of first-order equations are performed to obtain fundamental linear frequencies and mode shapes. The first order of perturbation which is linear the solution is represented by

$$y_0(x,T_0,T_1)=[A(T_1)e^{i\omega T_0}+cc]Y(x) \tag{4.15}$$

Where cc, ω, A(T_1) represent to the complex conjugate, natural frequency, complex amplitude respectively. By substituting equation (4.9) into equation (4.7)

$$(1+\eta)Y^{iv}(\mathrm{x})+(N_t-\mathrm{K_p})Y''(x)+(\mathrm{K_w}-\omega^2)Y(x)=0 \tag{4.16}$$

S-S	**C-C**
$y^*(0)=0 \quad y^*(L)=0$	$y^*(0)=0 \quad y^*(L)=0$
$y^{*\prime\prime}(0)=0 \quad y^{*\prime\prime}(L)=0$	$y^{*\prime}(0)=0 \quad y^{*\prime}(L)=0$

The following shape function for any beam segment can be considered for solution of the equations

$$Y(x) = C_1 e^{i\beta_1 x} + C_2 e^{i\beta_2 x} + C_3 e^{i\beta_3 x} + C_4 e^{i\beta_4 x} \tag{4.17}$$

The boundary conditions then become

$$Y(x)' = C_1 i\beta_1 e^{i\beta_1 x} + C_2 i\beta_2 e^{i\beta_2 x} + C_3 i\beta_3 e^{i\beta_3 x} + C_4 i\beta_4 e^{i\beta_4 x} \tag{4.18}$$

$$Y(x)'' = -C_1 {\beta_1}^2 e^{i\beta_1 x} - C_2 {\beta_2}^2 e^{i\beta_2 x} - C_3 {\beta_3}^2 e^{i\beta_3 x} - C_4 {\beta_4}^2 e^{i\beta_4 x} \tag{4.19}$$

$$Y(x)''' = -C_1 i{\beta_1}^3 e^{i\beta_1 x} - C_2 i{\beta_2}^3 e^{i\beta_2 x} - C_3 i{\beta_3}^3 e^{i\beta_3 x} - C_4 i{\beta_4}^3 e^{i\beta_4 x} \tag{4.20}$$

$$Y(x)^{iv} = C_1 {\beta_1}^4 e^{i\beta_1 x} + C_2 {\beta_2}^4 e^{i\beta_2 x} + C_3 {\beta_3}^4 e^{i\beta_3 x} + C_4 {\beta_4}^4 e^{i\beta_4 x} \tag{4.21}$$

Using the boundary conditions, the natural frequencies will be obtained. Using the functions in equation above will give the dispersion relation shown below:

$$\begin{aligned}(1+\eta)\left(C_1 {\beta_1}^4 e^{i\beta_1 x} + C_2 {\beta_2}^4 e^{i\beta_2 x} + C_3 {\beta_3}^4 e^{i\beta_3 x} + C_4 {\beta_4}^4 e^{i\beta_4 x}\right) \\ + \left(N_t - \mathrm{K_p}\right)\left(-C_1 {\beta_1}^2 e^{i\beta_1 x} - C_2 {\beta_2}^2 e^{i\beta_2 x} - C_3 {\beta_3}^2 e^{i\beta_3 x} \right. \\ \left. - C_4 {\beta_4}^2 e^{i\beta_4 x}\right) \\ + (\mathrm{K_w} - \omega^2)\left(C_1 e^{i\beta_1 x} + C_2 e^{i\beta_2 x} + C_3 e^{i\beta_3 x} + C_4 e^{i\beta_4 x}\right) = 0\end{aligned} \tag{4.22}$$

$$((1+\eta){\beta_1}^4 - \left(N_t - \mathrm{K_p}\right){\beta_1}^2 + (\mathrm{K_w} - \omega^2))C_1 e^{i\beta_1 x} = 0 \tag{4.23}$$

$$(1+\eta){\beta_1}^4 - \left(N_t - \mathrm{K_p}\right){\beta_1}^2 + (\mathrm{K_w} - \omega^2) = 0 \tag{4.24}$$

Which can be written as

$$(1+\eta){\beta_n}^4 - \left(N_t - \mathrm{K_p}\right){\beta_n}^2 + (\mathrm{K_w} - \omega^2) = 0 \tag{4.25}$$

Let u=${\beta_n}^2$ where n=1,2,3,4

$$(1+\eta)\mathrm{u}^2 - \left(\mathrm{N_t} - \mathrm{K_p}\right)\mathrm{u} + (\mathrm{K_w} - \omega^2) = 0 \tag{4.26}$$

Applying a quadratic equation formula

$$\mathrm{u} = \frac{-\mathrm{b} \pm \sqrt{\mathrm{b}^2 - 4\mathrm{ac}}}{2\mathrm{a}} \tag{4.27}$$

$$u = \frac{N_t - K_p \pm \sqrt{{N_t}^2 - 2N_tK_p + {K_p}^2 - 4K_w + 4\omega^2 - 4\eta K_w + 4\eta\omega^2}}{2 + 2\eta}$$

$${\beta_n}^2 = \frac{N_t - K_p \pm \sqrt{{N_t}^2 - 2N_tK_p + {K_p}^2 - 4K_w + 4\omega^2 - 4\eta K_w + 4\eta\omega^2}}{2 + 2\eta}$$

$$\beta_n = \sqrt{\frac{N_t - K_p \pm \sqrt{{N_t}^2 - 2N_tK_p + {K_p}^2 - 4K_w + 4\omega^2 - 4\eta K_w + 4\eta\omega^2}}{2 + 2\eta}} \qquad (4.28)$$

4.1.1.2 The Non-linear problem

The secular and non-secular terms assuming a solution of the form are separated to find the solvability condition.

$$y_0(x, T_0, T_1) = \phi(x, T_1)e^{i\omega T_0} + cc + W(x, T_0, T_1) \qquad (4.29)$$

We know that for solvability condition we will use the order($\boldsymbol{\epsilon}$) expansion which is given as

$$y_0(x, T_0, T_1) = \left(AT_1e^{i\omega T_0} + cc\right)Y(x) \qquad (4.30)$$

$$\cos\Theta = \frac{1}{2}\left(e^{i\Theta} + e^{-i\Theta}\right) \qquad (4.31)$$

$$\begin{aligned}(1 + \eta){y_1}^{iv} + {D_0}^2y_1 + N_t{y_1}'' - k_p{y_1}'' + k_wy_1 \\ = -2D_0D_1y_0 + \frac{1}{2}\int_0^L \left[{y_0}'^2 dx\right] {y_0}'' - K_{NL}y^3 + F\cos\Omega t \\ - 2\mu D_0y_0 \qquad (4.32)\end{aligned}$$

Substituting the above equation into an order($\boldsymbol{\epsilon}$) gives

$$\begin{aligned}(1 + \eta){y_1}^{iv} + {D_0}^2y_1 + N_t{y_1}'' - k_p{y_1}'' + k_wy_1 \\ = -2D_0D_1y_0 + \frac{1}{2}\int_0^1 \left[{y_0}'^2 dx\right] {y_0}'' - K_{NL}y^3 + F\cos\Omega t \\ - 2\mu D_0y_0 \qquad (4.33)\end{aligned}$$

Pourkiaee et al [43] wrote the general solution for the above equation as

$$y_1 = A(T_1)e^{i\omega T_0}\Omega t + \bar{A}(T_1)e^{-i\omega T_0} \tag{4.34}$$

$$\begin{aligned}&\left[(1+\eta)\phi^{iv} - \omega^2\phi + N_t\phi'' - \mathrm{k_p}\phi'' + \mathrm{k_w}\phi\right]e^{i\omega T_0}\\ &\quad = -2D_0D_1\left(A(T_1)e^{i\omega T_0}\right)Y(x)\\ &\quad + \frac{1}{2}\int_0^1 \left[\left(A(T_1)e^{i\omega T_0} + \bar{A}(T_1)e^{-i\omega T_0}\right)'^2 Y'^2(x)dx\right]\left(A(T_1)e^{i\omega T_0}\Omega t\right.\\ &\quad \left.+ \bar{A}(T_1)e^{-i\omega T_0}\right)Y''(x) - \mathrm{K_{NL}}\left(A(T_1)e^{i\omega T_0} + \bar{A}(T_1)e^{-i\omega T_0}\right)^3 Y^3(x)\\ &\quad + F cos\Omega t - 2\mu D_0\left(A(T_1)e^{i\omega T_0}\right)Y(x) + cc + NST\end{aligned} \tag{4.35}$$

$$\begin{aligned}&\left[(1+\eta)\phi^{iv} - \omega^2\phi + N_t\phi'' - \mathrm{k_p}\phi'' + \mathrm{k_w}\phi\right]e^{i\omega T_0}\\ &\quad = -2i\omega A'Y(x)e^{i\omega T_0}\\ &\quad + \frac{1}{2}\left(A^3e^{3i\omega T_0} + 3A^2\bar{A}e^{i\omega T_0} + 3A\bar{A}^2e^{-2i\omega T_0}\right.\\ &\quad \left.+ \bar{A}^3e^{-3i\omega T_0}\right)\left(\int_0^1 Y'^2(x)dx\right)Y''(x) - 3A^2\bar{A}\mathrm{K_{NL}}Y(x)e^{i\omega T_0}Y^3(x)\\ &\quad + \frac{\mathrm{F}}{2}\left(\mathrm{e}^{\mathrm{i}\Omega t} + \mathrm{e}^{-\mathrm{i}\Omega t}\right) - 2\mu i\omega AY(x)e^{i\omega T_0} + cc + NST\end{aligned} \tag{4.36}$$

$$\begin{aligned}&\left[(1+\eta)\phi^{iv} - \omega^2\phi + N_t\phi'' - \mathrm{k_p}\phi'' + \mathrm{k_w}\phi\right]\\ &\quad = -2i\omega A'Y(x) + \frac{3}{2}(A^2\bar{A})\left(\int_0^1 Y'^2(x)dx\right)Y''(x) - 3A^2\bar{A}\mathrm{K_{NL}}Y^3(x)\\ &\quad + \frac{\mathrm{F}}{2}\left(\mathrm{e}^{\mathrm{i}\Omega t} + \mathrm{e}^{-\mathrm{i}\Omega t}\right)e^{-i\omega T_0} - 2\mu i\omega AY(x) + cc + NST\end{aligned} \tag{4.37}$$

Where $A'$is the derivative of A with respect to T_1, cc denotes the complex conjugate of prior terms and NST represents the non-secular terms.

In the case of a primary resonance in order to show the nearness of the excitation frequency Ω to the natural frequencyω, detuning parameter is described in the form of

$$\Omega = \omega + \varepsilon\sigma \tag{4.38}$$

Simplifying the following term

$$\cos(\Omega t) = \frac{\mathrm{e}^{\mathrm{i}\Omega t} + \mathrm{e}^{-\mathrm{i}\Omega t}}{2} = \frac{\mathrm{e}^{\mathrm{i}\Omega t}}{2} + cc \tag{4.39}$$

$$\frac{e^{i\Omega T}}{2} = \frac{e^{i(\omega+\varepsilon\sigma)T_0}}{2} = \frac{e^{i\omega T_0}e^{i\sigma T_1}}{2} \quad , T_0 = \varepsilon T_1$$

Where σ is a detuning parameter of order(1).

$$\left[(1+\eta)\phi^{iv} - \omega^2\phi + N_t\phi'' - k_p\phi'' + k_w\phi\right] = -2i\omega A'Y(x) + \frac{3}{2}(A^2\bar{A})(\int_0^1 Y'^2 dx)\,Y'' - 3A^2\bar{A}K_{NL}Y^3(x) + \frac{F}{2}e^{i\sigma T_1} - 2\mu i\omega AY(x) \quad (4.40)$$

$$0 = \int_0^1 \left[-2i\omega(A'+\mu A)Y + \frac{3}{2}(A^2\bar{A})\left(\int_0^1 Y'^2 dx\right)Y'' - 3A^2\bar{A}K_{NL}Y^3(x) + \frac{F}{2}e^{i\sigma T_1}\right]Y(x) \quad (4.41)$$

$$0 = -2i\omega(A'+\mu A)\int_0^1 Y^2 dx + \frac{3}{2}(A^2\bar{A})(\int_0^1 Y'^2 dx)\left(\int_0^1 Y''Y dx\right) - 3A^2\bar{A}K_{NL}\int_0^1 Y^4 dx + \frac{e^{i\sigma T_1}}{2}\int_0^1 FY dx \quad (4.42)$$

Applying integration by part

$$\int_0^1 Y''Y dx = YY' - \int_0^1 Y'^2 dx = -\int_0^1 Y'^2 dx \quad (4.43)$$

Substituting the above equation

$$0 = -2i\omega(A'+\mu A)\int_0^1 Y^2 dx - \frac{3}{2}(A^2\bar{A})(\int_0^1 Y'^2 dx)^2 - 3A^2\bar{A}K_{NL}\int_0^1 Y^4 dx + \frac{e^{i\sigma T_1}}{2}\int_0^1 FY dx \quad (4.44)$$

$$0 = -2i\omega(A'+\mu A) - \frac{3}{2}(A^2\bar{A})b^2 - 3A^2\bar{A}dK_{NL} + \frac{e^{i\sigma T_1}}{2}f \quad (4.45)$$

Where $\int_0^1 Y^2\,dx = 1$ $\quad \int_0^1 Y^4\,dx = d$ $\quad \int_0^1 Y'^2 dx = b$ $\int_0^1 FY\,dx = f$ (4.46)

And we will obtain the final equation as

$$2i\omega(A' + \mu A) + 3(A^2\bar{A})\left(d\mathrm{K}_{\mathrm{NL}} + \frac{b^2}{2}\right) - \frac{\mathrm{e}^{\mathrm{i}\sigma T_1}}{2} f = 0 \tag{4.47}$$

Expressing A in polar form leads to

$$A = \frac{1}{2} a(T_1) e^{i\theta T_1} \tag{4.48}$$

Where a *and* θ are real-valued functions of T_1 representing the amplitude and the phase of the response, respectively. Substituting the above equation below and separating the real and imaginary parts, and introducing $\psi = \sigma T_1 - \boldsymbol{\theta}$, the modulation equations can be expressed as

$$2i\omega(\frac{1}{2}ae^{i\theta})' + 2i\omega\mu\left(\frac{1}{2}ae^{i\theta}\right) + 3\left(\left(\frac{1}{2}ae^{i\theta}\right)^2\left(\frac{1}{2}ae^{-i\theta}\right)\right)\left(d\mathrm{K}_{\mathrm{NL}} + \frac{b^2}{2}\right) - \frac{\mathrm{e}^{\mathrm{i}\sigma T_1}}{2} f = 0 \tag{4.49}$$

$$2i\omega(\frac{1}{2}ae^{i\theta})' + i\omega\mu\left(ae^{i\theta}\right) + 3\left(\left(\frac{1}{4}a^2 e^{2i\theta}\right)\left(\frac{1}{2}ae^{-i\theta}\right)\right)\left(d\mathrm{K}_{\mathrm{NL}} + \frac{b^2}{2}\right) - \frac{\mathrm{e}^{\mathrm{i}\psi}\mathrm{e}^{\mathrm{i}\theta}}{2} f = 0 \tag{4.50}$$

And removing $e^{i\theta}$

$$i\omega a' - \omega a\theta' + i\omega\mu a + \frac{3}{8}\mathrm{a}^3\left(d\mathrm{K}_{\mathrm{NL}} + \frac{b^2}{2}\right) - \frac{\mathrm{e}^{\mathrm{i}\psi}}{2} f = 0 \tag{4.51}$$

$$\psi = \sigma T_1 - \theta \tag{4.52}$$

$$\theta' = \sigma - \psi' \tag{4.53}$$

$$\mathrm{e}^{\mathrm{i}\psi} = cos\psi + isin\psi \tag{4.54}$$

$$i\omega a' - \omega a\sigma + \omega a\psi' + i\omega\mu a + \frac{3}{8}\mathrm{a}^3\left(d\mathrm{K}_{\mathrm{NL}} + \frac{b^2}{2}\right) - \frac{cos\psi}{2} f - i\frac{sin\psi}{2} f = 0 \tag{4.55}$$

Collecting like terms

Real Part

$$\omega a\psi' = \omega a\sigma - \frac{3}{8}\mathrm{a}^3\left(d\mathrm{K}_{\mathrm{NL}} + \frac{b^2}{2}\right) + \frac{cos\psi}{2} f \tag{4.56}$$

$$Imaginary\ Part \qquad \omega a' + \omega\mu a = \frac{sin\psi}{2} f \tag{4.57}$$

Free Vibration

For free vibrations values of $f, \mu\ and\ \sigma = 0$. For simple boundary condition

$$If\ a' = 0\ then\ a = a_0$$

$$-\psi' = \frac{3}{8}\frac{\mathrm{a_0}^2\left(\mathrm{dK_{NL}} + \frac{\mathrm{b}^2}{2}\right)}{\omega} \tag{4.58}$$

$$\Theta' = \sigma - \psi' = 0 - \psi' = -\psi' \tag{4.59}$$

$$\Theta' = \frac{3}{8}\frac{\mathrm{a_0}^2}{\omega}\left(\mathrm{dK_{NL}} + \frac{\mathrm{b}^2}{2}\right) \tag{4.60}$$

$$\omega_{\mathrm{NL}} = \omega + \Theta' \tag{4.61}$$

$$\omega_{\mathrm{NL}} - \omega = \frac{3}{8}\frac{\mathrm{a_0}^2\left(\mathrm{dK_{NL}} + \frac{\mathrm{b}^2}{2}\right)}{\omega} \tag{4.62}$$

$$\omega_{\mathrm{NL}} = \omega + \frac{3}{8}\frac{\mathrm{a_0}^2\left(\mathrm{dK_{NL}} + \frac{\mathrm{b}^2}{2}\right)}{\omega} \tag{4.63}$$

Let $\boldsymbol{\lambda} = \frac{\mathbf{3}}{\mathbf{8}}\frac{\left(\boldsymbol{d}\mathbf{K_{NL}} + \frac{\boldsymbol{b}^2}{2}\right)}{\boldsymbol{\omega}}$ (4.64)

The equation then becomes

$$\omega_{NL} = \omega + \mathrm{a_0}^2\lambda \tag{4.65}$$

For forced and damped vibration

$$a' = \psi' = 0$$

$$\omega a\sigma + \omega\mu a - \frac{3}{8}\mathrm{a}^3\left(d\mathrm{K_{NL}} + \frac{b^2}{2}\right) + \frac{cos\psi}{2} f - \frac{sin\psi}{2} f = 0 \tag{4.66}$$

$$\omega a\sigma + \omega\mu a - \frac{3}{8}\mathrm{a}^3\left(d\mathrm{K_{NL}} + \frac{b^2}{2}\right) + \frac{cos\psi}{2} f = \frac{sin\psi}{2} f \tag{4.67}$$

$$(\omega a\sigma - \frac{3}{8}\mathrm{a}^3(d\mathrm{K}_{\mathrm{NL}} + \frac{b^2}{2}))^2 = \left(-\frac{cos\psi}{2}f\right)^2 \quad (4.69)$$

$$(\omega\mu a)^2 = (\frac{sin\psi}{2}f)^2 \quad (4.70)$$

$$(\omega a\sigma - \frac{3}{8}\mathrm{a}^3(d\mathrm{K}_{\mathrm{NL}} + \frac{b^2}{2}))^2 + (\omega\mu a)^2 = (\frac{sin\psi}{2}f)^2 + \left(\frac{cos\psi}{2}f\right)^2 \quad (4.71)$$

$$(\omega a\sigma - \frac{3}{8}\mathrm{a}^3(d\mathrm{K}_{\mathrm{NL}} + \frac{b^2}{2}))^2 + (\omega\mu a)^2 = \left(\frac{f}{2}\right)^2 (sin^2\psi + cos^2\psi) \quad (4.72)$$

$$sin^2\psi + cos^2\psi = 1 \quad (4.73)$$

$$(\omega a\sigma - \frac{3}{8}\mathrm{a}^3(d\mathrm{K}_{\mathrm{NL}} + \frac{b^2}{2}))^2 + (\omega\mu a)^2 = \left(\frac{f}{2}\right)^2 \quad (4.74)$$

$$(\omega^2 a^2)\sigma^2 - \left(\frac{3}{4}\omega a^4\left(d\mathrm{K}_{\mathrm{NL}} + \frac{b^2}{2}\right)\right)\sigma + \left(\frac{9}{(8*8)}a^6\left(d\mathrm{K}_{\mathrm{NL}} + \frac{b^2}{2}\right)^2 + (\omega^2 a^2)\mu^2 - \frac{f^2}{4}\right) = 0 \quad (4.75)$$

Applying quadratic equation formula

$$\sigma = \frac{\frac{3}{4}\mathrm{a}^4(\mathrm{dK}_{\mathrm{NL}} + \frac{b^2}{2}) \pm \omega a\sqrt{\frac{9}{(16)}a^6(\mathrm{dK}_{\mathrm{NL}} + \frac{b^2}{2})^2 - (\frac{9}{(16)}a^6(d\mathrm{K}_{\mathrm{NL}} + \frac{b^2}{2})^2 - (4\omega^2 a^2)\mu^2 + f^2}}{2\omega^2 a^2}$$

$$\sigma = \frac{3}{8\omega}\mathrm{a}^2\left(\mathrm{dK}_{\mathrm{NL}} + \frac{b^2}{2}\right) \pm \sqrt{-\mu^2 + \frac{f^2}{(4\omega^2 a^2)}} \quad (4.76)$$

$$\sigma = \frac{3}{16\omega}\mathrm{a}^2\left(\mathrm{dK}_{\mathrm{NL}} + \frac{b^2}{2}\right) \pm \sqrt{\frac{f^2}{(4\omega^2 a^2)} - \mu^2} \quad (4.77)$$

$$\sigma = \mathrm{a}^2\lambda \pm \sqrt{\frac{f^2}{(4\omega^2 a^2)} - \mu^2} \quad (4.78)$$

4.2.1 Nonlocal Elasticity Theory

Multiple scale method is applied to the nonlocal nanobeam

$$y^{iv} + \ddot{y} - \gamma^2\ddot{y}^2 + N_t(y'' - \gamma^2 y^{iv}) - K_p(y'' - \gamma^2 y^{iv}) + \mathrm{K_w}(\mathrm{y} - \gamma^2 y'') + \mathrm{K_{NL}}(\mathrm{y}^3 - 3\gamma^2(2\mathrm{y}y'^2 + y^2 y'') = \frac{1}{2}\int_0^{\mathrm{L}} [y'^2\mathrm{dx}]\,[y'' - \gamma^2 y^{iv}] + \bar{F}cos\Omega t - 2\bar{\mu}\dot{y} \quad (4.79)$$

Where $\bar{y} = \sqrt{\mathcal{E}}y$, $\bar{\mu} = \mathcal{E}\mu$, $\bar{F} = \mathcal{E}\sqrt{\mathcal{E}}F$ transformation is performed for the damping and forcing terms based on multiple scale method. So that they are counter effect of non-linearity.

$$\sqrt{\mathcal{E}}(y^{iv} + \ddot{y} - \gamma^2\ddot{y}^2) + \sqrt{\mathcal{E}}N_t(y'' - \gamma^2 y^{iv}) - \sqrt{\mathcal{E}}K_p(y'' - \gamma^2 y^{iv}) + \sqrt{\mathcal{E}}\mathrm{K_w}(\mathrm{y} - \gamma^2 y'') + \mathcal{E}\sqrt{\mathcal{E}}\mathrm{K_{NL}}(\mathrm{y}^3 - 3\gamma^2(2\mathrm{y}y'^2 + y^2 y'') = \frac{\mathcal{E}\sqrt{\mathcal{E}}}{2}\left(\int_0^{\mathrm{L}} [y'^2\mathrm{dx}]\,[y'' - \gamma^2 y^{iv}] + Fcos\Omega t - 2\mu\dot{y}\right) \quad (4.80)$$

$$y^{iv} + \ddot{y} - \gamma^2\ddot{y}^2 + N_t(y'' - \gamma^2 y^{iv}) - K_p(y'' - \gamma^2 y^{iv}) + \mathrm{K_w}(\mathrm{y} - \gamma^2 y'') + \mathcal{E}\mathrm{K_{NL}}(\mathrm{y}^3 - 3\gamma^2(2\mathrm{y}y'^2 + y^2 y'') = \frac{\mathcal{E}}{2}\int_0^{\mathrm{L}} [y'^2\mathrm{dx}]\,[y'' - \gamma^2 y^{iv}] + F\mathcal{E}cos\Omega t - 2\mathcal{E}\mu\dot{y} \quad (4.81)$$

The analytical solution will be approximated using multiple scale method which is an important perturbation technique. According to the following expansion

$$y(x,t;\epsilon) = \hat{u}(T_0, T_1, T_2, T_3, \ldots\ldots; \epsilon) \quad (4.82)$$

Where T_n , are defined $T_0 = tT_1 = \epsilon t\ T_2 = \epsilon^2 tT_3 = \epsilon^3 t$

Thus, instead of determining u as a function of t, we determine u as a function of $\mathrm{T_0}$, $\mathrm{T_1}$, $\mathrm{T_2}$,...

$$\frac{\mathrm{d}}{\mathrm{dt}} = \frac{\mathrm{dT_0}}{\mathrm{dt}}\frac{\partial}{\partial \mathrm{T_0}} + \frac{\mathrm{dT_1}}{\mathrm{dt}}\frac{\partial}{\partial \mathrm{T_1}} + \frac{\mathrm{dT_2}}{\mathrm{dt}}\frac{\partial}{\partial \mathrm{T_2}} + \cdots \quad (4.83)$$

$$\frac{\mathrm{d}}{\mathrm{dt}} = \epsilon^0\mathrm{D_0} + \epsilon^1\mathrm{D_1} + \cdots \quad (4.84)$$

$$\frac{d^2}{dt^2} = \epsilon^0 D_0{}^2 + 2\epsilon D_0 D_1 + \epsilon^2 D_1{}^2 \ldots \tag{4.85}$$

Which ε is a small dimensionless parameter and D_n is the new differential operator, which is defined as

$$D_n = \frac{\partial}{\partial T_n} \ , n = 0,1,2,3, \ldots \tag{4.86}$$

$$\begin{aligned} y^{iv} + \ddot{y} - \gamma^2\ddot{y}^2 + N_t(y'' - \gamma^2 y^{iv}) - K_p(y'' - \gamma^2 y^{iv}) + K_w(y - \gamma^2 y'') + \mathcal{E}K_{NL}(y^3 \\ - 3\gamma^2(2yy'^2 + y^2 y'') \\ = \frac{\mathcal{E}}{2}\int_0^L [y'^2 dx]\,[y'' - \gamma^2 y^{iv}] + F\mathcal{E}cos\Omega t - 2\mathcal{E}\mu\dot{y} \end{aligned} \tag{4.87}$$

Categorizing the obtained result into their respective orders

Order (1):

$$\begin{aligned} y_0{}^{iv} + D_0{}^2 y_0 - \gamma^2 D_0{}^2 y_0'' + N_t(y_0'' - \gamma^2 y_0{}^{iv}) - K_p(y_0'' - \gamma^2 y_0{}^{iv}) + K_w(y_0 \\ - \gamma^2 y_0'') = 0 \end{aligned} \tag{4.88}$$

Order ($\boldsymbol{\epsilon}$)

$$\begin{aligned} y_1{}^{iv} + D_0{}^2 y_1 - \gamma^2 D_0{}^2 y_1'' + N_t(y_1'' - \gamma^2 y_1{}^{iv}) - K_p(y_1'' - \gamma^2 y_1{}^{iv}) \\ + K_w(y_0 - \gamma^2 y_0'') \\ = -2D_0 D_1 y_0 + 2\gamma^2 D_0 D_1 y_0'' + \frac{1}{2}\int_0^L [y_0'^2 dx]\,[y_0'' - \gamma^2 y_0{}^{iv}] \\ - K_{NL}(y_0{}^3 - 3\gamma^2(2y_0 y_0'^2 + y_0{}^2 y_0'') + Fcos\Omega t \\ - 2\mu D_0 y_0 \end{aligned} \tag{4.89}$$

Fundamental expressions are obtained by solving the first order of expansion. For solvability condition the second order of expansion is used.

4.2.1.1 The Linear Problem

As seen above the first order of perturbation is linear. This section solves first-order equations to derive fundamental linear frequencies and mode shapes. The linear solution of the first order of perturbation is represented by

$$y_0(x, T_0, T_1) = [A(T_1)e^{i\omega T_0} + cc]Y(x) \tag{4.90}$$

Where cc, ω, A(T_1) represent to the complex conjugate, natural frequency, complex amplitude respectively.

$$Y^{iv} + {D_0}^2 Y - \gamma^2 {D_0}^2 Y'' + N_t(Y'' - \gamma^2 Y^{iv}) - K_p(Y'' - \gamma^2 Y^{iv}) + \mathrm{K_w}(\mathrm{Y} - \gamma^2 Y'') = 0 \tag{4.91}$$

$$Y^{iv} - N_t\gamma^2 Y^{iv} + K_p\gamma^2 Y^{iv} - \gamma^2 {D_0}^2 Y'' + N_t Y'' - K_p Y'' - \mathrm{K_w}\gamma^2 Y'' + {D_0}^2 Y + \mathrm{K_w Y} = 0 \tag{4.92}$$

$$\left(1 - N_t\gamma^2 + K_p\gamma^2\right)Y^{iv} + (\gamma^2\omega^2 + N_t - K_p - \mathrm{K_w}\gamma^2)Y'' + (\mathrm{K_w} - \omega^2)\mathrm{Y} = 0 \tag{4.93}$$

The following shape function for any beam segment can be considered for solution of the equations

$$Y(x) = C_1 e^{i\beta_1 x} + C_2 e^{i\beta_2 x} + C_3 e^{i\beta_3 x} + C_4 e^{i\beta_4 x} \tag{4.94}$$

The boundary conditions then become

$$Y(x)' = C_1 i\beta_1 e^{i\beta_1 x} + C_2 i\beta_2 e^{i\beta_2 x} + C_3 i\beta_3 e^{i\beta_3 x} + C_4 i\beta_4 e^{i\beta_4 x} \tag{4.95}$$

$$Y(x)'' = -C_1{\beta_1}^2 e^{i\beta_1 x} - C_2{\beta_2}^2 e^{i\beta_2 x} - C_3{\beta_3}^2 e^{i\beta_3 x} - C_4{\beta_4}^2 e^{i\beta_4 x} \tag{4.96}$$

$$Y(x)''' = -C_1 i{\beta_1}^3 e^{i\beta_1 x} - C_2 i{\beta_2}^3 e^{i\beta_2 x} - C_3 i{\beta_3}^3 e^{i\beta_3 x} - C_4 i{\beta_4}^3 e^{i\beta_4 x} \tag{4.97}$$

$$Y(x)^{iv} = C_1{\beta_1}^4 e^{i\beta_1 x} + C_2{\beta_2}^4 e^{i\beta_2 x} + C_3{\beta_3}^4 e^{i\beta_3 x} + C_4{\beta_4}^4 e^{i\beta_4 x} \tag{4.98}$$

Using the boundary conditions the natural frequencies will be obtained. Using the functions in the above equation will give the dispersion relation shown below:

$$\begin{aligned}&\left(1 - N_t\gamma^2 + K_p\gamma^2\right)\left(C_1{\beta_1}^4 e^{i\beta_1 x} + C_2{\beta_2}^4 e^{i\beta_2 x} + C_3{\beta_3}^4 e^{i\beta_3 x} + C_4{\beta_4}^4 e^{i\beta_4 x}\right)\\ &+ \left(\gamma^2\omega^2 + N_t - K_p - \mathrm{K_w}\gamma^2\right)\left(-C_1{\beta_1}^2 e^{i\beta_1 x} - C_2{\beta_2}^2 e^{i\beta_2 x} - C_3{\beta_3}^2 e^{i\beta_3 x}\right.\\ &\left. - C_4{\beta_4}^2 e^{i\beta_4 x}\right) + (\mathrm{K_w} - \omega^2)\left(C_1 e^{i\beta_1 x} + C_2 e^{i\beta_2 x} + C_3 e^{i\beta_3 x} + C_4 e^{i\beta_4 x}\right)\\ &= 0\end{aligned} \tag{4.99}$$

$$\left(1 - N_t\gamma^2 + K_p\gamma^2\right){\beta_1}^4 - \left(\gamma^2\omega^2 + N_t - K_p - \mathrm{K_w}\gamma^2\right){\beta_1}^2 + (\mathrm{K_w} - \omega^2) = 0 \tag{4.100}$$

Which can be written as

$$\left(1 - N_t\gamma^2 + K_p\gamma^2\right){\beta_n}^4 - \left(\gamma^2\omega^2 + N_t - K_p - \mathrm{K_w}\gamma^2\right){\beta_n}^2 + (\mathrm{K_w} - \omega^2) = 0 \quad (4.101)$$

Let u=${\beta_n}^2$ where n=1, 2, 3, 4

$$\left(1 - N_t\gamma^2 + K_p\gamma^2\right)u^2 - \left(\gamma^2\omega^2 + N_t - K_p - \mathrm{K_w}\gamma^2\right)u + (\mathrm{K_w} - \omega^2) = 0 \quad (4.102)$$

4.2.1.2 The Non-linear problem

The secular and non-secular terms assuming a solution of the form are separated to find the solvability condition.

$$y_0(x, T_0, T_1) = \phi(x, T_1)e^{i\omega T_0} + cc + W(x, T_0, T_1) \quad (4.103)$$

We know that for solvability condition we will use the order($\boldsymbol{\epsilon}$) expansion which is given as

$$\begin{aligned} &{y_1}^{iv} + {D_0}^2 y_1 - \gamma^2 {D_0}^2 {y_1}'' + N_t\left({y_1}'' - \gamma^2 {y_1}^{iv}\right) - K_p\left({y_1}'' - \gamma^2 {y_1}^{iv}\right) \\ &\qquad + \mathrm{K_w}(y_1 - \gamma^2 {y_1}'') \\ &\qquad = -2D_0 D_1 y_0 + 2\gamma^2 \mathrm{D_0 D_1} {y_0}'' + \frac{1}{2}\int_0^{\mathrm{L}} \left[{y_0'}^2 \mathrm{dx}\right]\left[{y_0}'' - \gamma^2 {y_0}^{iv}\right] \\ &\qquad - \mathrm{K_{NL}}\left({y_0}^3 - 3\gamma^2\left(2y_0{y_0'}^2 + {y_0}^2 {y_0}''\right)\right) + F\cos\Omega t \\ &\qquad - 2\mu D_0 y_0 \end{aligned} \quad (4.104)$$

Pourkiaee et al [43] wrote the general solution for the above equation as

$$y_1 = A(T_1)e^{i\omega T_0}\Omega t + \bar{A}(T_1)e^{-i\omega T_0} \quad (4.105)$$

$$\begin{aligned} &(\phi^{iv} - \omega^2\phi + \gamma^2\omega^2\phi'' + N_t\left(\phi'' - \gamma^2\phi^{iv}\right) - K_p\left(\phi'' - \gamma^2\phi^{iv}\right) \\ &\qquad + \mathrm{K_w}(\phi - \gamma^2\phi''))e^{i\omega T_0} \\ &\qquad = -2D_0 D_1\left(A(T_1)e^{i\omega T_0}\right)Y(x) \\ &\qquad + 2\gamma^2 \mathrm{D_0 D_1}\left(A(T_1)e^{i\omega T_0}\Omega t + \bar{A}(T_1)e^{-i\omega T_0}\right)Y''(x) \\ &\qquad + \frac{1}{2}\int_0^1 \left[\left(A(T_1)e^{i\omega T_0} + \bar{A}(T_1)e^{-i\omega T_0}\right)'^2 Y'^2(x)dx\right]\left(A(T_1)e^{i\omega T_0}\Omega t\right. \\ &\qquad + \bar{A}(T_1)e^{-i\omega T_0}\big)Y''(x) - \gamma^2\left(A(T_1)e^{i\omega T_0}\right)Y(x)^{iv} \\ &\qquad - \mathrm{K_{NL}}(\left(A(T_1)e^{i\omega T_0} + \bar{A}(T_1)e^{-i\omega T_0}\right)^3 Y^3(x) \end{aligned}$$

$$-3\gamma^2\Big(2\big(A(T_1)e^{i\omega T_0}\big)Y(x)Y(x)'^2 + \big(A(T_1)e^{i\omega T_0}\big)Y(x)^2\big(A(T_1)e^{i\omega T_0}\Omega t + \bar{A}(T_1)e^{-i\omega T_0}\big)Y''(x)\Big) + Fcos\Omega t - 2\mu D_0\big(A(T_1)e^{i\omega T_0}\big)Y(x) + cc + NST \tag{4.106}$$

$$[(1 - N_t\gamma^2 + K_p\gamma^2)\phi^{iv}(x) + (\gamma^2\omega^2 + N_t - K_p - K_w\gamma^2)\phi''(\mathrm{x}) + (\mathrm{K_w} - \omega^2)\phi]e^{i\omega T_0} = -2i\omega Y(x)D_1Ae^{i\omega T_0} + 2\gamma^2 i\omega Y''(x)\mathrm{D}_1Ae^{i\omega T_0} + \frac{3A^2\bar{A}e^{i\omega T_0}}{2}\int_0^{\mathrm{L}}\big[Y(x)'^2\mathrm{dx}\big]\big[Y(x)'' - \gamma^2Y(x)^{iv}\big] - \mathrm{K_{NL}}(3A^2\bar{A}Y^3(x) - 3\gamma^2\Big(6A^2\bar{A}Y(x)Y(x)'^2 + (3A^2\bar{A})Y(x)^2Y''(x)\Big)e^{i\omega T_0} + \frac{\mathrm{F}}{2}(\mathrm{e}^{\mathrm{i}\Omega t} + \mathrm{e}^{-\mathrm{i}\Omega t}) - 2\mu i\omega AY(x)e^{i\omega T_0} + cc + NST \tag{4.107}$$

$$[(1 - N_t\gamma^2 + K_p\gamma^2)\phi^{iv}(x) + (\gamma^2\omega^2 + N_t - K_p - K_w\gamma^2)\phi''(\mathrm{x}) + (\mathrm{K_w} - \omega^2)\phi] = -2i\omega Y(x)D_1A + 2\gamma^2 i\omega Y''(x)\mathrm{D}_1A + \frac{3A^2\bar{A}}{2}\int_0^{\mathrm{L}}\big[Y(x)'^2\mathrm{dx}\big]\big[Y(x)'' - \gamma^2Y(x)^{iv}\big] - \mathrm{K_{NL}}(3A^2\bar{A}Y(x)^3 - 3\gamma^2\big(6A^2\bar{A}Y(x)Y'(\mathrm{x})^2 + (3A^2\bar{A})Y(x)^2Y''(x)\big) + \frac{\mathrm{F}}{2}(\mathrm{e}^{\mathrm{i}\Omega t}) - 2\mu i\omega AY(x) + cc + NST \tag{4.108}$$

Where $A'$is the derivative of A with respect to T_1, cc denotes the complex conjugate of prior terms and NST represents the non-secular terms. In the case of a primary resonance in order to show the nearness of the excitation frequency Ω to the natural frequencyω, detuning parameter is described in the form of

$$\Omega = \omega + \mathcal{E}\sigma \tag{4.109}$$

Where σ is a detuning parameter

$$-2i\omega Y(x)D_1A + 2\gamma^2 i\omega Y''(x)\mathrm{D}_1A + \frac{3A^2\bar{A}}{2}\int_0^{\mathrm{L}}\big[Y(x)'^2\mathrm{dx}\big]\big[Y(x)'' - \gamma^2Y(x)^{iv}\big] - \mathrm{K_{NL}}(3A^2\bar{A}Y(x)^3 - 3\gamma^2\big(6A^2\bar{A}Y(x)Y'(\mathrm{x})^2 + (3A^2\bar{A})Y(x)^2Y''(x)\big) + \frac{\mathrm{F}}{2}(\mathrm{e}^{\mathrm{i}\Omega t}) - 2\mu i\omega AY(x) + cc + NST = 0 \tag{4.110}$$

$$2i\omega(D_1A+\mu A)+2\gamma^2 i\omega \mathrm{D}_1 A z_1+\frac{3A^2\bar{A}}{2}({z_1}^2+\gamma^2 z_1 z_2)+\mathrm{K}_{\mathrm{NL}}(3A^2\bar{A})z_3-\frac{\mathrm{F}}{2}\left(\mathrm{e}^{\mathrm{i}\Omega t}\right)$$
$$=0 \tag{4.111}$$

Where

$$\int_0^1 Y(x)^2 dx = 1 \quad \int_0^1 {Y'}^2 dx = z_1 \quad \int_0^1 {Y''}^2 dx = z_2 \quad \int_0^1 FY\, dx = f \tag{4.112}$$

$$\int_0^1 Y(x)^4 - 3\gamma^2\left(2\int_0^1 Y^2(x)Y'(\mathrm{x})^2 dx + \int_0^1 Y(x)^3 Y''(x)\right) = z_3 \tag{4.113}$$

Expressing A in polar form leads to

$$A=\frac{1}{2}a(T_1)e^{i\theta T_1} \tag{4.114}$$

Where a *and* θ are real-valued functions of T_1 representing the amplitude and the phase of the response, respectively. Substituting the above equation below and separating the real and imaginary parts, and introducing $\psi= \sigma T_1$-$\boldsymbol{\theta}$, the modulation equations can be expressed as

$$2i\omega(D_1A+\mu A)+2\gamma^2 i\omega \mathrm{D}_1 A z_1+\frac{3A^2\bar{A}}{2}({z_1}^2+\gamma^2 z_1 z_2)+\mathrm{K}_{\mathrm{NL}}(3A^2\bar{A})z_3-\frac{\mathrm{F}}{2}\left(\mathrm{e}^{\mathrm{i}\Omega t}\right)$$
$$=0 \tag{4.115}$$

$$2i\omega(\frac{1}{2}ae^{i\theta})'+2i\omega\mu\left(\frac{1}{2}ae^{i\theta}\right)+2\gamma^2 i\omega(\frac{1}{2}ae^{i\theta})'z_1$$
$$+\frac{3\left((\frac{1}{4}a^2e^{2i\theta})(\frac{1}{2}ae^{-i\theta})\right)}{2}({z_1}^2+\gamma^2 z_1 z_2)$$
$$+3\mathrm{K}_{\mathrm{NL}}\left(\left(\frac{1}{2}ae^{i\theta}\right)^2\left(\frac{1}{2}ae^{-i\theta}\right)\right)(z_3)-\frac{\mathrm{e}^{\mathrm{i}\sigma T_1}}{2}f=0 \tag{4.116}$$

$$2i\omega(\frac{1}{2}ae^{i\theta})'+i\omega\mu\left(ae^{i\theta}\right)+\gamma^2 i\omega(ae^{i\theta})'z_1$$
$$+\frac{3\left((\frac{1}{4}a^2e^{2i\theta})(\frac{1}{2}ae^{-i\theta})\right)}{2}({z_1}^2+\gamma^2 z_1 z_2)$$
$$+3\mathrm{K}_{\mathrm{NL}}\left(\left(\frac{1}{4}a^2e^{2i\theta}\right)\left(\frac{1}{2}ae^{-i\theta}\right)\right)(z_3)-\frac{\mathrm{e}^{\mathrm{i}\psi}\mathrm{e}^{\mathrm{i}\theta}}{2}f=0 \tag{4.117}$$

And removing $e^{i\theta}$

$$i\omega(D_1a+\mu a)-\omega aD_1\theta+\gamma^2 i\omega D_1az_1-\gamma^2\omega aD_1\theta z_1+\frac{3\mathrm{a}^3}{16}({z_1}^2+\gamma^2 z_1z_2)$$
$$+\frac{3}{8}\mathrm{a}^3\mathrm{K}_{\mathrm{NL}}(z_3)-\frac{\mathrm{e}^{\mathrm{i}\psi}}{2}f=0 \tag{4.118}$$

Substituting the following equation into above

$$\psi=\sigma T_1-\theta \tag{4.119}$$

$$\theta'=\sigma-\psi' \tag{4.120}$$

$$\mathrm{e}^{\mathrm{i}\psi}=cos\psi+isin\psi \tag{4.121}$$

$$i\omega(D_1a+\mu a)-\omega aD_1\theta+\gamma^2 i\omega D_1az_1-\gamma^2\omega aD_1\theta z_1+\frac{3\mathrm{a}^3}{16}({z_1}^2+\gamma^2 z_1z_2)$$
$$+\frac{3}{8}\mathrm{a}^3\mathrm{K}_{\mathrm{NL}}(z_3)-\frac{cos\psi}{2}f-i\frac{sin\psi}{2}f=0 \tag{4.122}$$

Collecting like terms

Real Part $$\omega a\psi'+\gamma^2\omega a\psi' z_1+\frac{3\mathrm{a}^3}{16}({z_1}^2+\gamma^2 z_1z_2)$$
$$=\omega a\sigma+\gamma^2\omega a\sigma z_1-\frac{3}{8}\mathrm{a}^3\mathrm{K}_{\mathrm{NL}}(z_3)+\frac{cos\psi}{2}f \tag{4.123}$$

Imaginary Part $$\omega(D_1a+\mu a)+\gamma^2\omega D_1az_1=\frac{sin\psi}{2}f \tag{4.124}$$

Free Vibration

For free vibrations values of f, μ and $\sigma=0$. For simple boundary condition

$$If\ a'=0\ then\ a=a_0$$

$$-\psi'(\omega a+\gamma^2\omega az_1)=\frac{3\mathrm{a}^3}{16}({z_1}^2+\gamma^2 z_1z_2)+\frac{3}{8}\mathrm{a}^3\mathrm{K}_{\mathrm{NL}}(z_3) \tag{4.125}$$

$$-\psi'=\frac{\frac{3\mathrm{a}^3}{16}({z_1}^2+\gamma^2 z_1z_2)+\frac{3}{8}\mathrm{a}^3\mathrm{K}_{\mathrm{NL}}(z_3)}{\omega a(1+\gamma^2 z_1)} \tag{4.126}$$

$$-\psi' = \frac{3a_0{}^2(z_1{}^2+\gamma^2 z_1 z_2)}{16\omega(1+\gamma^2 z_1)} + \frac{3a_0{}^2\mathrm{K_{NL}}(z_3)}{8\omega(1+\gamma^2 z_1)} \tag{4.127}$$

$$-\psi' = \frac{3a_0{}^2(z_1{}^2+\gamma^2 z_1 z_2)}{16\omega(1+\gamma^2 z_1)} + \frac{3a_0{}^2\mathrm{K_{NL}}(z_3)}{8\omega(1+\gamma^2 z_1)} \tag{4.128}$$

$$\theta' = \sigma - \psi' = 0 - \psi' = -\psi' \tag{4.129}$$

$$\theta' = \frac{3a_0{}^2(z_1{}^2+\gamma^2 z_1 z_2)}{16\omega(1+\gamma^2 z_1)} + \frac{3a_0{}^2\mathrm{K_{NL}}(z_3)}{8\omega(1+\gamma^2 z_1)} \tag{4.130}$$

$$\omega_{NL} = \omega + \theta' \tag{4.131}$$

$$\omega_{NL} = \omega + \frac{3a_0{}^2(z_1{}^2+\gamma^2 z_1 z_2)}{16\omega(1+\gamma^2 z_1)} + \frac{3a_0{}^2\mathrm{K_{NL}}(z_3)}{8\omega(1+\gamma^2 z_1)} \tag{4.132}$$

Let $\lambda = \frac{3}{16\omega(1+\gamma^2 z_1)}[(z_1{}^2+\gamma^2 z_1 z_2) + 2\mathrm{K_{NL}}(z_3)]$ (4.133)

The equation then becomes

$$\omega_{NL} = \omega + \mathrm{a_0}{}^2\lambda \tag{4.134}$$

For forced and damped vibration $a' = \psi' = 0$

$$(\omega a\sigma + \gamma^2\omega a\sigma z_1 - \frac{3}{8}\mathrm{a}^3\mathrm{K_{NL}}(z_3) - \frac{3\mathrm{a}^3}{16}(z_1{}^2+\gamma^2 z_1 z_2))^2 = (-\frac{cos\psi}{2}f)^2 \tag{4.135}$$

$$(\omega\mu a + \gamma^2\omega D_1 a z_1)^2 = \left(\frac{sin\psi}{2}f\right)^2 \tag{4.136}$$

Adding

$$(\omega a\sigma + \gamma^2\omega a\sigma z_1 - \frac{3}{8}\mathrm{a}^3\mathrm{K_{NL}}(z_3) - \frac{3\mathrm{a}^3}{16}(z_1{}^2+\gamma^2 z_1 z_2))^2 + (\omega\mu a + \gamma^2\omega D_1 a z_1)^2$$
$$= \left(\frac{f}{2}\right)^2 (sin^2\psi + cos^2\psi) \tag{4.137}$$

$$sin^2\psi + cos^2\psi = 1 \tag{4.138}$$

$$(\omega a\sigma + \gamma^2\omega a\sigma z_1 - \frac{3}{8}\mathrm{a}^3\mathrm{K}_{\mathrm{NL}}(z_3) - \frac{3\mathrm{a}^3}{16}({z_1}^2 + \gamma^2 z_1 z_2))^2 + (\omega\mu a + \gamma^2\omega D_1 a z_1)^2 = \left(\frac{f}{2}\right)^2 \tag{4.139}$$

$$(\omega a\sigma + \gamma^2\omega a\sigma {z_1}^2 - \frac{3}{8}\mathrm{a}^3\mathrm{K}_{\mathrm{NL}}(z_3) - \frac{3\mathrm{a}^3}{16}({z_1}^2 + \gamma^2 z_1 z_2))^2 + (\omega^2 a^2)\mu^2 - \frac{f^2}{4} = 0 \tag{4.140}$$

$$\begin{aligned}
&\omega^2 a^2(1 + 2\gamma^2 z_1 + \gamma^4 z_1)\sigma^2 \\
&\quad - \left(\frac{3}{4}\omega a^4\mathrm{K}_{\mathrm{NL}}(z_3)(1 + \gamma^2 z_1) + \frac{3}{8}\omega a^4\big(({z_1}^2 + \gamma^2 z_1 z_2)\big)(1 + \gamma^2 z_1)\right)\sigma \\
&\quad + \left[\frac{9}{(8*8)}a^6\mathrm{K}_{\mathrm{NL}}(z_3)(\mathrm{K}_{\mathrm{NL}}(z_3) + {z_1}^2 + \gamma^2 z_1 z_2) - \frac{9}{(16*16)}a^6({z_1}^2 + \gamma^2 z_1 z_2) - \frac{f^2}{4}\right] = 0
\end{aligned} \tag{4.141}$$

Applying quadratic equation formula

$$\sigma = \frac{\frac{3}{4}\omega a^4\mathrm{K}_{\mathrm{NL}}(z_3)(1 + \gamma^2 z_1) + \frac{3}{8}\omega a^4\big(({z_1}^2 + \gamma^2 z_1 z_2)\big)(1 + \gamma^2 z_1) \pm \sqrt{\frac{3}{4}\omega a^4\mathrm{K}_{\mathrm{NL}}(z_3)(1 + \gamma^2 z_1) + \frac{3}{8}\omega a^4\big(({z_1}^2 + \gamma^2 z_1 z_2)\big)(1 + \gamma^2 z_1)^2 - 4ac}}{2\omega^2 a^2\left(1 + 2\gamma^2 z_1 + \gamma^4 {Z_1}^2\right)}$$

$$\sigma = \mathrm{a}^2\lambda \pm \frac{1}{(1 + \gamma^2 z_1)}\sqrt{\frac{f^2}{(4\omega^2 a^2)} - \mu^2} \tag{4.142}$$

CHAPTER 5
RESULT AND DISCUSSION

Numerical results in tabular form and graphically are given in this section for two types of boundary conditions. Linear natural frequencies are presented for simply supported (SS) and clamped-clamped (CC) boundary conditions. After obtaining linear natural frequencies, nonlinear frequencies are calculated for the free and un-damped situation.

5.1 Numerical results using modified Couple Stress Theory

Table 5.1. The first Three frequencies for Simple-Simple nanobeams for different Temperature, Winkler and Pasternak parameter, nonlinear foundation and material length scale parameter

			K_L=10			K_L=100			K_L=200		
	ΔT		K_P=5	K_P=50	K_P=100	K_P=5	K_P=50	K_P=100	K_P=5	K_P=50	K_P=100
h/l	(K)		K_{NL}=10	K_{NL}=100	K_{NL}=200	K_{NL}=10	K_{NL}=100	K_{NL}=200	K_{NL}=10	K_{NL}=100	K_{NL}=200
						Temperature ΔT is low and room					
1	0	ω_1	24.6239	32.411	39.2931	26.3882	33.7708	40.4221	28.2195	35.2203	41.6407
		ω_2	94.6532	103.613	112.737	95.1274	104.047	113.136	95.6516	104.526	113.577
		ω_3	211.566	220.811	230.649	211.779	221.015	230.844	212.015	221.241	231.06
	100	ω_1	25.0057	32.702	39.5335	26.7449	34.0502	40.6559	28.5532	35.4883	41.8676
		ω_2	95.0527	103.979	113.073	95.525	104.41	113.47	96.047	104.888	113.91
		ω_3	211.969	221.197	231.018	212.181	221.4	231.213	212.417	221.626	231.429
	200	ω_1	25.3818	32.9904	39.7725	27.0968	34.3274	40.8883	28.8832	35.7543	42.0933
		ω_2	95.4506	104.342	113.408	95.9209	104.773	113.804	96.4408	105.249	114.242
		ω_3	212.371	221.582	231.387	212.583	221.785	231.581	212.818	222.01	231.797
2	0	ω_1	16.4059	26.7074	34.7385	18.9513	28.3423	36.0106	21.4278	30.0547	37.3733
		ω_2	59.7014	73.0807	85.5261	60.4505	73.6939	86.0506	61.272	74.3693	86.6297
		ω_3	132.092	146.443	160.894	132.432	146.75	161.173	132.809	147.09	161.483
	100	ω_1	16.9736	27.0598	35.0102	19.4448	28.6746	36.2728	21.8655	30.3683	37.626
		ω_2	60.3329	73.5975	85.9681	61.0742	74.2064	86.4899	61.8875	74.8771	87.0661
		ω_3	132.736	147.024	161.423	133.074	147.33	161.701	133.45	147.669	162.01
	200	ω_1	17.5229	27.4077	35.2798	19.9262	29.0032	36.5331	22.2947	30.6787	37.877
		ω_2	60.9578	74.1106	86.4078	61.6916	74.7154	86.927	62.4969	75.3816	87.5003
		ω_3	133.377	147.603	161.95	133.714	147.907	162.228	134.087	148.245	162.536
3	0	ω_1	14.3774	25.5116	33.8278	17.2253	27.2184	35.1329	19.9176	28.9973	36.5284
		ω_2	50.6477	65.8917	79.471	51.5286	66.5712	80.0353	52.4899	67.3181	80.6576
		ω_3	111.313	128.014	144.323	111.716	128.365	144.634	112.163	128.754	144.979
	100	ω_1	15.022	25.8803	34.1068	17.7668	27.5643	35.4016	20.3877	29.3222	36.7869
		ω_2	51.3906	66.4644	79.9465	52.2589	67.1381	80.5074	53.2071	67.8787	81.1261
		ω_3	112.076	128.679	144.912	112.477	129.028	145.222	112.92	129.415	145.566
	200	ω_1	15.64	26.2439	34.3835	18.2923	27.9059	35.6682	20.8473	29.6436	37.0435
		ω_2	52.1228	67.0322	80.4191	52.9791	67.7002	80.9768	53.9146	68.4348	81.5919
		ω_3	112.834	129.34	145.499	113.232	129.687	145.808	113.673	130.072	146.151
4	0	ω_1	13.5962	25.0796	33.5033	16.5788	26.814	34.8205	19.3612	28.618	36.228
		ω_2	47.0693	63.1826	77.2397	48.0158	63.8909	77.8201	49.0461	64.6687	78.46

		ω_3	103.055	120.903	138.054	103.49	121.274	138.379	103.972	121.686	138.74
		ω_1	14.276	25.4546	33.7849	17.1408	27.165	35.0916	19.8445	28.9472	36.4886
	100	ω_2	47.8677	63.7797	77.7288	48.7987	64.4814	78.3056	49.8128	65.2522	78.9415
		ω_3	103.879	121.606	138.67	104.311	121.975	138.994	104.789	122.385	139.353
		ω_1	14.925	25.8242	34.0642	17.6849	27.5116	35.3605	20.3164	29.2726	36.7473
	200	ω_2	48.653	64.3711	78.2149	49.5693	65.0665	78.7881	50.5679	65.8304	79.4202
		ω_3	104.697	122.305	139.283	105.125	122.673	139.606	105.6	123.079	139.964
		ω_1	13.2189	24.8771	33.352	16.2708	26.6247	34.675	19.0982	28.4407	36.0881
	0	ω_2	45.3174	61.8886	76.1848	46.2998	62.6115	76.7732	47.3674	63.405	77.4217
		ω_3	98.9995	117.465	135.053	99.453	117.848	135.386	99.9545	118.271	135.755
		ω_1	13.9173	25.2551	33.6348	16.8431	26.9782	34.9471	19.588	28.7719	36.3497
5	100	ω_2	46.1462	62.498	76.6806	47.1112	63.2139	77.2652	48.1609	64.0	77.9097
		ω_3	99.8572	118.189	135.683	100.307	118.569	136.015	100.804	118.99	136.382
		ω_1	14.5822	25.6276	33.9154	17.3965	27.3271	35.2172	20.0659	29.0993	36.6095
	200	ω_2	46.9603	63.1015	77.1733	47.9089	63.8106	77.7542	48.9415	64.5894	78.3946
		ω_3	100.708	118.908	136.31	101.153	119.286	136.64	101.646	119.705	137.006

						Temperature ΔT is high				
		ω_1	24.089	32.0065	38.9602	25.8898	33.3828	40.0986	27.754	34.8484	41.3267
	200	ω_2	94.101	103.109	112.274	94.578	103.545	112.674	95.1052	104.027	113.117
		ω_3	211.011	220.279	230.14	211.224	220.483	230.335	211.461	220.71	230.552
		ω_1	23.542	31.5968	38.6243	25.3816	32.9903	39.7723	27.2805	34.4726	41.0102
1	400	ω_2	93.5456	102.603	111.809	94.0254	103.04	112.211	94.5557	103.524	112.655
		ω_3	210.455	219.746	229.63	210.669	219.951	229.826	210.906	220.178	230.043
		ω_1	22.982	31.1818	38.2855	24.863	32.593	39.4434	26.7987	34.0926	40.6913
	600	ω_2	92.9869	102.094	111.342	93.4695	102.533	111.745	94.003	103.02	112.192
		ω_3	209.897	219.212	229.119	210.111	219.417	229.315	210.349	219.645	229.533
		ω_1	15.5916	26.215	34.3614	18.2509	27.8788	35.647	20.811	29.618	37.0231
	200	ω_2	58.8221	72.3641	84.9146	59.5822	72.9833	85.4429	60.4155	73.6652	86.0261
		ω_3	131.201	145.64	160.163	131.544	145.948	160.444	131.923	146.291	160.755
		ω_1	14.7323	25.7133	33.9802	17.5226	27.4075	35.2796	20.1752	29.1749	36.6695
2	400	ω_2	57.9294	71.6404	84.2987	58.701	72.2658	84.8308	59.5467	72.9544	85.4182
		ω_3	130.305	144.833	159.43	130.649	145.143	159.712	131.032	145.487	160.024
		ω_1	13.8197	25.2015	33.5946	16.7626	26.928	34.9084	19.5188	28.7249	36.3125
	600	ω_2	57.0227	70.9092	83.6782	57.8065	71.541	84.2142	58.6651	72.2365	84.8059
		ω_3	129.402	144.021	158.692	129.749	144.333	158.976	130.134	144.679	159.29
		ω_1	13.4408	24.9957	33.4405	16.4516	26.7355	34.7601	19.2524	28.5445	36.17
	200	ω_2	49.6082	65.0961	78.8126	50.5071	65.7837	79.3815	51.4876	66.5394	80.0089
		ω_3	110.254	127.095	143.508	16.4516	127.449	143.821	111.113	127.84	144.168
		ω_1	12.4338	24.469	33.0486	15.6397	26.2437	34.3833	18.5634	28.0844	35.808
3	400	ω_2	48.5463	64.2905	78.1485	49.4646	64.9867	78.7223	50.4653	65.7516	79.3549
		ω_3	109.186	126.169	142.688	109.597	126.525	143.003	110.052	126.92	143.353
		ω_1	11.3377	23.9306	32.652	14.7832	25.7425	34.0023	17.8478	27.6166	35.4423
	600	ω_2	47.4607	63.4748	77.4789	48.3996	64.1798	78.0575	49.4219	64.9542	78.6954
		ω_3	108.106	125.236	141.864	108.522	125.595	142.181	108.982	125.993	142.532
		ω_1	12.6016	24.5547	33.1121	15.7734	26.3236	34.4443	18.6762	28.1591	35.8666
	200	ω_2	45.9488	62.3524	76.562	46.918	63.07	77.1476	47.9718	63.8578	77.793
		ω_3	101.911	119.929	137.202	102.351	120.304	137.529	102.839	120.719	137.892
		ω_1	11.5215	24.0183	135.482	14.9246	25.824	34.064	17.9651	27.6925	35.5015
4	400	ω_2	44.8004	61.511	75.8783	45.7938	62.2383	76.4691	46.8729	63.0365	77.1202
		ω_3	100.753	118.947	136.344	101.199	119.325	136.674	101.692	119.743	137.039
		ω_1	10.329	23.4696	32.3156	14.0246	25.3144	33.6794	17.2247	27.218	35.1326
	600	ω_2	43.6217	60.6579	75.1884	44.6413	61.3953	75.7846	45.7477	62.2043	76.4415
		ω_3	99.583	117.957	135.482	100.034	118.338	135.813	100.532	118.76	136.181
		ω_1	12.1936	24.3478	32.959	15.4494	26.1308	34.2972	18.4034	27.9789	35.7253
	200	ω_2	44.1525	61.0408	75.4977	45.1602	61.7736	76.0914	46.2541	62.5777	76.7457
		ω_3	97.808	116.463	134.182	98.267	116.849	134.517	98.7745	117.276	134.889
		ω_1	11.0738	23.8067	32.5613	14.5818	25.6273	33.9152	17.6813	27.5093	35.3588
5	400	ω_2	42.9561	60.181	74.8042	43.9912	60.9241	75.4034	45.1134	61.7394	76.0636
		ω_3	96.6018	115.452	133.306	97.0665	115.841	133.643	97.5803	116.272	134.016
		ω_1	9.82716	23.2531	32.1588	13.6592	25.1138	33.5289	16.9285	27.0316	34.9884
	600	ω_2	41.7253	59.3088	74.1043	42.7902	60.0627	74.7091	43.9431	60.8895	75.3754
		ω_3	95.3803	114.432	132.423	95.8509	114.824	132.763	96.3712	115.259	133.139

Table 5.2. The first three frequencies for Clamped-Clamped nanobeams for different Temperature, Winkler and Pasternak parameter, nonlinear foundation and material length scale parameter

			K_L=10			K_L=100			K_L=200		
			K_P=5	K_P=50	K_P=100	K_P=5	K_P=50	K_P=100	K_P=5	K_P=50	K_P=100
h/l	ΔT(K)		K_{NL}=10	K_{NL}=100	K_{NL}=200	K_{NL}=10	K_{NL}=100	K_{NL}=200	K_{NL}=10	K_{NL}=100	K_{NL}=200
			Temperature ΔT is low and room								
1	0	ω_1	53.6874	58.59	63.5518	54.5192	59.353	64.256	55.4287	60.1896	65.0295
		ω_2	146.964	153.839	161.11	147.27	154.131	161.389	147.609	154.455	161.698
		ω_3	287.381	295.02	303.276	287.538	295.173	303.425	287.712	295.342	303.589
	100	ω_1	53.9067	58.7891	63.7338	54.7351	59.5496	64.436	55.6411	60.3834	65.2073
		ω_2	147.265	154.125	161.382	147.57	154.417	161.66	147.908	154.74	161.969
		ω_3	287.712	295.342	303.589	287.868	295.494	303.737	288.042	295.663	303.901
	200	ω_1	54.1249	58.9875	63.9152	54.9501	59.7455	64.6154	55.8526	60.5766	65.3846
		ω_2	147.564	154.411	161.654	147.869	154.702	161.932	148.207	155.025	162.24
		ω_3	288.041	295.663	303.901	288.198	295.815	304.049	288.371	295.984	304.213
2	0	ω_1	33.905	41.1759	47.8548	35.2074	42.2546	48.7861	36.6001	43.4218	49.8005
		ω_2	91.8279	102.439	112.986	92.3167	102.878	113.384	92.8567	103.362	113.824
		ω_3	178.854	190.878	203.38	179.105	191.113	203.601	179.384	191.375	203.846
	100	ω_1	34.2506	41.4548	48.0907	35.5402	42.5264	49.0175	36.9203	43.6864	50.0271
		ω_2	92.3075	102.866	113.37	92.7937	103.302	113.766	93.331	103.785	114.205
		ω_3	179.384	191.373	203.844	179.634	191.608	204.064	179.912	191.869	204.309
	200	ω_1	34.5923	41.7316	48.3252	35.8696	42.7963	49.2476	37.2374	43.9491	50.2527
		ω_2	92.7845	103.291	113.753	93.2682	103.725	114.148	93.8028	104.206	114.585
		ω_3	179.912	191.868	204.307	180.162	192.102	204.527	180.439	192.362	204.771
3	0	ω_1	28.7864	37.037	44.2735	30.3093	38.2327	45.2785	31.9164	39.5189	46.3696
		ω_2	77.4219	89.7294	101.552	78.001	90.2296	101.994	78.639	90.782	102.483
		ω_3	150.394	164.504	178.838	150.693	164.778	179.09	151.024	165.081	179.368
	100	ω_1	29.1919	37.3442	44.5252	30.6947	38.5304	45.5246	32.2826	39.8069	46.61
		ω_2	77.9899	90.2145	101.976	78.5648	90.7119	102.416	79.1986	91.2614	102.904
		ω_3	151.024	165.079	179.365	151.321	165.351	179.615	151.651	165.653	179.894
	200	ω_1	29.5912	37.6486	44.7753	31.0748	38.8255	45.7693	32.6442	40.0926	46.849
		ω_2	78.5534	90.6967	102.399	79.1242	91.1915	102.837	79.7536	91.7382	103.322
		ω_3	151.651	165.651	179.89	151.947	165.922	180.14	152.276	166.224	180.417
4	0	ω_1	26.7643	35.4666	42.9312	28.3959	36.7135	43.9669	30.1053	38.051	45.0898
		ω_2	71.6992	84.827	97.2173	72.3241	85.3558	97.6791	73.0121	85.9396	98.1896
		ω_3	139.064	154.21	169.404	139.387	154.501	169.669	139.745	154.825	169.964
	100	ω_1	27.1996	35.7859	43.1892	28.8066	37.022	44.2188	30.4929	38.3488	45.3355
		ω_2	72.3119	85.3389	97.6592	72.9316	85.8645	98.189	73.6139	86.4449	98.6272
		ω_3	139.744	154.822	169.959	140.066	155.112	170.223	140.423	155.434	170.517
	200	ω_1	27.6274	36.1019	43.4454	29.2108	37.3276	44.4691	30.8751	38.6439	45.5796
		ω_2	72.9191	85.8474	98.099	73.5337	86.37	98.5567	74.2105	86.947	99.0627
		ω_3	140.422	155.432	170.512	140.742	155.721	170.776	141.097	156.042	171.068
5	0	ω_1	25.7747	34.7133	42.2904	27.4651	35.9863	43.3414	29.229	37.3499	44.48
		ω_2	68.8896	82.4575	95.1397	69.5397	83.0015	95.6115	70.255	83.6017	96.133
		ω_3	133.494	149.204	164.852	133.831	149.505	165.125	134.204	149.839	165.427
	100	ω_1	26.2262	35.0386	42.5513	27.8893	36.3002	43.596	29.6279	37.6524	44.7282
		ω_2	69.527	82.9834	95.5905	70.1712	83.5239	96.0601	70.8802	84.1204	96.5792
		ω_3	134.203	149.837	165.422	134.538	150.137	165.694	134.909	150.469	165.995
	200	ω_1	26.6693	35.3605	42.8105	28.3064	36.611	43.849	30.0209	37.9522	44.9748
		ω_2	70.1581	83.5058	96.039	70.7966	84.0429	96.5064	71.4994	84.6358	97.0231
		ω_3	134.909	150.466	165.99	135.242	150.765	166.261	135.611	151.096	166.561

			Temperature ΔT is high								
1	200	ω_1	53.3843	58.3149	63.3006	54.2207	59.0815	64.0075	55.1352	59.9218	64.784
		ω_2	146.55	153.445	160.735	146.857	153.738	161.014	147.197	154.063	161.325
		ω_3	286.927	294.578	302.846	287.084	294.731	302.995	287.258	294.9	303.16
	400	ω_1	53.0793	58.0384	63.0483	53.9204	58.8086	63.758	54.8399	59.6528	64.5375
		ω_2	146.135	153.05	160.359	146.443	153.343	160.639	146.784	153.669	160.95
		ω_3	286.472	294.135	302.415	286.629	294.288	302.564	286.803	294.457	302.729
	600	ω_1	52.7724	57.7604	62.7949	53.6183	58.5343	63.5074	54.5429	59.3824	64.2899
		ω_2	145.718	152.653	159.982	146.027	152.948	160.263	146.369	153.274	160.574
		ω_3	286.015	293.691	301.984	286.173	293.844	302.133	286.347	294.014	302.298
2	200	ω_1	33.4238	40.789	47.5284	34.7441	41.8777	48.466	36.1546	43.0551	49.4869

		ω_2	91.1641	101.85	112.456	91.6563	102.29	112.855	92.2003	102.778	113.298
		ω_3	178.122	190.194	202.739	178.375	190.43	202.961	178.655	190.693	203.208
		ω_1	32.9347	40.3979	47.1994	34.2738	41.4969	48.1434	35.7028	42.6848	49.171
	400	ω_2	90.495	101.256	111.923	90.9909	101.7	112.324	91.5387	102.19	112.769
		ω_3	177.388	189.508	202.097	177.641	189.745	202.32	177.923	190.008	202.567
		ω_1	32.4374	40.0025	46.8679	33.7962	41.1121	47.8184	35.2446	42.3108	48.8528
	600	ω_2	89.8205	100.659	111.387	90.3201	101.105	111.791	90.872	101.598	112.237
		ω_3	176.65	188.819	201.453	176.905	189.057	201.676	177.187	189.321	201.924
		ω_1	28.2183	36.6099	43.9247	29.7703	37.8191	44.9375	31.4049	39.1189	46.0367
	200	ω_2	76.6336	89.0579	100.965	77.2186	89.5617	101.41	77.8634	90.1183	101.901
		ω_3	149.523	163.711	178.111	149.824	163.986	178.364	150.157	164.29	178.644
		ω_1	27.6373	36.1771	43.5728	29.2202	37.4003	44.5939	30.8839	38.7141	45.7011
3	400	ω_2	75.8365	88.3808	100.374	76.4276	88.8885	100.822	77.079	89.4492	101.316
		ω_3	148.648	162.914	177.381	148.95	163.19	177.635	149.285	163.496	177.916
		ω_1	27.0425	35.7385	43.2177	265838.	36.9762	44.2467	30.3529	38.3045	45.3627
	600	ω_2	75.0303	87.6981	99.78	75.6277	88.2097	100.23	76.2859	88.7747	100.728
		ω_3	147.767	162.113	176.648	148.071	162.39	176.903	148.408	162.698	177.185
		ω_1	26.1526	35.0223	42.5737	27.8201	36.2845	43.6179	29.5628	37.6373	44.7495
	200	ω_2	70.8473	84.1176	96.606	71.4797	84.6509	97.0707	72.1758	85.2395	97.5844
		ω_3	138.122	153.364	168.637	138.447	153.657	168.904	138.808	153.982	169.2
		ω_1	25.5247	34.5716	42.2128	27.2307	35.8496	43.2657	29.0088	37.2182	44.4063
4	400	ω_2	69.9844	83.4018	95.9905	70.6245	83.9396	96.4582	71.3289	84.5331	96.9752
		ω_3	137.173	152.513	167.867	137.501	152.808	168.135	137.864	153.135	168.432
		ω_1	24.8794	34.1142	41.8483	26.6267	35.4087	42.9102	28.4426	36.7937	44.06
	600	ω_2	69.1099	82.6792	95.3707	69.758	83.2217	95.8414	70.4711	83.8203	96.3617
		ω_3	136.218	151.658	167.093	136.548	151.954	167.362	136.914	152.283	167.661
		ω_1	25.1391	34.2604	41.9286	26.8696	35.5496	42.9884	28.6701	36.9293	44.1362
	200	ω_2	68.0026	81.7284	94.5161	68.6612	82.2772	94.991	69.3856	82.8826	95.5159
		ω_3	132.513	148.33	164.065	132.852	148.633	164.339	133.228	148.969	164.643
		ω_1	24.4853	33.8006	41.5632	26.2589	35.1067	42.6322	28.0986	36.5032	43.7893
5	400	ω_2	67.1032	80.9922	93.8879	67.7704	81.5459	94.366	68.5043	82.1568	94.8944
		ω_3	131.524	147.451	163.273	131.866	147.755	163.549	132.244	148.093	163.854
		ω_1	23.8117	33.3337	41.1943	25.632	34.6574	42.2725	27.5136	36.0712	43.4392
	600	ω_2	66.1906	80.2487	93.2552	66.867	80.8075	93.7365	67.6106	81.4239	94.2684
		ω_3	130.528	146.566	162.478	130.872	146.872	162.755	131.253	147.212	163.062

Table 5.3. The nonlinear correction term of the 1st mode SS nanobeam with different h/l, T, , Kp and kw values when K_{nl}=10,100 and 200

			K_L=10			K_L=100			K_L=200		
	ΔT		K_P=5	K_P=50	K_P=100	K_P=5	K_P=50	K_P=100	K_P=5	K_P=50	K_P=100
h/l	(K)		K_{NL}=10	K_{NL}=100	K_{NL}=200	K_{NL}=10	K_{NL}=100	K_{NL}=200	K_{NL}=10	K_{NL}=100	K_{NL}=200
Temperature ΔT is low and room											
	0	ω_1	0.970163	3.1829	3.32792	0.905299	2.20647	3.23497	0.84655	2.11566	3.1403
1	100	ω_1	0.95535	2.27828	3.30768	0.893225	2.18836	3.21637	0.836656	2.09968	3.12328
	200	ω_1	0.941194	2.25866	3.28781	0.881625	2.17069	3.19808	0.827097	2.08406	3.10653
	0	ω_1	1.45614	2.79002	3.76424	1.26056	2.62908	3.63127	1.11487	2.47929	3.49887
2	100	ω_1	1.40743	2.75369	3.73503	1.22857	2.59861	3.60502	1.09255	2.45368	3.47537
	200	ω_1	1.36331	2.71873	3.70649	1.19888	2.56917	3.57934	1.07152	2.42886	3.45234
	0	ω_1	1.66158	2.9208	3.86558	1.38687	2.73764	3.72199	1.1994	2.56969	3.5798
3	100	ω_1	1.59028	2.87918	3.83396	1.3446	2.70329	3.69374	1.17175	2.54122	3.55464
	200	ω_1	1.52744	2.8393	3.80311	1.30597	2.67019	3.66613	1.14591	2.51367	3.53002
	0	ω_1	1.75705	2.97111	3.90303	1.44095	2.77893	3.75538	1.23387	2.60375	3.60948
4	100	ω_1	1.67338	2.92734	3.87049	1.3937	2.74302	3.72637	1.20382	2.57414	3.5837
	200	ω_1	1.60062	2.88544	3.83876	1.35083	2.70847	3.69803	1.17586	2.54553	3.55847
	0	ω_1	1.8072	2.99529	3.92073	1.46823	2.79869	3.77114	1.25086	2.61999	3..62347
5	100	ω_1	1.71651	2.95046	3.88776	1.41834	2.76202	3.74177	1.21958	2.58983	3.59739
	200	ω_1	1.63824	2.90758	3.8556	1.37322	2.72675	3.71308	1.19054	2.56183	3.57187
Temperature ΔT is high											
	200	ω_1	0.991706	2.3281	3.35635	0.922727	2.23211	3.26107	0.860748	2.13824	3.16416
1	400	ω_1	1.01475	2.35828	3.38554	0.941202	2.25867	3.28782	0.875688	2.16155	3.18858
	600	ω_1	1.03947	2.38967	3.4155	0.960834	2.2862	3.31524	0.891431	2.18564	3.21357

2	200	ω_1	1.53218	2.84243	3.80555	1.30893	2.67279	3.66831	1.14791	2.51584	3.53196
	400	ω_1	1.62155	2,89789	3.84825	1.36334	2.71875	3.70651	1.18409	2.55405	3.56602
	600	ω_1	1.7282	2.95674	3.89242	1.42515	2.76716	3.74592	1.22389	2.59406	3.60108
3	200	ω_1	1.7773	2.98108	3.91035	1.45209	2.78709	3.7619	1.24084	2.61046	3.61527
	400	ω_1	1.92131	3.04525	3.95672	1.52747	2.83932	3.80313	1.2869	2.65323	3.65182
	600	ω_1	2.10706	3.11376	4.00478	1.61597	2.8946	3.84575	1.3385	2.69817	3.6895
4	200	ω_1	1.89573	3.03462	3.94914	1.51452	2.8307	3.79639	1.27913	2.64619	3.64585
	400	ω_1	2.07345	3.10239	3.88876	1.60066	2.88546	3.83878	1.32976	2.69077	3.68334
	600	ω_1	2.31283	3.17493	4.04647	1.70338	2.94355	3.88262	1.38692	2.73768	3.72202
5	200	ω_1	1.95916	3.06041	3.96748	1.54629	2.85159	3.81268	1.29809	2.66323	3.66027
	400	ω_1	2.1572	3.12997	3.99026	1.63829	2.90761	3.85562	1.3511	2.70869	3.69821
	600	ω_1	2.43094	3.20449	4.06621	1.74895	2.96706	3.90005	1.4118	2.75656	3.73736

Table 5.4. The nonlinear correction term of the 1st mode C-C nanobeam with different h/l, T, K_p and K_w values when K_{nl}=10,100 and 200

			***K_L*=10**			***K_L*=100**			***K_L*=200**		
	ΔT		***K_P*=5**	***K_P*=50**	***K_P*=100**	***K_P*=5**	***K_P*=50**	***K_P*=100**	***K_P*=5**	***K_P*=50**	***K_P*=100**
h/l	(K)		***K_NL*=10**	***K_NL*=100**	***K_NL*=200**	***K_NL*=10**	***K_NL*=100**	***K_NL*=200**	***K_NL*=10**	***K_NL*=100**	***K_NL*=200**
			Temperature ΔT is low and room								
1	0	ω_1	0.656696	1.65038	2.58206	0.646678	1.62917	2.55376	0.636066	1.60652	2.52338
	100	ω_1	0.653559	1.6441	2.57383	0.643659	1.62111	2.54579	0.633179	1.60069	2.51567
	200	ω_1	0.650445	1.63789	2.56569	0.640679	1.61711	2.53788	0.630326	1.59492	2.50803
2	0	ω_1	1.03672	2.31075	3.34851	0.998374	2.25177	3.28459	0.960389	2.19123	3.21764
	100	ω_1	1.02437	2.2931	3.32998	0.987202	2.23531	3.26702	0.950302	2.17597	3.20104
	200	ω_1	1.01241	2.27582	3.31174	0.976358	2.2192	3.24971	0.940491	2.16099	3.18478
3	0	ω_1	1.21859	2.54434	3.57326	1.15736	2.46477	3.49395	1.09909	2.38455	3.41173
	100	ω_1	1.19856	2.52046	3.55039	1.13988	2.44287	3.47244	1.08381	2.36453	3.39158
	200	ω_1	1.17938	2.49721	3.52793	1.12308	2.42151	3.45131	1.06909	2.34498	3.37242
4	0	ω_1	1.30911	2.64329	3.661	1.23389	2.55351	3.57476	1.16383	2.46375	3.48573
	100	ω_1	1.28429	2.61633	3..63622	1.21265	2.52897	3.55155	1.14558	2.44148	3.46408
	200	ω_1	1.26069	2.59013	3.61192	1.19235	2.50508	3.52877	1.12808	2.41976	3.4428
5	0	ω_1	1.35844	2.69278	3.70322	1.27482	2.59753	3.61341	1.19789	2.5027	3.52091
	100	ω_1	1.33071	2.66418	3.67748	1.25136	2.57159	3.58935	1.17792	2.47923	3.49849
	200	ω_1	1.30444	2.63641	3.65225	1.229	2.54636	3.56574	1.15882	2.45638	3.47648
			Temperature ΔT is high								
1	200	ω_1	0.661087	1.65913	2.59348	0.650889	1.6376	2.56484	0.640095	1.61464	2.5341
	400	ω_1	0.665558	1.66801	2.60505	0.655175	1.64616	2.57605	0.644191	1.62287	2.54494
	600	ω_1	0.67011	1.67702	2.61677	0.659538	1.65485	2.58741	0.648358	1.63121	2.55592
2	200	ω_1	1.05436	2.33565	3.37448	1.0143	2.27493	3.3092	0.974731	2.21272	3.24093
	400	ω_1	1.07284	2.36132	3.40103	1.03092	2.29879	3.33434	0.989653	2.23481	3.26466
	600	ω_1	1.09219	2.3878	3.42818	1.04828	2.32335	3.36003	1.0052	2.25753	3.28889
3	200	ω_1	1.24765	2.57823	3.6054	1.1826	2.4958	3.52414	1.12104	2.41288	3.44
	400	ω_1	1.27863	2.61343	3.63839	1.20936	2.52795	3.5551	1.14421	2.44216	3.46895
	600	ω_1	1.31174	2.65	3.67225	1.20162	2.56129	3.58685	1.16808	2.47247	3.49861
4	200	ω_1	1.34542	2.68166	3.69587	1.26478	2.58838	3.60739	1.19022	2.49535	3.51616
	400	ω_1	1.38454	2.72164	3.7317	1.2978	2.62461	3.64089	1.21825	2.5281	3.54737
	600	ω_1	1.42686	2.76334	3.76855	1.33322	2.66232	3.6753	1.26078	2.5621	3.57938
5	200	ω_1	1.39919	2.73357	3.73946	1.30908	2.63444	3.64727	1.22687	2.53601	3.55242
	400	ω_1	1.44338	2.77614	3.77675	1.34589	2.67284	3.68205	1.25777	2.57061	3.58476
	600	ω_1	1.49149	2.82063	3.81512	1.38558	2.7129	3.7178	1.29082	2.60656	3.61795

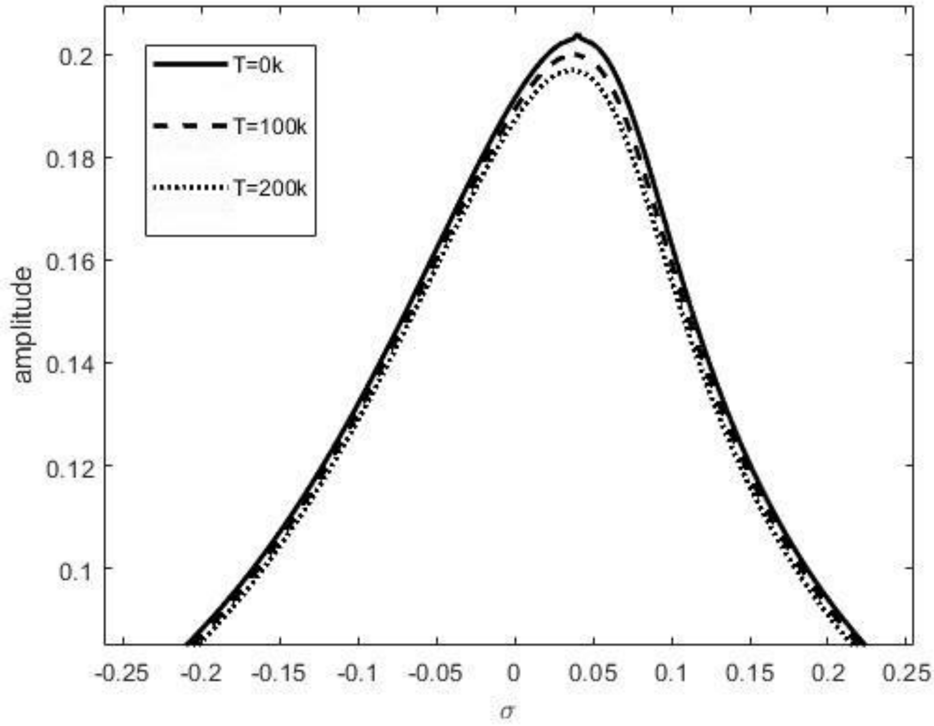

Figure 5.1. Frequency-response curves of S-S nanobeams for different Low Temperature values T=0k, T=100k and T=200k , the first mode and (h/l=1, $K_{nl} = 10,\ K_p = 5\ and\ K_w = 10$)

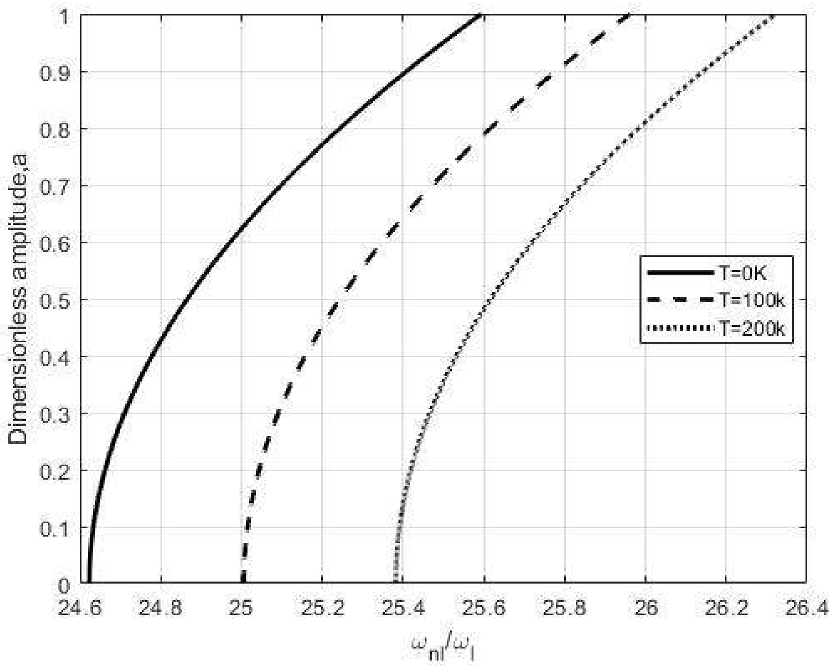

Figure 5.2. Amplitude and Nonlinear natural frequency change of S-S nanobeams for different Low Temperature values when h/l=1, $K_{nl} = 10,\ K_p = 5\ and\ K_w = 10$

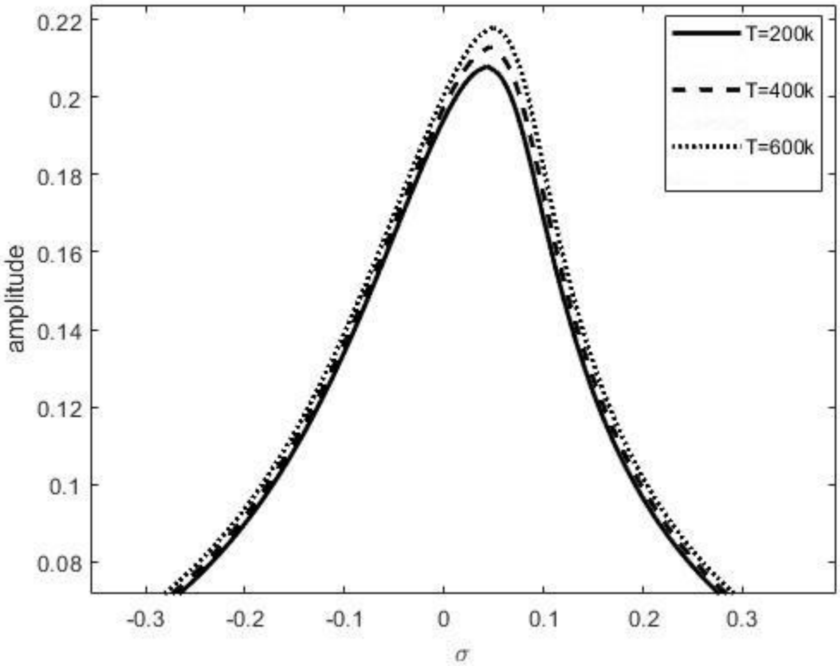

Figure 5.3. Frequency-response curves of SS nanobeams for different High Temperature values T=200k, T=400k and T=600k , the first mode and (h/l=1, $K_{nl} = 10,\ K_p = 5\ and\ K_w = 10$)

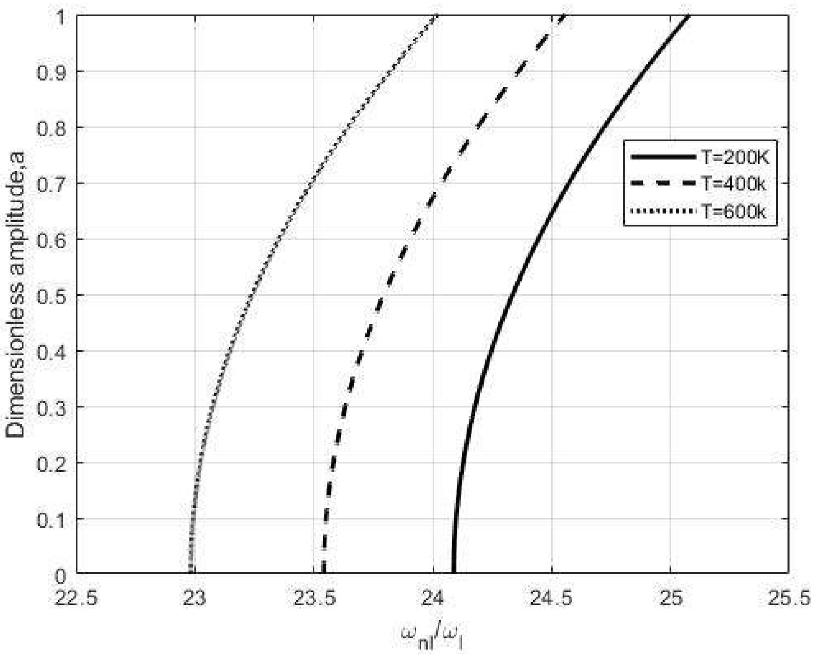

Figure 5.4. Amplitude and Nonlinear natural frequency change of S-S nanobeams for different High Temperature values when h/l=1, $K_{nl} = 10,\ K_p = 5\ and\ K_w = 10$

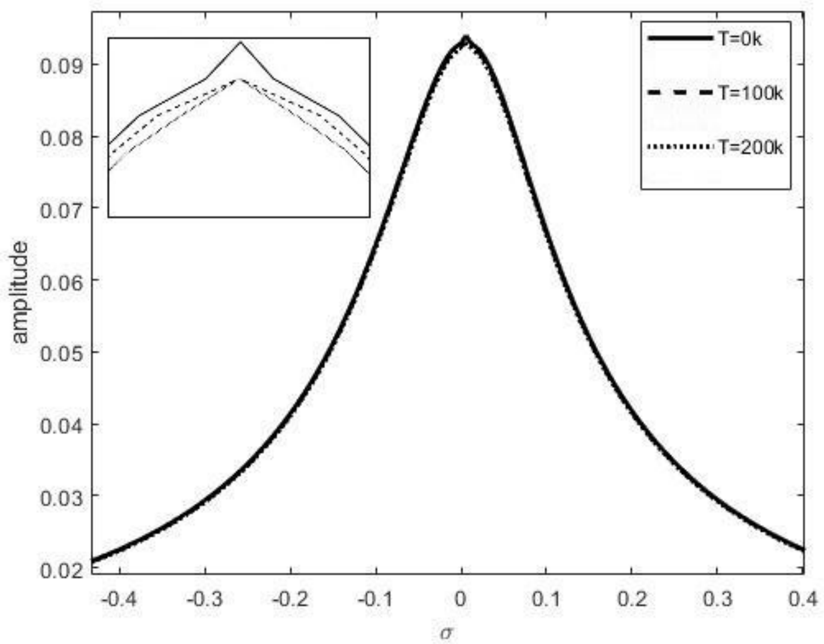

Figure 5.5. Frequency-response curves of CC nanobeams for different Low Temperature values T=0k, T=100k and T=200k, the first mode and (h/l=1, $K_{nl} = 10,\ K_p = 5\ and\ K_w = 10$)

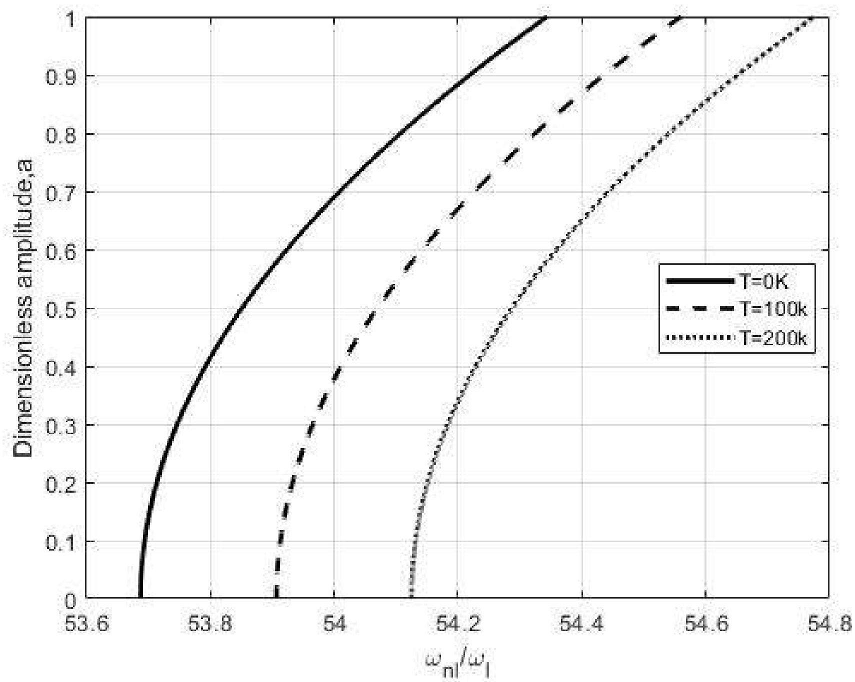

Figure 5.6. Amplitude and Nonlinear natural frequency change of C-C nanobeams for different Low Temperature values, the first mode and (h/l=1, $K_{nl} = 10,\ K_p = 5\ and\ K_w = 10$)

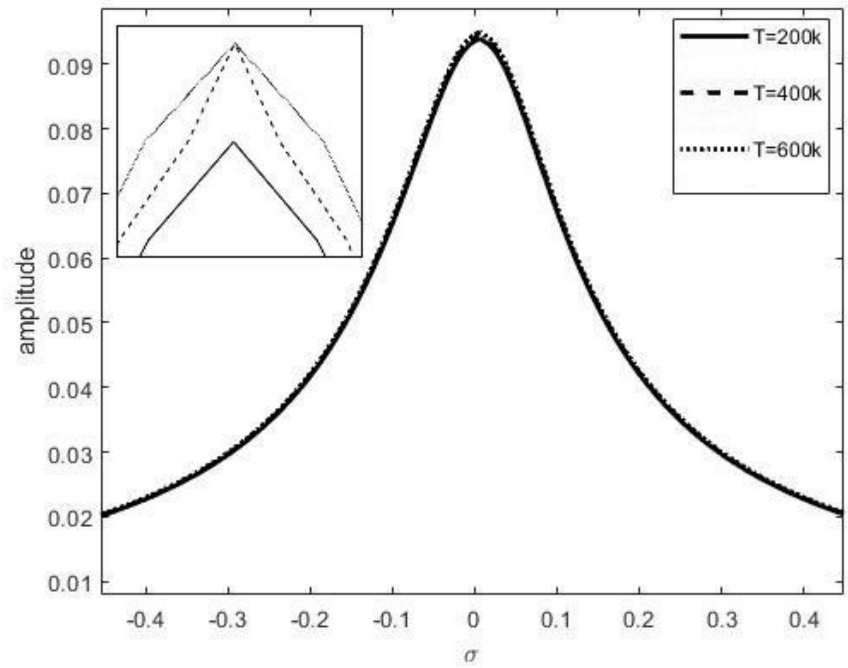

Figure 5.7. Frequency-response curves of C-C nanobeams for different High Temperature values T=200k, T=400k and T=600k, the first mode and (h/l=1, $K_{nl} = 10,\ K_p = 5\ and\ K_w = 10$)

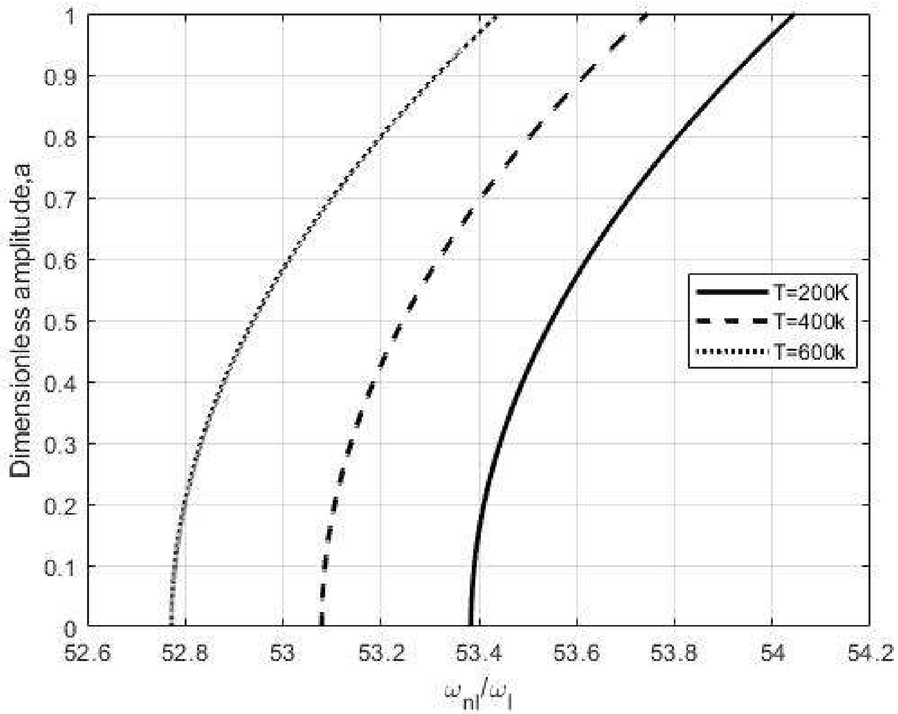

Figure 5.8 Amplitude and Nonlinear natural frequency change of C-C nanobeams for different High Temperature values, the first mode and (h/l=1, $K_{nl} = 10,\ K_p = 5\ and\ K_w = 10$)

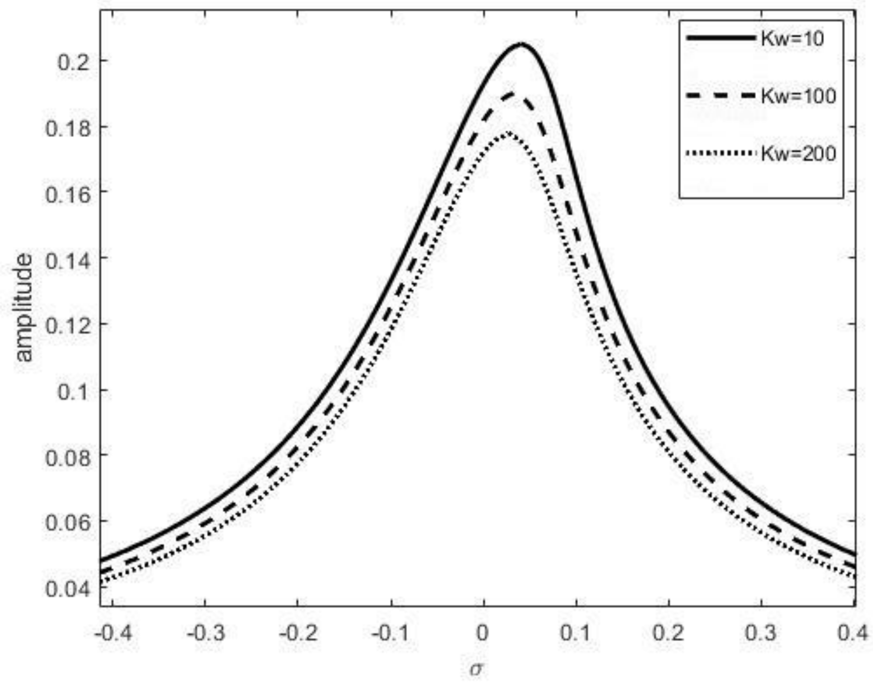

Figure 5.9. Frequency-response curves of S-S nanobeams for different Winkler parameters Kw=10, Kw=100 and Kw=200, the first mode and (h/l=1, $K_{nl} = 10,\ K_p = 5\ and\ T = 0K$)

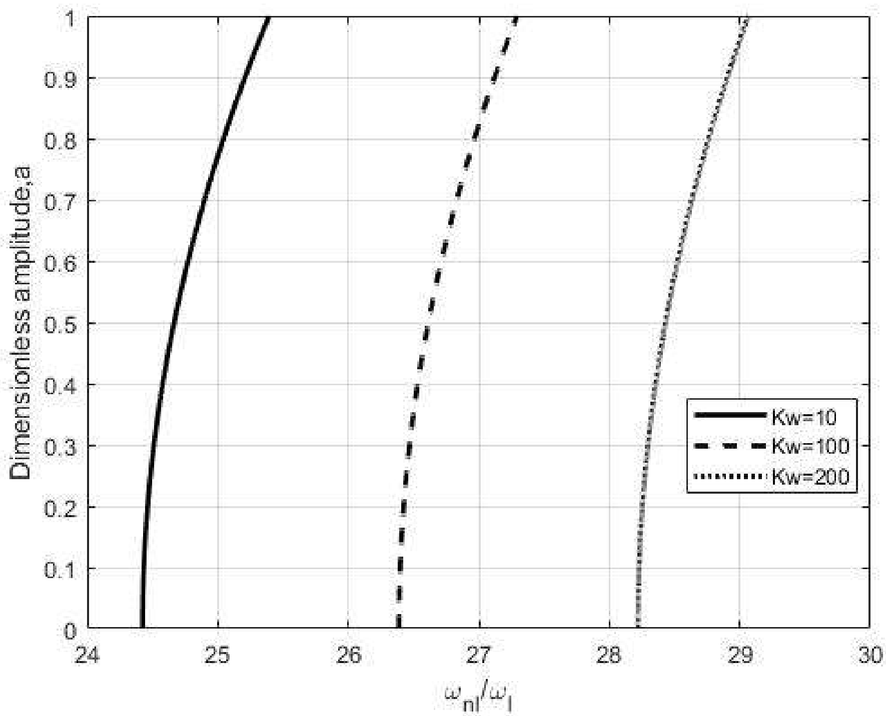

Figure 5.10. Amplitude and Nonlinear natural frequency change of S-S nanobeams for different Winkler parameter Kw=0, Kw=100 and Kw=200, the first mode and (h/l=1, $K_{nl} = 10,\ K_p = 5\ and\ T = 0K$)

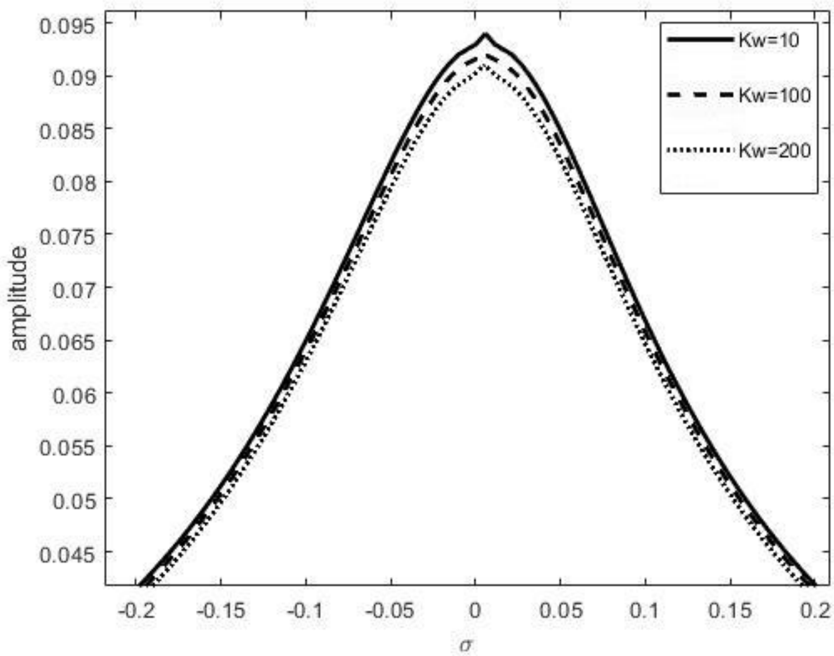

Figure 5.11. Frequency-response curves of CC nanobeams for different Winkler parameters Kw=10, Kw=100 and Kw=200, the first mode and (h/l=1, $K_{nl} = 10,\ K_p = 5\ and\ T = 0K$)

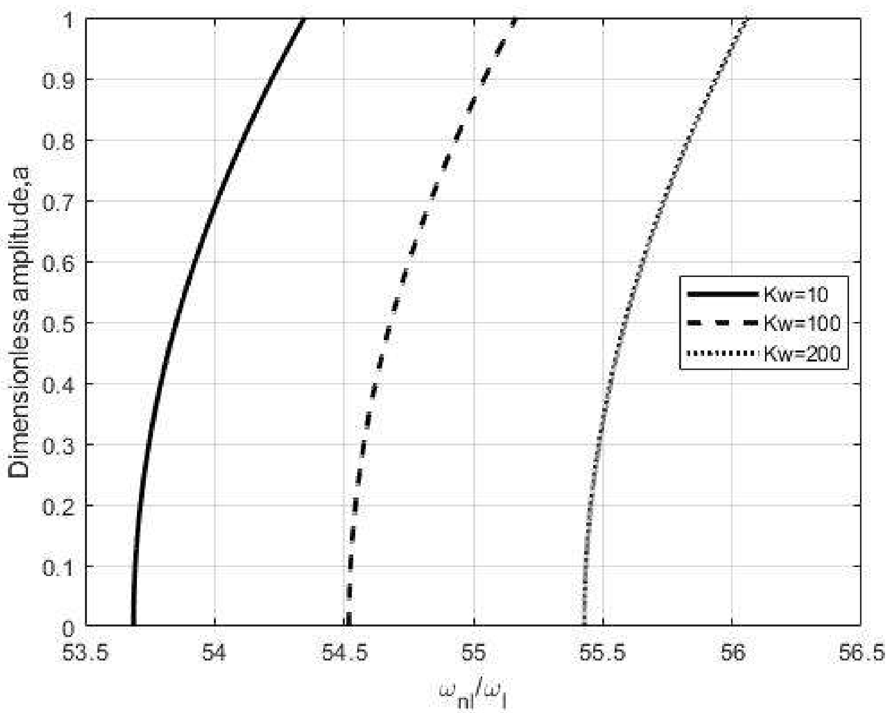

Figure 5.12. Amplitude and Nonlinear natural frequency change of CC nanobeams for different Winkler parameter Kw=0, Kw=100 and Kw=200, the first mode and (h/l=1, $K_{nl} = 10,\ K_p = 5\ and\ T = 0K$)

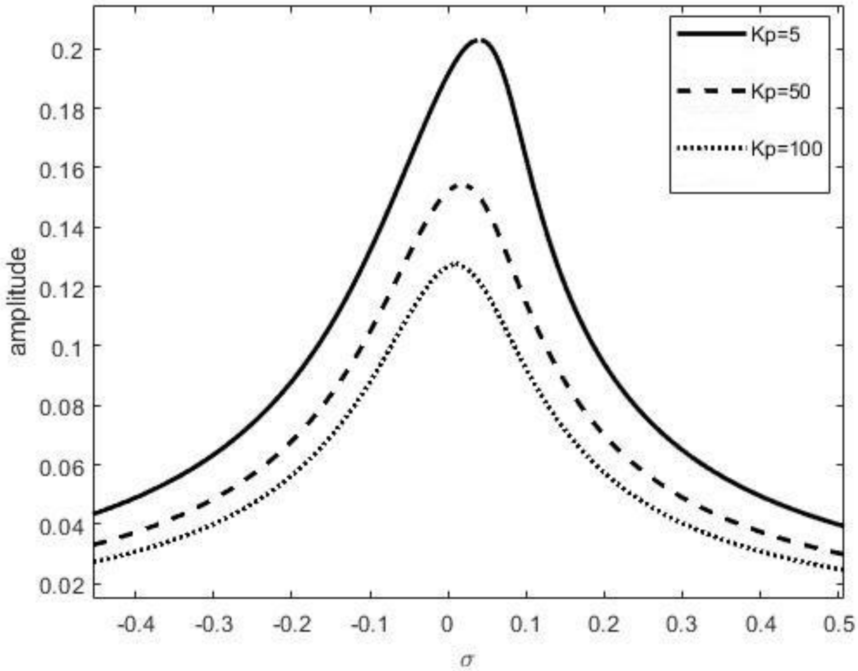

Figure 5.13. Frequency-response curves of SS nanobeams for different Pasternak parameters Kp=5, Kp=50 and Kp=100, the first mode and (h/l=1, $K_{nl} = 10,\ K_w = 10\ \ and\ \ T = 0K$

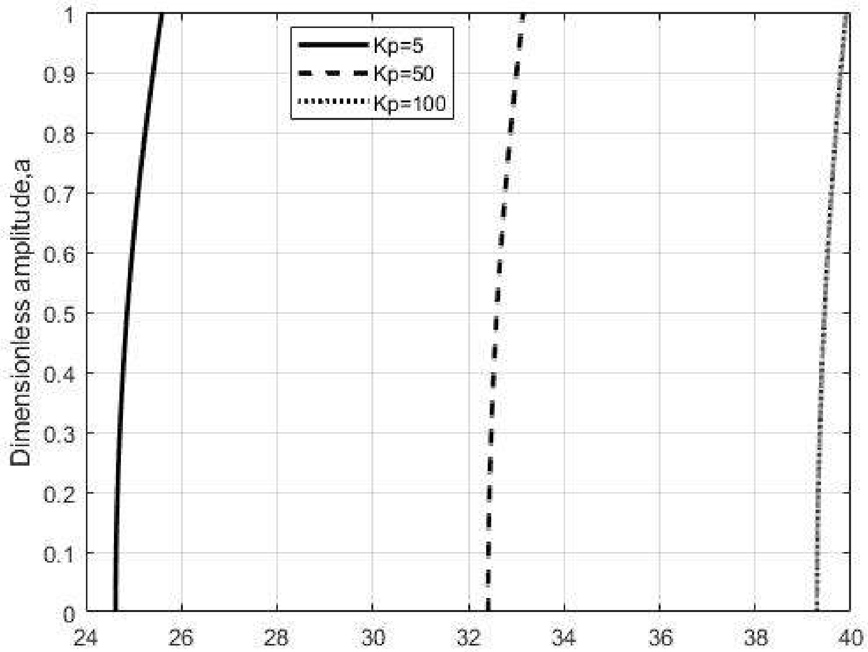

Figure 5.14. Amplitude and Nonlinear natural frequency change of SS nanobeams for different Pasternak parameters Kp=5, Kp=50 and Kp=100, the first mode and (h/l=1, $K_{nl} = 10,\ K_w = 10\ \ and\ \ T = 0K$)

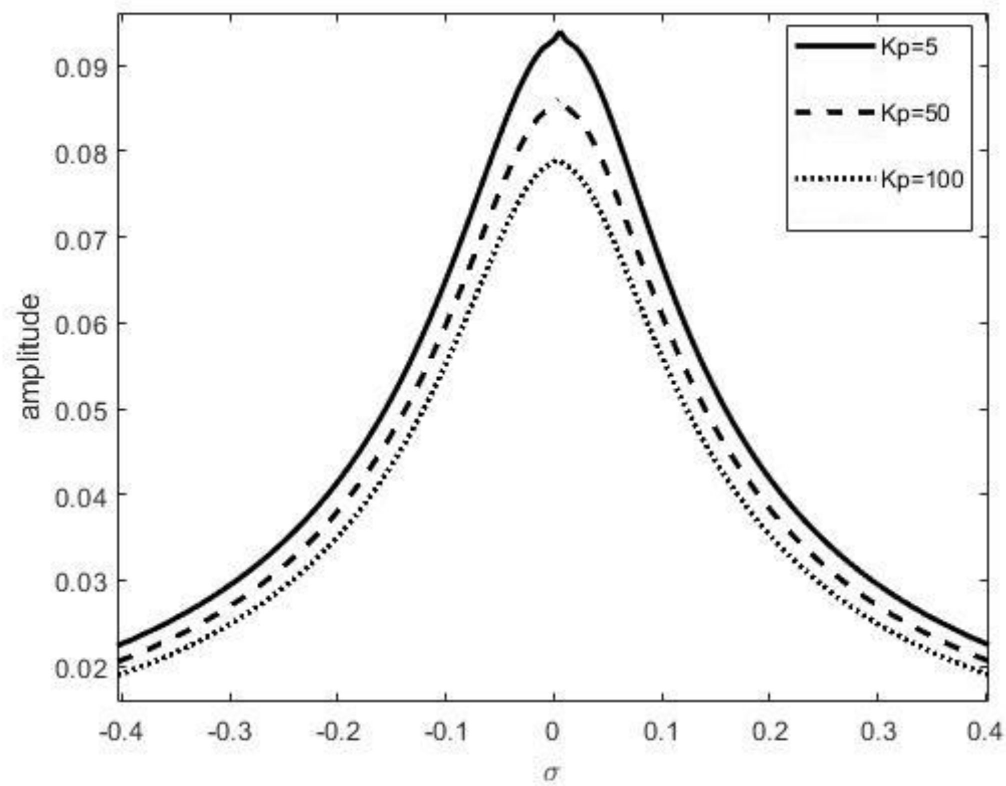

Figure 5.15. Frequency-response curves of CC nanobeams for different Pasternak parameters Kp=5, Kp=50 and Kp=100, the first mode and (h/l=1, $K_{nl} = 10,\ K_w = 10\ \ and\ \ T = 0K$)

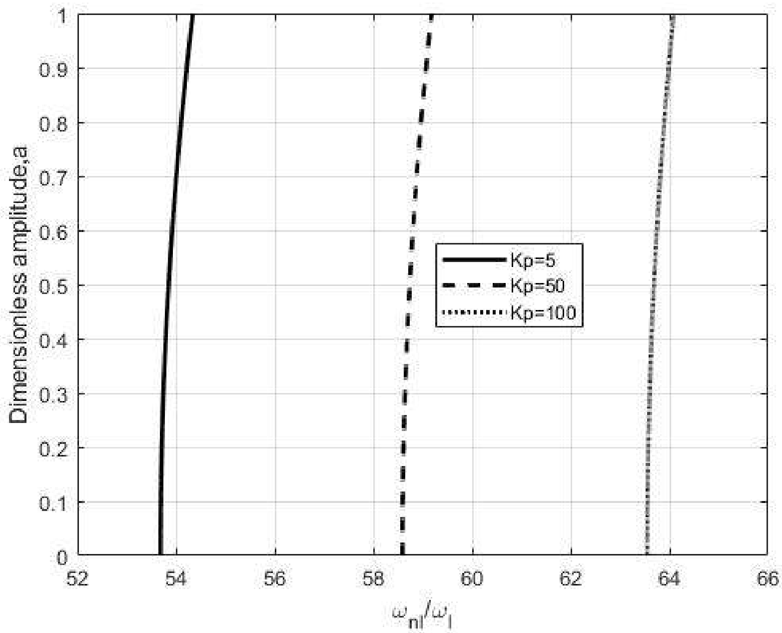

Figure 5.16. Amplitude and Nonlinear natural frequency change of C-C nanobeams for different Pasternak parameters Kp=5, Kp=50 and Kp=100, the first mode and (h/l=1, $K_{nl} = 10,\ K_w = 10\ \ and\ \ T = 0K$)

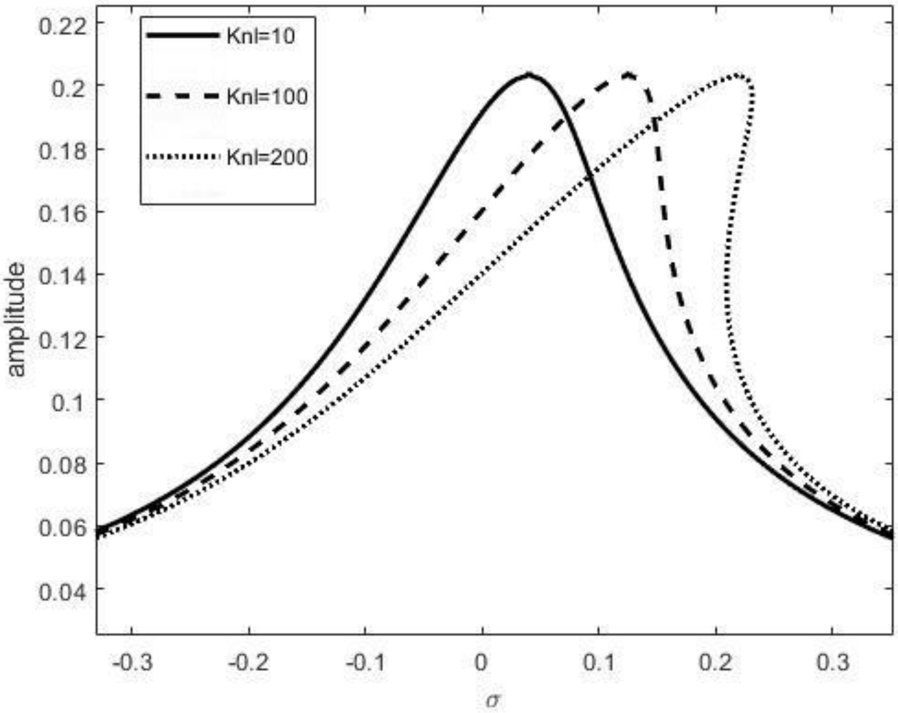

Figure 5.17. Frequency-response curves of SS nanobeams for different Nonlinear foundation parameters Knl=10, Knl=100 and Knl=200, the first mode and (h/l=1, $K_p = 5,\ K_w = 10\ and\ T = 0K$)

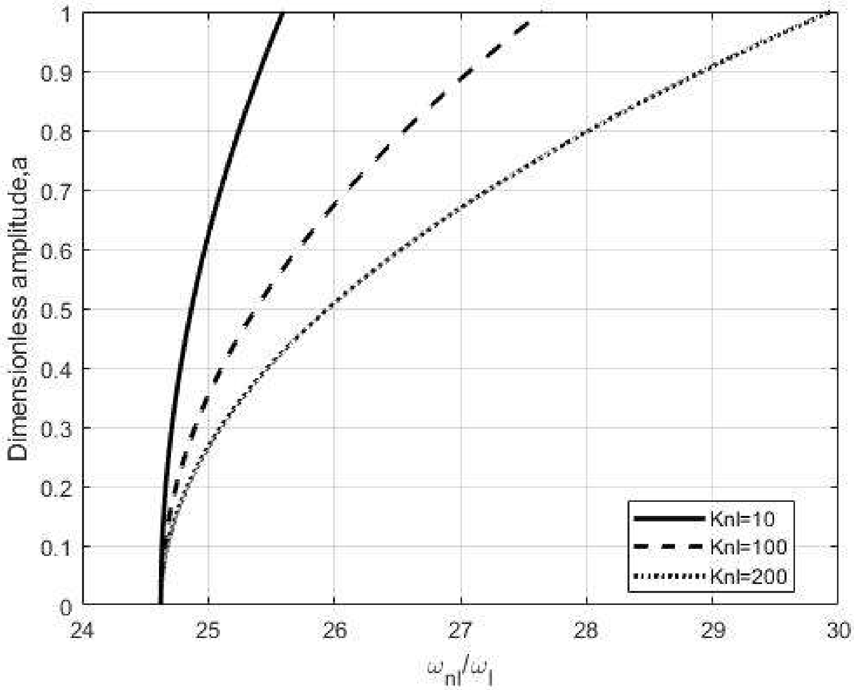

Figure 5.18. Amplitude and Nonlinear natural frequency change of S-S nanobeams for different nonlinear foundation parameters (Knl=10, Knl=100 and Kw=200), the first mode and h/l=1, $K_w = 10,\ K_p = 5\ and\ T = 0K$)

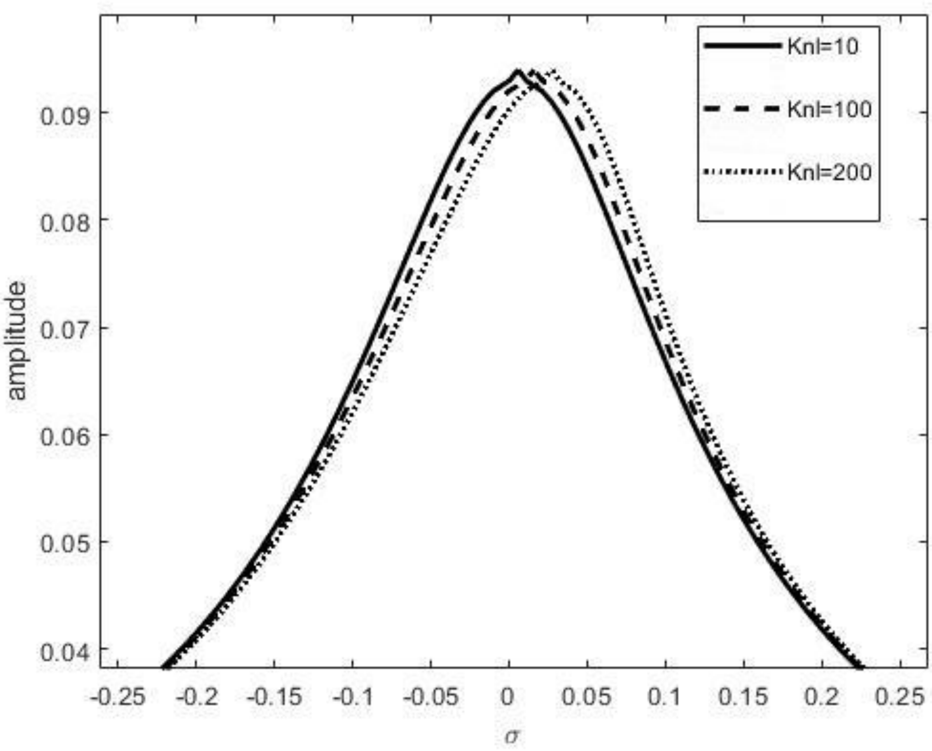

Figure 5.19. Frequency-response curves of C-C nanobeams for different Nonlinear foundation parameters Knl=10, Knl=100 and Knl=200, the first mode and (h/l=1, $K_p = 5,\ K_w = 10\ and\ T = 0K$)

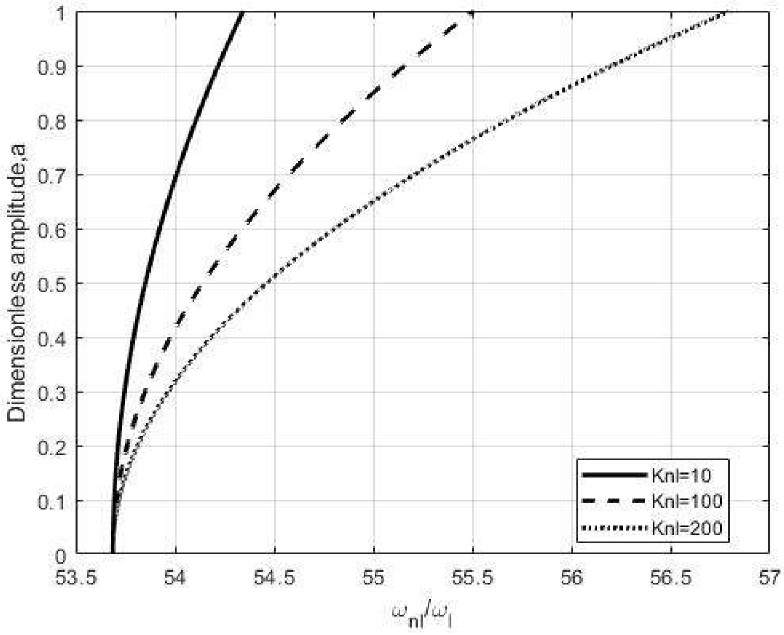

Figure 5.20. Amplitude and Nonlinear natural frequency change of CC nanobeams for different nonlinear foundation parameters Knl=10, Knl=100 and Kw=200, the first mode and (h/l=1, $K_w = 10,\ K_p = 5\ and\ T = 0K$)

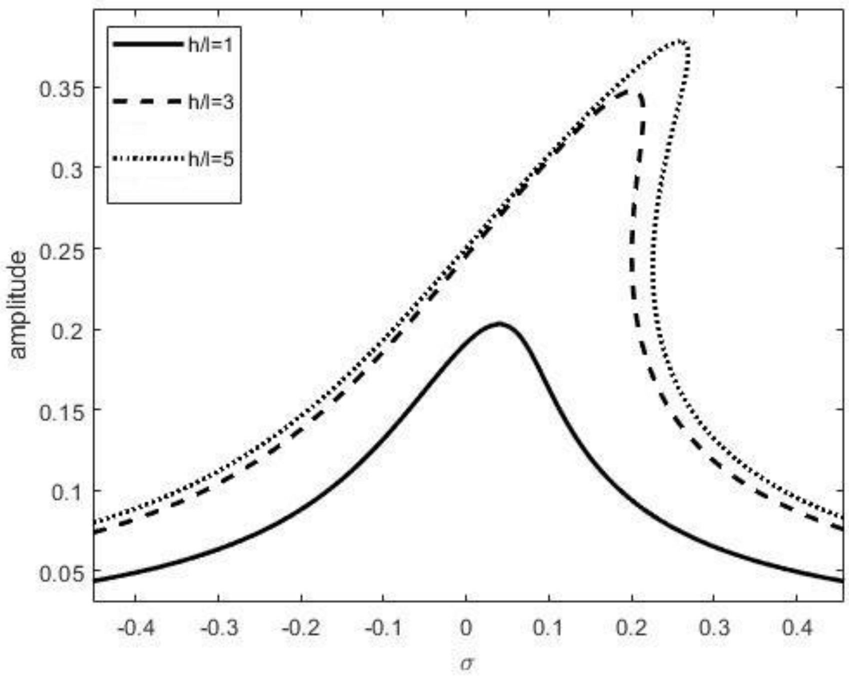

Figure 5.21. Frequency-response curves of SS nanobeams for different material length scale parameter h/l=1 and h/l=2 and h/l=3, the first mode and (K_{nl}= 10, $K_p = 5,\ K_w = 10\ and\ T = 0K$)

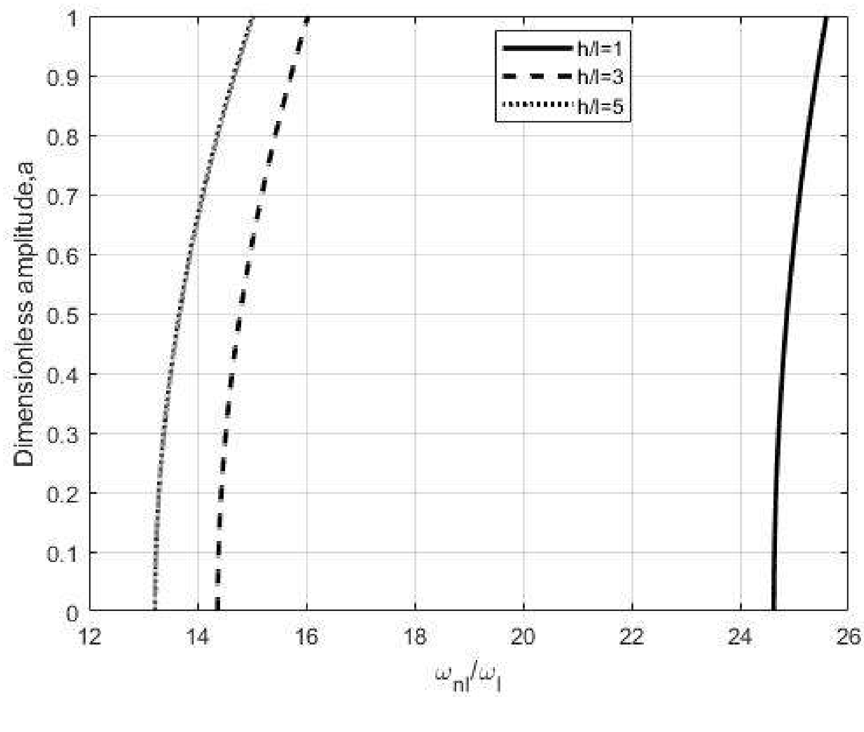

Figure 5.22. Amplitude and Nonlinear natural frequency change of S-S nanobeams for different material length scale parameter h/l=1, h/l=3 and h/l=5, the first mode and (K_{nl}= 10, $K_w = 10,\ K_p = 5\ and\ T = 0K$)

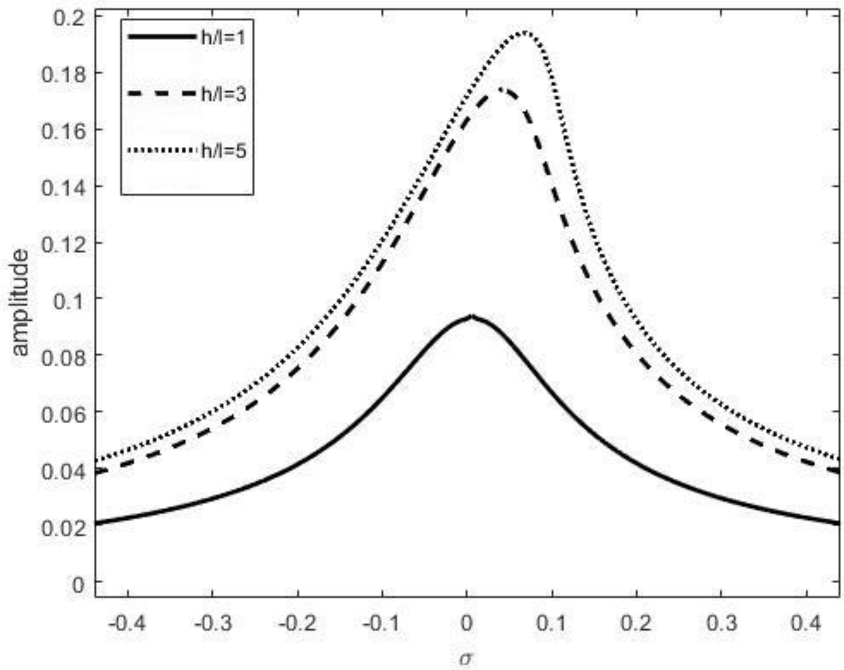

Figure 5.23. Frequency-response curves of C-C nanobeams for different material length scale parameter h/l=1 and h/l=3 and h/l=5, the first mode and K_{nl}= 10, $K_p = 5,\ K_w = 10\ \ and\ \ T = OK$

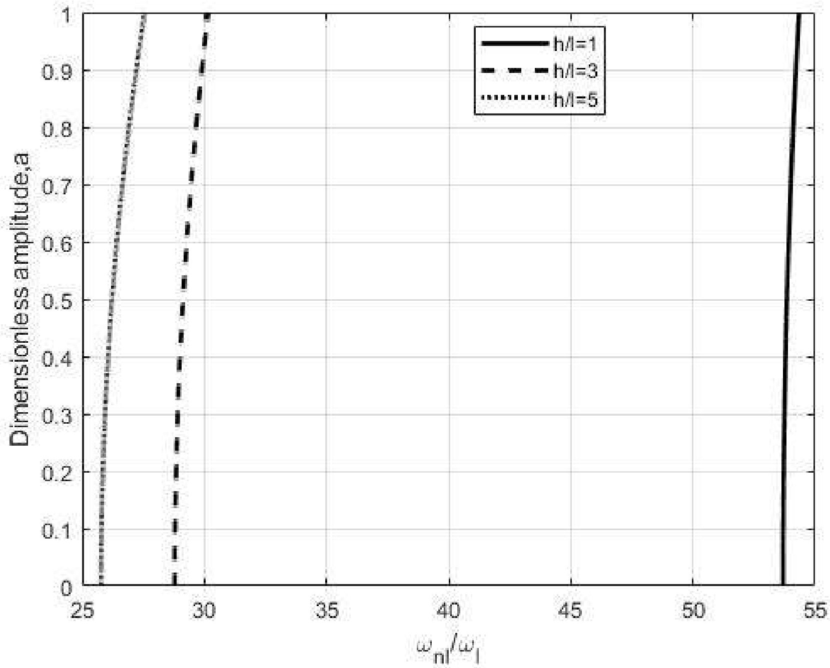

Figure 5.24. Amplitude and Nonlinear natural frequency change of C-C nanobeams for different material length scale parameter h/l=1, h/l=3 and h/l=5, the first mode and (K_{nl}= 10, $K_w = 10,\ K_p = 5\ \ and\ \ T = 0K$)

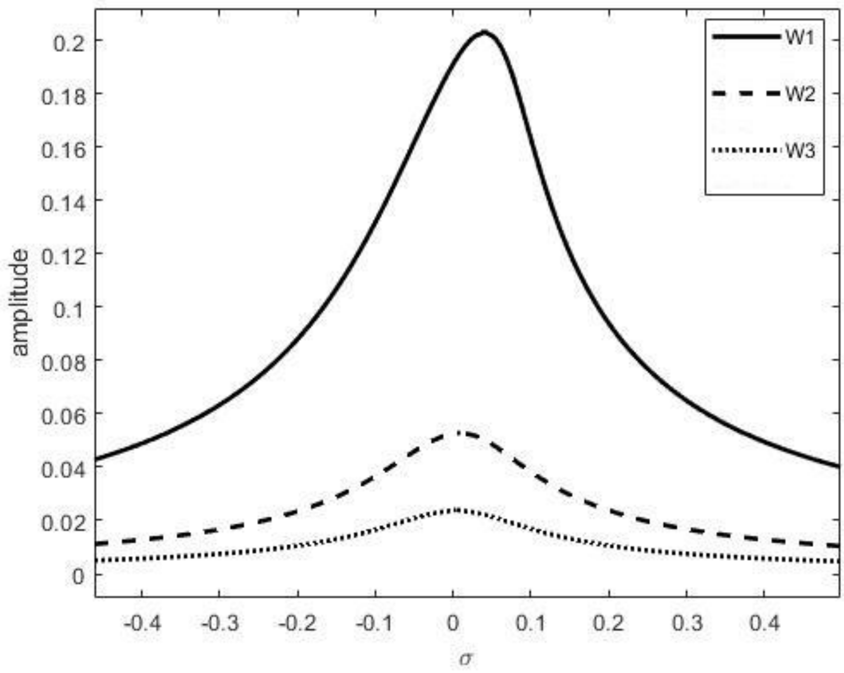

Figure 5.25. 1st mode (ω_1), 2nd mode (ω_2) and 3rd mode ($\omega_{3)}$ frequency-response curves of SS nanobeams for (h/l=1, K_{nl}= 10, $K_p = 5,\ K_w = 10\ \ and\ \ T = 0K$)

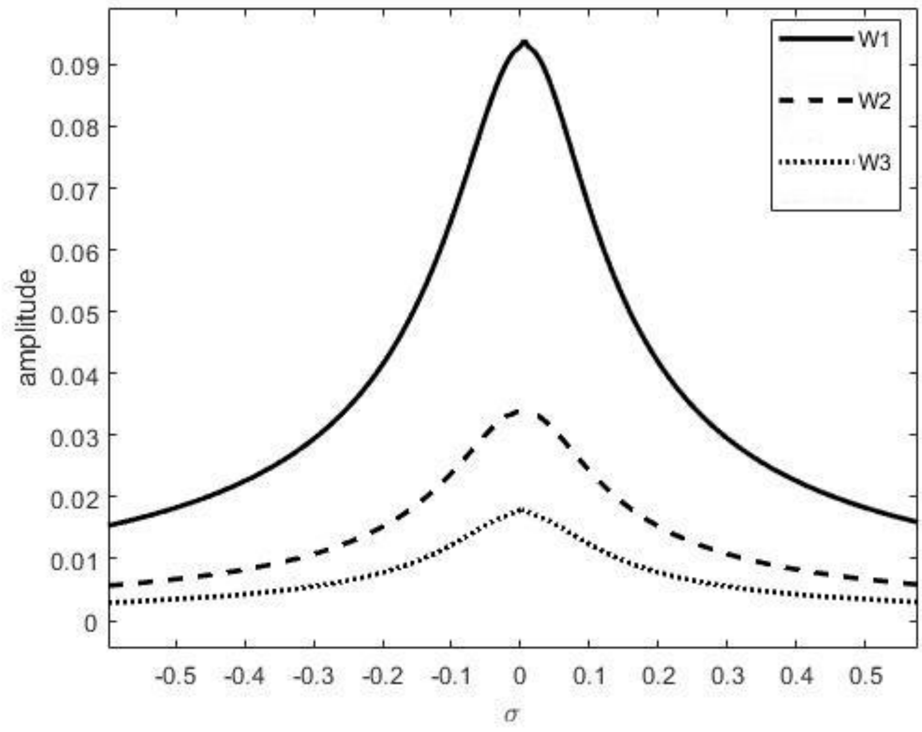

Figure 5.26. 1st mode (ω_1), 2nd mode (ω_2) and 3rd mode ($\omega_{3)}$ frequency-response curves of C-C nanobeams for (h/l=1, K_{nl}= 10, $K_p = 5,\ K_w = 10\ \ and\ \ T = 0K$)

5.2 Numerical Results using Nonlocal Elasticity Theory

Table 5.5: Effect of Temperature on C-C Boundary condition nanobeams on nonlinear foundation based on nonlocal theory

			K_L=10			K_L=100			K_L=200		
e_oa /L	ΔT (K)		K_P=5	K_P=50	K_P=100	K_P=5	K_P=50	K_P=100	K_P=5	K_P=50	K_P=100
			Temperature ΔT is low and room								
0	0	ω_1	23.9143	78.0638	91.3191	25.7273	78.6381	91.8105	27.6024	79.2714	92.3535
		ω_2	63.5888	139.862	156.427	64.2926	140.183	156.715	65.0657	140.539	157.034
		ω_3	122.972	220.285	238.913	123.337	220.489	239.101	123.742	220.716	239.31
	100	ω_1	24.3998	78.6177	91.7869	26.1792	79.188	92.2758	28.0241	79.8169	92.8161
		ω_2	64.2786	140.536	157.027	64.9749	140.855	157.313	65.7399	141.21	157.631
		ω_3	123.741	221.03	239.599	124.104	221.234	239.786	124.506	221.46	239.995
	200	ω_1	24.8748	79.1674	92.2521	26.6225	79.7338	92.7386	28.4386	80.3585	93.2762
		ω_2	64.9604	141.206	157.624	65.6495	141.524	157.91	66.4067	141.877	158.226
		ω_3	124.506	221.773	240.282	124.866	221.976	240.469	125.266	222.201	240.677
0.1	0	ω_1	23.0822	74.1135	91.4914	24.9557	74.7182	91.9819	26.8847	75.3844	92.5239
		ω_2	53.8346	116.255	140.267	54.6641	116.641	140.588	57.5318	117.069	140.943
		ω_3	89.2907	158.885	189.092	89.7933	159.168	189.33	90.3484	159.482	189.594
	100	ω_1	23.7143	74.8558	92.093	25.5415	75.4545	92.5804	27.4293	76.1143	93.1189
		ω_2	54.8548	117.267	141.108	55.6691	117.651	141.427	56.5601	118.075	141.78
		ω_3	90.6047	160.15	190.157	91.1	160.431	190.393	91.6472	160.742	190.656
	200	ω_1	24.3293	75.5907	92.6908	26.1135	76.1837	93.175	27.9628	76.8372	93.7101
		ω_2	55.8561	118.272	141.944	56.6561	118.651	142.26	57.5318	119.072	142.611
		ω_3	91.9	161.405	191.215	92.3884	161.684	191.45	92.928	161.993	191.711
0.2	0	ω_1	21.2855	69.3394	90.989	23.304	69.9854	91.4822	25.3589	70.6962	92.0272
		ω_2	41.035	99.5596	129.776	42.1173	100.011	130.123	43.2882	129.099	130.506
		ω_3	60.6274	128.361	166.777	61.3651	128.711	167.047	62.1746	129.099	167.346
	100	ω_1	22.2428	70.294	91.7185	24.1815	70.9313	92.2078	26.1676	71.6327	92.7485
		ω_2	42.6283	100.887	130.798	43.6712	101.332	131.141	44.8015	101.824	131.522
		ω_3	62.7832	130.045	168.077	63.4959	130.391	168.345	64.2786	130.774	168.642
	200	ω_1	23.1603	71.2358	92.4423	25.025	71.8647	92.9278	26.9518	72.5571	93.4643
		ω_2	44.1642	102.197	131.811	45.1717	102.637	132.152	46.2653	103.123	132.53
		ω_3	64.8675	131.709	169.368	65.5576	132.05	169.633	66.3159	132.428	169.928
0.3	0	ω_1	19.5287	66.8639	90.5675	21.712	67.5336	91.063	23.9042	68.2699	91.6104
		ω_2	33.3506	93.7733	126.763	34.6737	94.252	127.118	36.0869	94.781	127.51
		ω_3	47.3877	118.747	160.387	61.0746	119.126	160.667	61.8879	119.545	160.978
	100	ω_1	20.8208	67.927	91.3552	22.8802	68.5863	91.8464	24.9704	69.3115	92.3892
		ω_2	35.4339	95.2513	127.86	36.6819	95.7226	128.212	38.0205	96.2435	128.601
		ω_3	50.249	120.612	161.773	64.6253	120.984	162.05	65.3944	121.397	162.359
	200	ω_1	22.0362	68.9737	92.1361	23.9916	69.6231	92.6071	25.9922	70.3376	93.1615
		ω_2	37.4013	96.7067	128.948	38.5857	97.1709	129.274	39.8605	97.6841	129.683
		ω_3	52.9559	122.448	163.146	67.9909	122.815	163.422	68.7223	123.222	163.727
0.4	0	ω_1	18.1866	65.6397	90.334	20.5123	66.3217	90.8308	22.82	67.0713	91.3796
		ω_2	29.0183	91.529	125.886	30.5297	92.0193	126.243	32.1257	92.5611	126.639
		ω_3	40.6783	114.841	157.911	41.7699	115.232	158.196	42.9502	115.665	158.511
	100	ω_1	19.7478	66.7568	91.149	21.9083	67.4275	91.6414	24.0826	68.165	92.1854
		ω_2	31.4637	93.0827	127.021	32.8628	93.5649	127.374	34.3506	94.0978	127.766
		ω_3	44.0632	116.788	159.333	45.0729	117.173	159.615	46.1689	117.599	159.928
	200	ω_1	21.1942	67.8555	91.9568	23.2205	68.5155	92.4448	25.2823	69.2414	92.9841
		ω_2	33.7323	94.611	128.145	35.041	95.0854	128.495	36.4399	95.6098	128.884
		ω_3	47.206	118.704	160.742	48.1498	119.082	161.022	49.1773	119.502	161.332
0.5	0	ω_1	17.2362	64.9805	90.203	19.6745	65.6694	90.7005	22.07	66.4264	91.2501
		ω_2	26.4531	90.5076	125.623	28.1028	91.0034	125.981	29.829	91.5512	126.377
		ω_3	36.892	112.918	156.721	38.0923	113.315	157.008	39.383	113.756	157.326
	100	ω_1	18.9983	66.1269	91.0323	21.2353	66.804	91.5253	23.472	67.5483	92.07
		ω_2	29.1559	92.1035	126.778	30.6605	92.5908	127.132	32.2501	93.1293	127.525
		ω_3	40.6504	114.908	158.161	41.7428	115.299	158.446	42.9239	115.732	158.761
	200	ω_1	20.6103	67.2538	91.8542	22.6889	67.9196	92.3428	24.7949	68.6518	92.8827
		ω_2	31.6286	93.6723	127.922	33.0208	94.1515	128.273	34.5018	94.681	128.663

		ω_3	44.0897	116.865	159.589	45.0988	117.25	159.87	46.1941	117.675	160.83
						Temperature ΔT is high					
		ω_1	23.2284	77.2951	90.6718	25.091	77.8751	91.1665	27.0103	78.5145	91.7133
	200	ω_2	62.6272	138.93	155.599	63.3416	139.253	155.888	64.1261	139.612	156.208
		ω_3	121.906	219.257	237.967	122.274	219.462	238.156	122.683	219.689	238.366
		ω_1	22.5193	76.518	90.019	24.434	77.1039	90.5175	26.403	77.7496	90.9111
0	400	ω_2	61.6493	137.991	154.766	62.375	138.317	155.056	63.1715	138.678	155.176
		ω_3	120.83	218.223	237.017	121.202	218.429	237.207	121.614	218.628	237.417
		ω_1	21.7847	75.7323	89.3613	23.7602	76.3242	89.8635	25.7794	76.9765	90.4182
	600	ω_2	60.6546	137.045	153.928	61.3921	137.373	154.22	62.2012	137.737	154.544
		ω_3	119.745	217.184	236.295	120.12	217.391	236.485	120.535	217.621	236.696
		ω_1	22.1824	73.0805	90.6575	24.1259	73.6937	91.1525	26.1163	74.3691	91.6994
	200	ω_2	52.399	114.847	139.203	53.2509	115.238	139.426	54.1817	115.672	139.784
		ω_3	87.4518	157.129	187.619	87.9649	157.415	187.859	88.5315	157.732	188.125
		ω_1	21.2429	72.0326	89.8159	23.265	72.6626	90.3219	25.3231	73.3396	90.8738
0.1	400	ω_2	50.9225	113.423	137.929	51.7987	113.83	138.264	52.7551	114.257	138.625
		ω_3	85.5736	155.353	186.134	86.0979	155.642	186.376	86.6766	155.963	186.644
		ω_1	20.2578	70.9691	88.9663	22.3692	71.6004	89.4707	24.5027	72.2953	90.0278
	600	ω_2	49.4013	111.98	136.745	50.3039	112.381	137.074	51.2883	112.825	137.438
		ω_3	83.6534	153.994	184.637	84.1897	154.286	184.881	84.7815	154.61	185.151
		ω_1	19.8938	68.005	89.9763	22.04	68.6636	90.475	24.2025	69.3879	91.026
	200	ω_2	38.7372	97.7047	128.359	39.8819	98.1642	128.709	41.1165	98.6723	129.097
		ω_3	57.5314	126.007	164.973	58.3083	126.364	165.245	59.1596	126.759	165.547
		ω_1	18.3962	66.6439	88.952	20.6983	67.3261	89.4565	22.9874	68.0545	90.0137
0.2	400	ω_2	36.2941	95.814	126.926	37.5135	96.2969	127.28	38.8235	96.8005	127.672
		ω_3	54.2593	123.609	163.148	55.0824	123.972	163.424	55.9827	124.375	163.729
		ω_1	16.7641	65.2544	87.9158	19.2623	65.9404	88.4262	21.7034	66.6944	88.9898
	600	ω_2	33.6741	93.8853	125.476	34.9849	94.3634	125.834	36.386	94.8917	126.231
		ω_3	50.777	121.163	161.303	67.574	121.534	161.582	52.6146	121.944	161.891
		ω_1	17.6005	65.3739	89.4731	19.9944	66.0587	89.9746	22.3557	66.8113	90.5286
	200	ω_2	30.2527	91.7022	125.239	31.7053	92.1916	125.597	33.245	92.7324	125.995
		ω_3	43.1446	116.134	158.462	55.8248	116.521	158.746	56.7134	116.95	159.061
		ω_1	15.4316	63.8492	88.3652	17.6285	64.2256	88.873	20.6914	65.3201	89.4338
0.3	400	ω_2	26.7991	89.5832	123.696	28.4287	89.6307	124.059	30.1362	90.6375	124.461
		ω_3	38.4331	113.461	156.154	50.0271	113.857	156.801	51.0167	114.296	157.12
		ω_1	12.9025	62.2871	87.2432	16.0148	63.0054	87.7574	18.8805	63.7941	88.3254
	600	ω_2	22.8288	87.4129	122.133	24.7215	87.9262	122.501	26.6675	88.493	122.908
		ω_3	33.034	110.724	154.541	43.4628	111.13	154.832	44.5983	111.579	155.155
		ω_1	15.7901	64.0718	89.2015	18.4208	64.7703	89.7043	20.9601	65.5378	90.26
	200	ω_2	25.2723	89.3485	124.31	26.9943	89.8507	124.671	28.787	90.4055	125.072
		ω_3	35.501	112.108	155.935	55.2115	112.508	156.223	56.1098	112.952	156.543
		ω_1	12.9574	62.4646	88.054	16.0591	63.1809	88.5635	18.9181	63.9674	89.1263
0.4	400	ω_2	20.8644	87.1134	122.713	22.9199	87.6284	123.079	25.0065	88.1972	123.485
		ω_3	29.4265	109.306	153.933	48.1816	109.717	154.225	54.5756	110.172	154.549
		ω_1	9.29818	60.815	86.8915	13.2837	61.5505	87.4079	16.627	62.3575	87.978
	600	ω_2	15.23	84.8194	121.096	17.9431	85.3483	121.467	20.5415	85.9322	121.878
		ω_3	21.7145	106.431	151.905	40.4091	106.853	152.201	41.628	107.32	152.529
		ω_1	14.467	63.3704	89.0501	17.3001	64.0766	89.554	19.9823	64.9125	90.1106
	200	ω_2	22.2059	88.266	124.018	24.1475	88.7744	124.38	26.1362	89.4208	124.782
		ω_3	30.9886	110.122	154.719	48.0136	110.53	155.009	49.0439	110.981	155.331
		ω_1	11.0226	61.7182	87.882	14.543	62.4431	88.3926	17.6493	63.2387	88.9565
0.5	400	ω_2	16.9244	85.9661	122.392	19.402	86.4879	122.759	27.3782	87.0641	123.165
		ω_3	23.6551	107.253	152.69	42.9435	107.671	152.984	44.0924	108.135	153.311
		ω_1	5.80502	60.0206	86.6983	11.122	60.7657	87.2158	14.9565	61.5831	87.7872
	600	ω_2	12.6032	83.6028	120.743	13.0296	84.1394	121.116	18.6773	84.7315	121.528
		ω_3	15.7969	104.305	150.634	36.912	104.735	150.932	38.2426	105.212	151.263

Table 5.6. Effect of Temperature on S-S Boundary condition nanobeams on nonlinear foundation based on nonlocal theory

			K_L=10			**K_L=100**			**K_L=200**	
e_oa	ΔT	**K_P=5**	**K_P=50**	**K_P=100**	**K_P=5**	**K_P=50**	**K_P=100**	**K_P=5**	**K_P=50**	**K_P=100**
/L	(K)	**K_{NL}=10**	**K_{NL}=100**	**K_{NL}=200**	**K_{NL}=10**	**K_{NL}=100**	**K_{NL}=200**	**K_{NL}=10**	**K_{NL}=100**	**K_{NL}=200**

Temperature ΔT is low and room

0	0	ω_1	12.5203	24.513	33.0819	15.7085	26.2848	34.4147	18.6214	28.1228	35.8381
		ω_2	42.0231	59.5186	74.2724	43.0806	60.2699	74.8758	44.226	61.0939	75.5406
		ω_3	91.347	111.092	129.548	91.8383	111.496	129.895	92.3811	111.944	130.28
	100	ω_1	13.2554	24.8966	33.3634	16.3005	26.6428	34.6889	19.1235	28.4577	36.1015
		ω_2	42.9155	60.152	74.7809	43.9515	60.8955	75.3803	45.0748	61.7111	76.0407
		ω_3	92.2758	111.857	130.205	92.7621	112.259	130.55	93.2996	112.703	130.933
	200	ω_1	13.9519	25.2743	33.6492	16.8718	26.9941	34.961	19.6127	28.7887	36.363
		ω_2	43.7897	60.7788	75.286	44.8055	61.5147	75.8814	45.9079	62.3223	76.5375
		ω_3	93.1953	112.617	130.858	93.6769	113.016	131.202	94.2091	113.457	131.582
0.1	0	ω_1	12.1618	24.3339	32.9487	15.4275	26.1178	34.2873	18.385	27.9667	35.7158
		ω_2	36.3978	55.6896	71.2408	37.6139	56.4919	71.8697	38.9205	57.3701	72.5621
		ω_3	68.0635	92.8969	114.329	68.7215	93.3801	114.722	69.4453	93.914	115.157
	100	ω_1	12.9212	24.7202	33.2351	16.0299	26.4781	34.5625	18.8933	28.3035	35.9801
		ω_2	37.4246	56.366	71.7708	38.6083	57.1588	72.3951	39.8823	58.027	73.0825
		ω_3	69.3051	93.8103	115.073	69.9514	94.2888	115.463	70.6625	94.8176	115.895
	200	ω_1	13.6347	25.1006	33.5189	16.6104	26.8335	34.8356	19.3883	28.6363	36.2425
		ω_2	38.4239	57.0344	72.2969	39.5778	57.8181	72.9167	40.8216	58.6765	73.5992
		ω_3	70.5247	94.715	115.811	71.1599	95.1889	116.199	71.8592	95.7127	116.629
0.2	0	ω_1	11.366	23.9441	32.6619	14.8049	25.755	34.0117	17.8658	27.6282	35.4541
		ω_2	28.49	50.8745	67.5436	30.028	51.7514	68.2065	31.6494	52.7087	68.9357
		ω_3	46.7661	78.64	103.08	47.7186	79.2102	103.516	48.7551	79.8389	103.998
	100	ω_1	12.1711	24.3366	32.9507	15.4314	26.1203	34.2892	18.3885	27.9691	35.7176
		ω_2	29.7906	51.614	68.1023	31.2647	52.4787	68.7599	32.825	53.4229	69.4833
		ω_3	48.5552	79.717	103.904	49.4733	80.2795	104.337	50.4739	80.8999	104.815
	200	ω_1	12.9262	24.7228	33.237	16.0277	26.4805	34.5644	18.8915	28.3058	35.9819
		ω_2	31.0367	52.3432	68.6566	32.4421	53.1959	69.3089	33.9483	54.1277	70.0266
		ω_3	50.2808	80.7796	104.722	51.1506	81.3348	105.151	52.1189	81.9472	105.625
0.3	0	ω_1	10.5325	23.5599	32.3813	14.1751	25.3982	33.7424	17.3475	27.2959	35.193
		ω_2	23.4457	48.231	65.5755	25.2923	49.1551	66.2582	27.1974	50.162	67.0086
		ω_3	36.4878	72.9969	98.8427	37.701	73.6108	99.2969	39.0046	74.287	99.7992
	100	ω_1	11.3967	23.9586	32.6726	14.8285	25.7685	34.022	17.8853	27.6408	35.4612
		ω_2	25.01	49.0105	66.1509	26.7488	49.9202	66.8277	28.5569	50.912	67.5718
		ω_3	38.7545	74.1559	99.7017	39.8987	74.7603	10.152	41.1328	75.4261	100.65
	200	ω_1	12.1997	24.3509	32.9613	15.4543	26.1336	34.2994	18.4074	27.9815	35.7274
		ω_2	26.482	49.7778	66.7214	28.13	50.6737	67.3925	29.8546	51.651	68.1304
		ω_3	40.8957	75.297	100.553	41.9816	75.8923	101.000	43.1562	76.5483	101.494
0.4	0	ω_1	9.85475	23.2647	32.1672	13.679	25.1247	33.537	16.9445	27.0416	34.9961
		ω_2	20.5039	46.8715	64.5822	22.5922	47.8219	65.2753	24.7064	48.8563	66.0368
		ω_3	31.1898	70.4982	97.0119	32.6007	71.1336	97.4747	34.0999	71.8331	97.9863
	100	ω_1	10.7734	23.6685	32.4604	14.355	25.499	33.8183	17.4947	27.3897	35.2658
		ω_2	22.2757	47.6732	65.1664	24.2117	48.608	65.8533	26.1956	49.626	66.6082
		ω_3	33.8135	71.6976	97.887	35.1191	72.3225	98.3456	36.5151	73.0105	98.8527
	200	ω_1	11.6196	24.0655	32.7555	15.0005	25.8679	34.0973	18.0282	27.7335	35.5335
		ω_2	23.9166	48.4617	65.7544	25.7295	49.3815	66.4263	27.6045	50.3839	67.1748
		ω_3	36.2477	72.8772	98.7678	37.4686	73.4921	99.2089	38.7801	74.1693	99.7116
0.5	0	ω_1	9.35098	23.0559	32.0165	13.3207	24.9314	33.3965	16.6566	26.8621	34.8576
		ω_2	18.7291	46.1227	64.0408	20.9947	47.0883	64.7397	23.3546	48.1384	65.5075
		ω_3	28.1803	69.2193	96.0866	29.7343	69.8664	96.5538	31.3708	70.5784	97.0703
	100	ω_1	10.3146	23.4632	32.311	14.0139	25.3085	33.675	17.216	27.2125	35.1284
		ω_2	20.6537	46.9372	64.6299	22.7283	47.8864	65.3225	24.831	48.9194	66.0835
		ω_3	31.0592	70.4405	96.97	32.4757	71.0765	97.433	33.9805	71.7765	97.9448
	200	ω_1	11.1955	23.8636	32.603	14.6745	25.6802	33.9552	17.7578	27.5585	35.3971
		ω_2	22.4137	47.7379	65.2137	24.3388	48.6714	65.9001	26.313	49.6881	66.6545
		ω_3	33.693	71.6406	97.8455	35.0032	72.2662	98.3043	36.4036	72.9549	98.8116

Temperature ΔT is high

0	200	ω_1	11.4325	23.9757	32.6851	14.856	25.7844	34.034	17.9081	27.6556	35.4727
		ω_2	40.7641	58.6365	73.5674	41.8535	59.399	74.1766	43.0316	60.2349	74.8476
		ω_3	90.0542	110.032	128.64	90.5526	110.44	128.989	91.1031	110.892	129.376
	400	ω_1	10.2296	23.426	32.284	13.9515	25.2741	33.649	17.1652	27.1805	35.1035
		ω_2	39.4651	57.741	72.8556	40.5893	58.5151	73.4707	41.803	59.3635	74.1481
		ω_3	88.7427	108.961	127.725	89.2483	109.373	128.077	89.8068	109.829	128.467
	600	ω_1	8.86509	22.8631	31.8779	12.9842	24.7532	33.2596	16.3887	26.6969	34.7304
		ω_2	38.1218	56.8313	72.1368	39.2845	57.6177	72.7579	40.5372	58.479	73.4419

		ω_3	93.1953	107.879	126.804	87.9248	108.296	127.158	88.4916	108.756	127.551
	200	ω_1	11.0431	23.7925	32.5509	14.5585	25.6141	33.9052	17.6621	27.497	35.3492
		ω_2	34.9368	54.7458	70.5055	36.2019	55.5617	71.1409	37.5577	56.4545	71.8403
		ω_3	66.3185	91.626	113.299	66.9936	92.1159	113.695	67.7358	92.6571	114.134
0.1	400	ω_1	9.79262	23.2385	32.1482	13.6343	25.1009	33.5188	16.9084	27.019	34.9787
		ω_2	33.4119	53.7855	69.7625	34.7326	54.6158	70.4046	36.1435	55.5237	71.1112
		ω_3	64.5263	90.3373	112.259	65.2199	90.8341	112.659	65.9821	91.3829	113.102
	600	ω_1	8.35701	22.6709	31.7404	12.6428	24.5758	33.1278	16.1195	26.5325	34.6042
		ω_2	31.814	52.8078	69.0115	33.1984	53.6532	69.6605	34.6718	54.5771	70.3746
		ω_3	62.6868	89.0299	111.21	63.3967	89.534	111.614	64.1805	90.0907	112.0616
	200	ω_1	10.1553	23.3936	32.2605	13.8719	25.2441	33.6265	17.1211	27.1526	35.0819
		ω_2	26.5981	49.8396	66.7676	28.2393	50.7345	67.4382	29.9576	51.7106	68.1756
		ω_3	44.1878	77.1346	101.937	45.1947	77.7158	102.377	46.2878	78.3566	102.864
0.2	400	ω_1	8.77922	22.83	31.8542	12.9257	24.7226	33.2368	16.3424	26.6685	34.3386
		ω_2	24.5609	48.7828	65.9825	26.3294	49.6967	66.661	28.1644	50.6928	67.4069
		ω_3	41.4495	75.5993	100.78	42.5213	76.1922	101.225	43.6813	76.8456	101.718
	600	ω_1	7.1427	22.252	31.4425	11.8751	24.1899	32.8425	15.5248	26.1754	34.3312
		ω_2	22.3386	47.7026	65.1879	24.2696	48.6368	65.8746	26.249	49.6542	66.6293
		ω_3	38.517	74.0321	99.6096	39.6681	74.6374	100.06	40.9091	75.3044	100.559
	200	ω_1	9.21297	23.0002	31.9764	13.2242	24.8799	33.354	16.5795	26.8144	34.8202
		ω_2	21.1063	47.1382	64.776	23.1404	48.0833	65.467	25.2087	49.1122	66.2263
		ω_3	33.1189	71.3726	97.6492	34.4508	72.0003	98.109	35.8728	72.6915	98.6173
0.3	400	ω_1	7.66962	22.4267	31.5664	12.1993	24.3507	32.9611	15.7741	26.324	34.4447
		ω_2	18.473	46.0194	63.9664	20.7666	46.987	64.6661	23.0489	48.0394	65.4347
		ω_3	29.3659	69.7105	96.441	30.8603	70.353	96.9065	32.4401	71.0602	97.4211
	600	ω_1	5.72428	21.838	31.1509	11.08	23.8097	32.5635	14.9254	25.8244	34.0643
		ω_2	15.3958	44.8727	63.1465	18.084	45.8646	63.8551	20.6647	46.9421	64.6334
		ω_3	25.0571	68.0077	95.2175	26.7928	68.6662	95.6889	28.5982	69.3905	96.21
	200	ω_1	8.42973	22.6979	31.7596	12.722	24.6007	33.1462	16.1574	26.5555	34.6219
		ω_2	17.7816	45.7642	63.7702	20.2322	46.7195	64.472	22.4986	47.7778	65.2429
		ω_3	27.1717	68.8149	95.7957	28.9034	69.4658	96.2643	30.468	70.1818	96.7823
0.4	400	ω_1	6.70855	22.1164	31.2616	11.6191	24.0653	32.7508	15.3299	26.0603	34.2435
		ω_2	14.5589	44.5925	62.7781	17.3771	45.5905	63.6586	20.049	46.6743	64.4392
		ω_3	22.4455	67.0894	94.3098	24.368	67.7568	95.0385	26.3401	68.4908	95.5631
	600	ω_1	4.35303	21.5193	30.9283	9.85652	23.5177	32.3506	14.041	25.5555	33.8609
		ω_2	10.3798	43.4082	62.1143	14.062	44.4327	62.8346	17.2551	45.5441	63.6254
		ω_3	22.3221	65.3184	93.3156	24.2544	66.0037	93.7966	26.235	66.7569	94.3282
	200	ω_1	7.83486	22.4837	31.6069	12.3039	24.4032	33.000	15.8551	26.3727	34.4818
		ω_2	15.7021	44.9787	63.2219	18.3454	45.9683	63.9297	20.8939	47.0434	64.7071
		ω_3	23.6564	67.5042	94.8585	25.4878	68.1676	95.3317	27.3793	68.8971	95.8548
0.5	400	ω_1	5.94385	21.8966	31.192	11.1951	23.8634	32.6028	15.011	25.874	34.1019
		ω_2	11.9303	43.8048	62.3922	15.2424	44.8203	63.1093	18.23	45.9223	63.8966
		ω_3	18.0312	65.7443	93.6143	20.3746	66.4252	94.0938	22.6963	67.1738	94.6237
	600	ω_1	3.04526	21.2933	30.7712	9.81365	23.3111	32.2007	14.011	25.3654	33.7177
		ω_2	9.51956	42.5986	61.5513	13.4396	43.6422	62.2781	15.1033	44.7732	63.0758
		ω_3	16.1473	63.936	92.3533	18.7229	64.636	92.8393	21.2305	65.405	93.3763

Table 5.7. The nonlinear correction term of the first three frequencies CC nanobeam with different γ, T, Knl, Kp and kw values

			K_L=10			**K_L=100**			**K_L=200**		
e_0a	ΔT		**K_P=5**	**K_P=50**	**K_P=100**	**K_P=5**	**K_P=50**	**K_P=100**	**K_P=5**	**K_P=50**	**K_P=100**
/L	(K)		**K_{NL}=10**	**K_{NL}=100**	**K_{NL}=200**	**K_{NL}=10**	**K_{NL}=100**	**K_{NL}=200**	**K_{NL}=10**	**K_{NL}=100**	**K_{NL}=200**
					Temperature ΔT is low and room						
	0	ω_1	1.46181	5.71425	5.45135	1.3588	5.67252	5.42217	1.26649	5.6272	5.39028
0	100	ω_1	1.42728	5.66802	5.41966	1.33027	5.6272	5.39094	1.2427	5.58286	5.35956
	200	ω_1	1.39485	5.62281	5.38848	1.30327	5.58287	5.37213	1.22005	5.53948	5.32932
	0	ω_1	1.84968	7.60165	6.83601	1.71081	7.54016	6.79954	1.58806	7.47349	6.75972
0.1	100	ω_1	1.79546	7.52402	6.78909	1.66701	7.46429	6.75366	1.55228	7.3996	6.71556
	200	ω_1	1.74558	7.44868	6.74564	1.62631	7.3907	6.71058	1.51877	7.32784	6.67226

0.2	0	ω_1	2.74263	9.85448	8.2581	2.50512	9.76354	8.21357	2.3021	9.66535	8.16496
	100	ω_1	2.62091	9.72023	8.19228	2.41081	9.63291	8.1488	2.22781	9.53856	8.10131
	200	ω_1	2.51398	9.59131	8.12803	2.32534	9.50736	8.08556	2.16032	9.41662	8.03915
0.3	0	ω_1	3.70824	11.0501	8.9325	3.33617	10.9405	8.88389	3.03022	10.8225	8.83079
	100	ω_1	3.47664	10.877	8.85547	3.16367	10.7725	8.80808	2.89912	10.6598	8.75634
	200	ω_1	3.28305	10.7119	8.78037	3.01551	10.612	8.72804	2.78337	9.86836	8.68374
0.4	0	ω_1	4.52977	11.6537	9.25382	4.01624	11.5339	9.20322	3.61004	11.4049	9.14794
	100	ω_1	4.17044	11.4587	9.17109	3.75912	11.3447	9.12183	3.61969	11.2219	9.068
	200	ω_1	3.88489	11.2731	9.09054	3.54583	11.1645	9.04252	3.52672	11.0474	8.99008
0.5	0	ω_1	5.16432	11.9826	9.42382	4.52427	11.857	9.37213	4.03316	11.7218	9.31568
	100	ω_1	4.68459	11.7749	9.33796	4.19118	11.6556	9.28766	3.7917	11.5271	9.23273
	200	ω_1	4.31773	11.5776	9.25444	3.92221	11.4641	9.20547	3.58909	11.3418	9.15197
Temperature ΔT is high											
0	200	ω_1	1.51313	5.77956	5.49575	1.4008	5.73651	5.46595	1.30126	5.68979	5.43336
	400	ω_1	1.56954	5.84697	5.54126	1.4463	5.80255	5.51075	1.33867	5.75435	5.46534
	600	ω_1	1.63193	5.91661	5.58782	1.49618	5.87073	5.5566	1.37906	5.82098	5.52251
0.1	200	ω_1	1.93254	7.71243	6.90026	1.77686	7.64826	6.86279	1.64145	7.5788	6.82186
	400	ω_1	2.02704	7.82816	6.96638	1.85085	7.76367	6.92929	1.70042	7.68866	6.88721
	600	ω_1	2.13606	7.94923	7.03442	1.93446	7.87915	6.99477	1.76603	7.8034	6.95148
0.2	200	ω_1	2.9414	10.0485	8.35125	2.65495	9.9522	8.3052	2.41772	9.84826	8.25494
	400	ω_1	3.1902	10.2545	8.44761	2.83537	10.1586	8.39998	2.55304	10.042	8.34799
	600	ω_1	3.51413	10.4737	8.54739	3.05839	10.3647	8.49806	2.71442	10.2476	8.44422
0.3	200	ω_1	4.12074	11.3021	9.04178	3.62732	11.1849	8.99137	3.24422	11.0589	8.93634
	400	ω_1	4.70898	11.5721	9.1552	4.12474	11.1986	9.10289	3.51194	11.3115	9.0458
	600	ω_1	5.65079	11.8625	9.27289	4.55258	11.7273	9.2186	3.86156	11.5823	9.15936
0.4	200	ω_1	5.22091	11.9389	9.37145	4.47524	11.8101	9.31879	3.93307	11.6719	9.26143
	400	ω_1	6.3703	12.2461	9.49349	5.13996	12.1073	9.43883	4.36317	11.9584	9.37924
	600	ω_1	8.90823	12.5784	9.62049	6.23558	12.4281	9.56368	4.98181	12.2672	9.50167
0.5	200	ω_1	6.15511	12.2871	9.54584	5.1471	12.1518	9.49213	4.45614	12.0598	9.4335
	400	ω_1	8.08522	12.616	9.6727	6.1282	12.4696	9.61684	5.04951	12.3127	9.5559
	600	ω_1	15.4353	12.9719	9.80481	8.05671	12.8138	9.74663	5.99023	12.6438	9.68318

Table 5.8. The nonlinear correction term of the first three frequencies SS nanobeam with different γ, T, Knl, Kp and kw values

			K_L=10			K_L=100			K_L=200		
e_0a /L	ΔT (K)		K_P=5 K_{NL}=10	K_P=50 K_{NL}=100	K_P=100 K_{NL}=200	K_P=5 K_{NL}=10	K_P=50 K_{NL}=100	K_P=100 K_{NL}=200	K_P=5 K_{NL}=10	K_P=50 K_{NL}=100	K_P=100 K_{NL}=200
Temperature ΔT is low and room											
0	0	ω_1	1.90804	3.03978	3.95278	1.52078	2.83488	3.79966	1.28289	2.6496	3.64875
	100	ω_1	1.80222	2.99295	3.91922	1.46555	2.79679	3.76963	1.24921	2.61842	3.62213
	200	ω_1	1.71225	2.94822	3.8861	1.41593	2.76031	3.74029	1.21805	2.58831	3.59608
0.1	0	ω_1	1.96425	3.06216	3.96872	1.54848	2.853	3.81378	1.29939	2.66439	3.66124
	100	ω_1	1.84884	3.0143	3.93452	1.49029	2.81418	3.78341	1.26443	2.63268	3.63435
	200	ω_1	1.75209	2.96862	3.90121	1.43821	2.77691	3.77034	1.23215	2.60209	3.60804
0.2	0	ω_1	2.10181	3.11201	4.00357	1.6136	2.89319	3.84468	1.33715	2.69703	3.68839
	100	ω_1	1.96278	3.06187	3.96848	1.54809	2.85273	3.81357	1.29914	2.66416	3.66106
	200	ω_1	1.84812	3.01399	3.9343	1.49044	2.84108	3.7832	1.2645	2.63247	3.63417
0.3	0	ω_1	2.26814	3.16276	4.03826	1.68529	2.93384	3.87537	1.3771	2.72987	3.71563
	100	ω_1	2.09615	3.11012	4.00226	1.61103	2.89168	3.84352	1.33539	2.6958	3.68753
	200	ω_1	1.95818	3.06002	3.9672	1.5458	2.85128	3.81244	1.2978	2.66298	3.66005
0.4	0	ω_1	2.42413	3.20289	4.06514	1.74641	2.96578	3.8991	1.40975	2.75554	3.73654
	100	ω_1	2.21743	3.14824	4.02842	1.66417	2.92224	3.86667	1.36551	2.72052	3.70796
	200	ω_1	2.05594	3.09631	3.99231	1.59256	2.88057	3.83503	1.3251	2.68679	3.68003
0.5	0	ω_1	2.55473	3.23189	4.08428	1.79339	2.98877	3.91567	1.43422	2.77395	3.75138
	100	ω_1	2.31606	3.17579	4.04705	1.70468	2.94423	3.88313	1.38762	2.73823	3.72246
	200	ω_1	2.13382	3.1225	4.01408	1.62794	2.90164	3.85108	1.34528	2.70385	3.69421
Temperature ΔT is high											
0	200	ω_1	2.08959	3.10791	4.00073	1.60805	2.8899	3.84216	1.33393	2.69436	3.68633

	400	ω_1	2.3353	3.18083	4.05043	1.7123	2.94825	3.86639	1.39172	2.74146	3.7251
	600	ω_1	2.69475	3.25915	4.10203	1.83987	3.01028	3.93162	1.45766	2.79212	3.76512
0.1	200	ω_1	2.16327	3.13184	4.01722	1.64091	2.90911	3.85676	1.35257	2.7099	3.69921
	400	ω_1	2.43951	3.15845	4.06754	1.75214	2.96861	3.90122	1.41286	2.75784	3.7384
	600	ω_1	2.85858	3.28678	4.1198	1.88955	3.03201	3.94726	1.48201	2.80841	3.77885
0.2	200	ω_1	2.35239	3.18524	4.05338	1.72187	2.95175	3.92596	1.39531	2.74428	3.7274
	400	ω_1	2.72111	3.26387	4.10509	1.84819	3.01401	3.93432	1.46179	2.79409	3.79164
	600	ω_1	3.34456	3.34865	4.15884	2.01171	3.08039	3.98155	1.53878	2.84673	3.8089
0.3	200	ω_1	2.593	3.23972	4.0894	1.80648	2.99495	3.92049	1.44089	2.77889	3.75538
	400	ω_1	3.11478	3.32257	4.14251	1.95824	3.06004	3.96723	1.51446	2.83065	3.79635
	600	ω_1	4.17331	3.41213	4.19777	2.15606	3.12404	4.01567	1.60057	2.88542	3.83874
0.4	200	ω_1	2.83392	3.3847	4.11731	1.87876	3.02895	3.94507	1.47853	2.80598	3.77692
	400	ω_1	3.56101	3.36928	4.17931	2.05603	3.09634	3.9927	1.55834	2.8593	3.81866
	600	ω_1	5.60579	3.46267	4.22798	2.71259	3.16881	4.0421	1.90424	2.91578	3.8618
0.5	200	ω_1	3.04909	3.31414	4.1372	1.9416	3.04594	3.96255	1.50672	2.82543	3.79227
	400	ω_1	4.01915	3.403	4.19223	2.1339	3.11447	4.01083	1.59145	2.87989	3.81323
	600	ω_1	8.66608	3.49942	4.24955	2.58208	3.18784	4.06091	1.80852	2.93763	3.8782

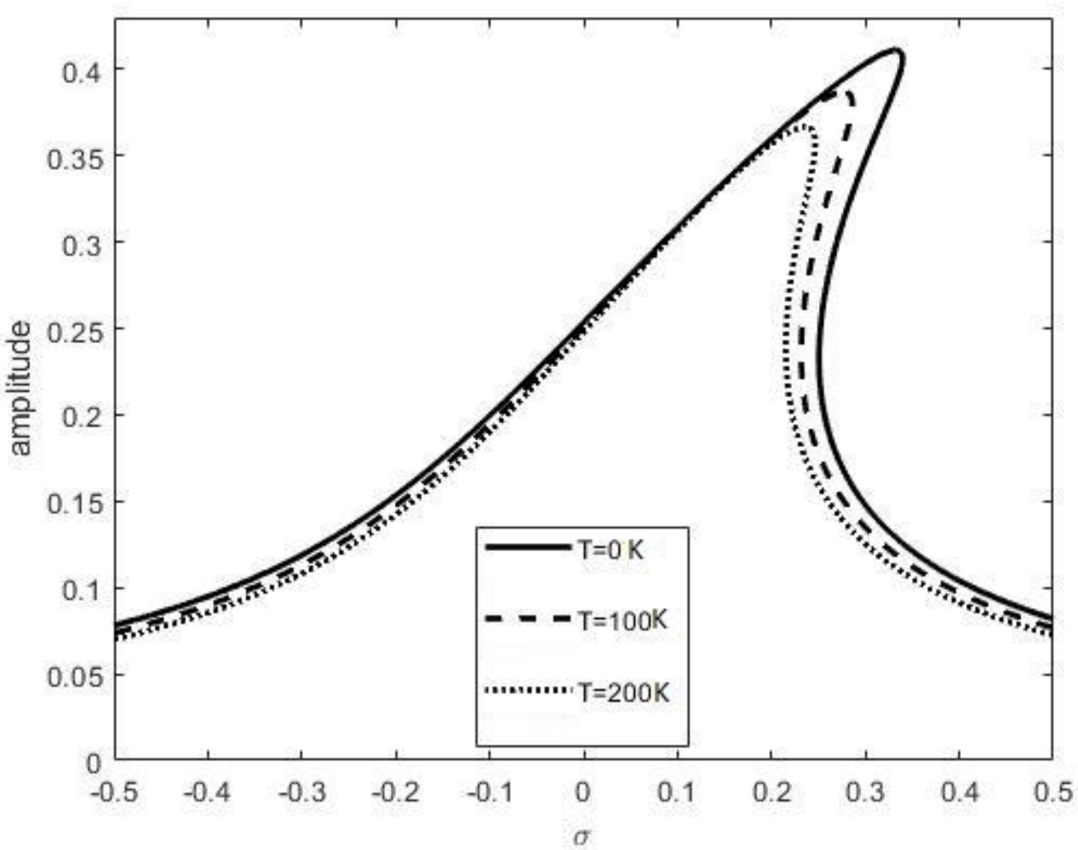

Figure 5.27. Frequency-response curves of S-S nanobeams for different Low Temperature values T=0K, T=100K and T=200K , the first mode and ($\boldsymbol{\gamma}$=0.1, $K_{nl} = 10,\ K_p = 5\ and\ K_w = 10$)

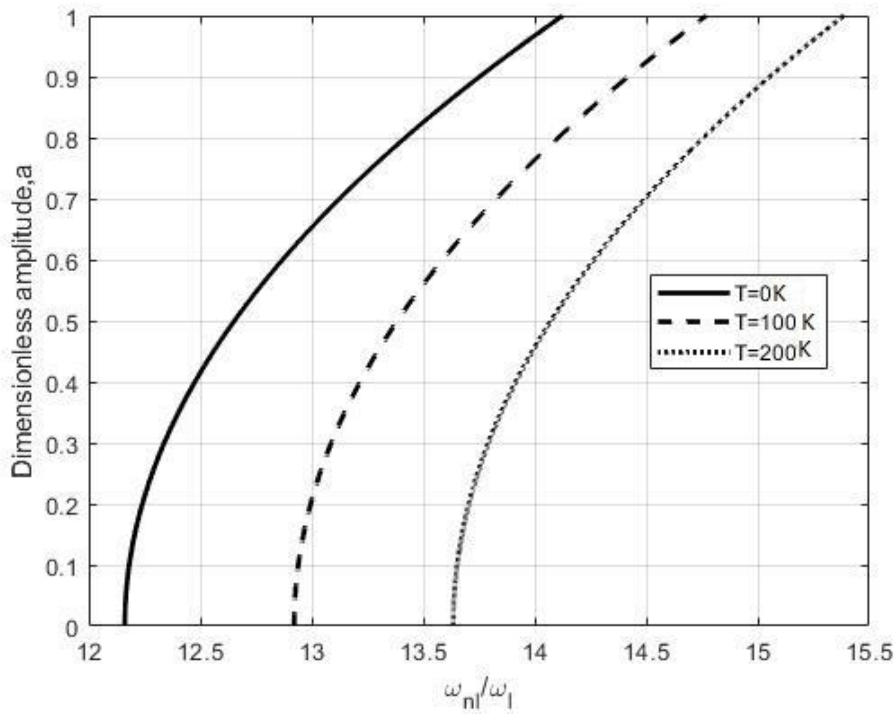

Figure 5.28. Amplitude and Nonlinear natural frequency change of SS nanobeams for different Low Temperature values when $\boldsymbol{\gamma}$=0.1, $K_{nl} = 10,\ K_p = 5\ and\ K_w = 10$

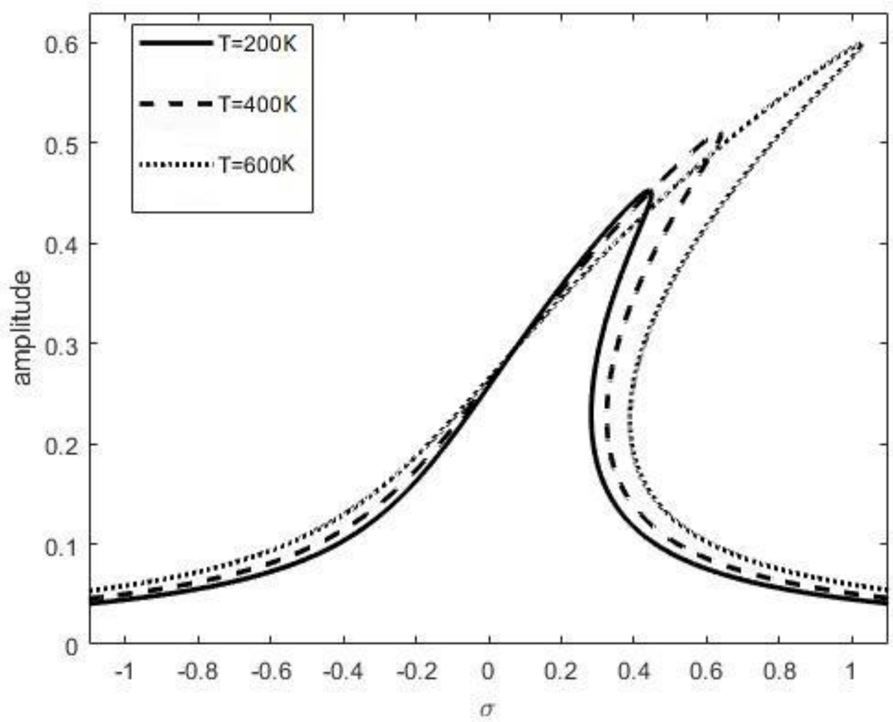

Figure 5.29. Frequency-response curves of SS nanobeams for different High Temperature values T=200K, T=400K and T=600K , the first mode and ($\boldsymbol{\gamma}$=0.1, $K_{nl} = 10,\ K_p = 5\ and\ K_w = 10$)

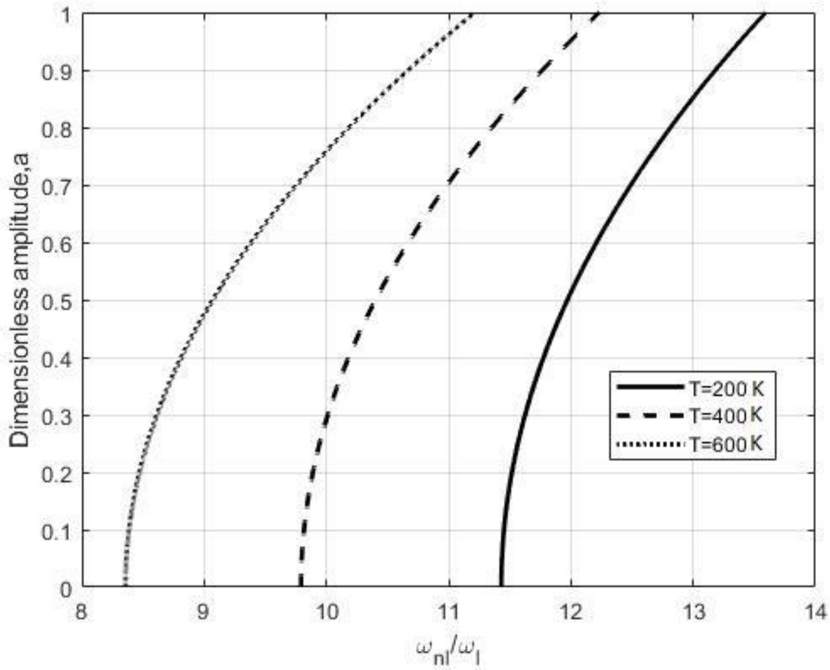

Figure 5.30. Amplitude and Nonlinear natural frequency change of S-S nanobeams for different High Temperature values when $\boldsymbol{\gamma}$=0.1, $K_{nl} = 10,\ K_p = 5\ and\ K_w = 10$

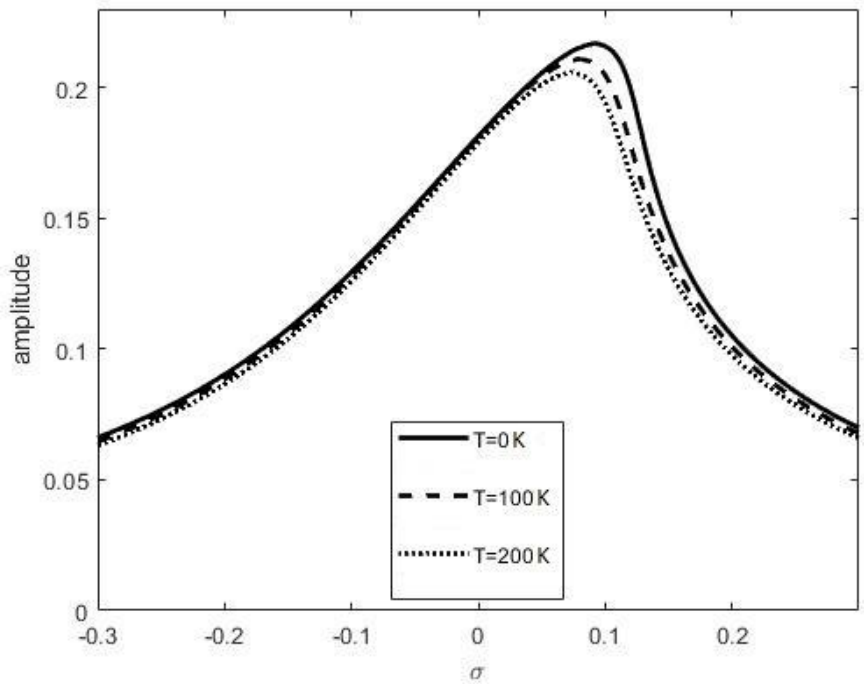

Figure 5.31. Frequency-response curves of C-C nanobeams for different Low Temperature values T=0K, T=100K and T=200K, the first mode and ($\boldsymbol{\gamma}$=0.1, $K_{nl} = 10,\ K_p = 5\ and\ K_w = 10$)

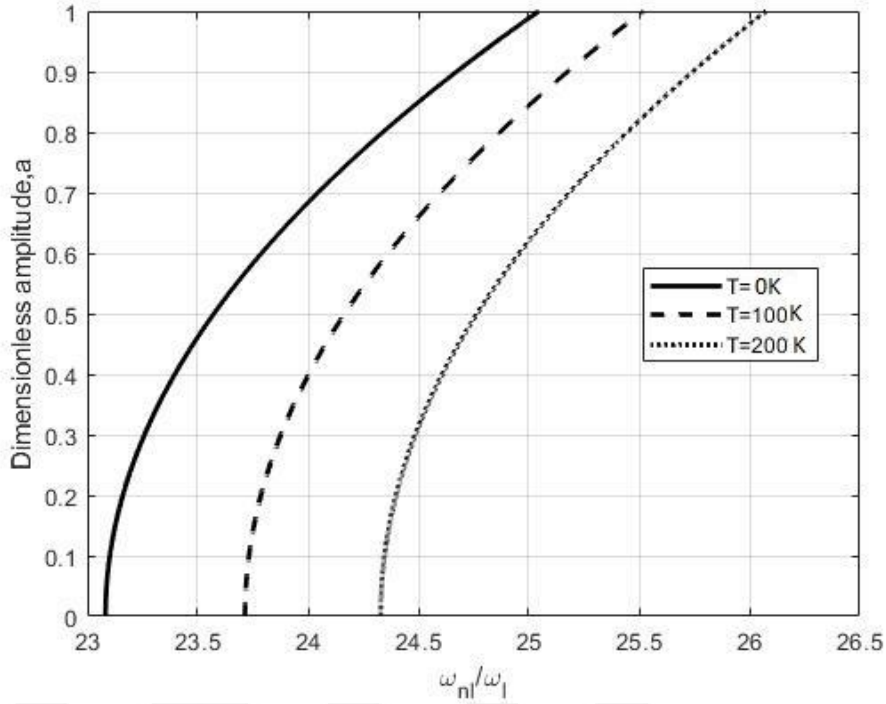

Figure 5.32. Amplitude and Nonlinear natural frequency change of C-C nanobeams for different Low Temperature values, the first mode and ($\boldsymbol{\gamma}$=0.1, $K_{nl} = 10,\ K_p = 5\ and\ K_w = 10$)

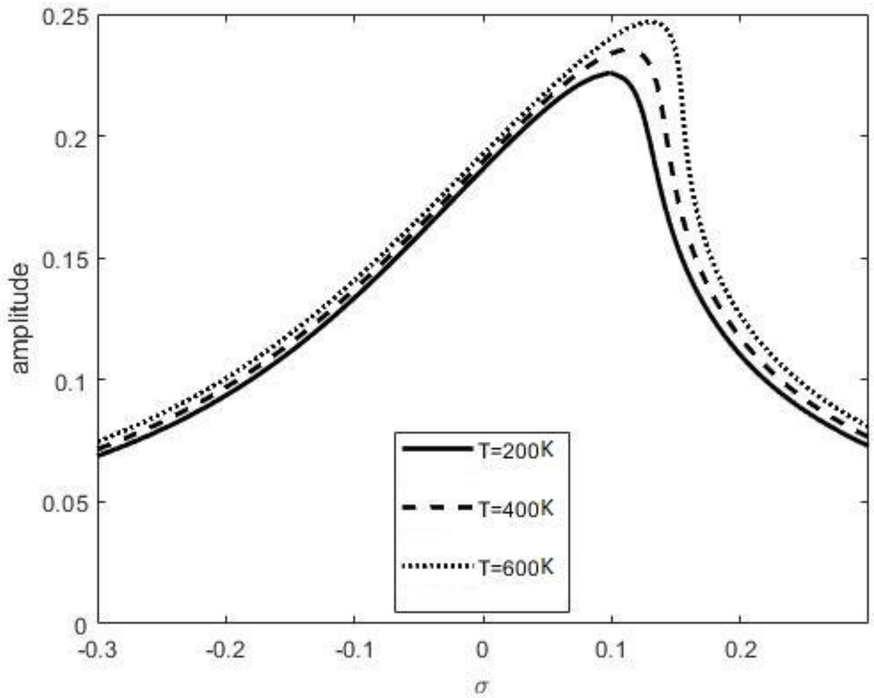

Figure 5.33. Frequency-response curves of C-C nanobeams for different High Temperature values T=200K, T=400K and T=600K, the first mode and ($\boldsymbol{\gamma}$=0.1, $K_{nl} = 10,\ K_p = 5\ and\ K_w = 10$)

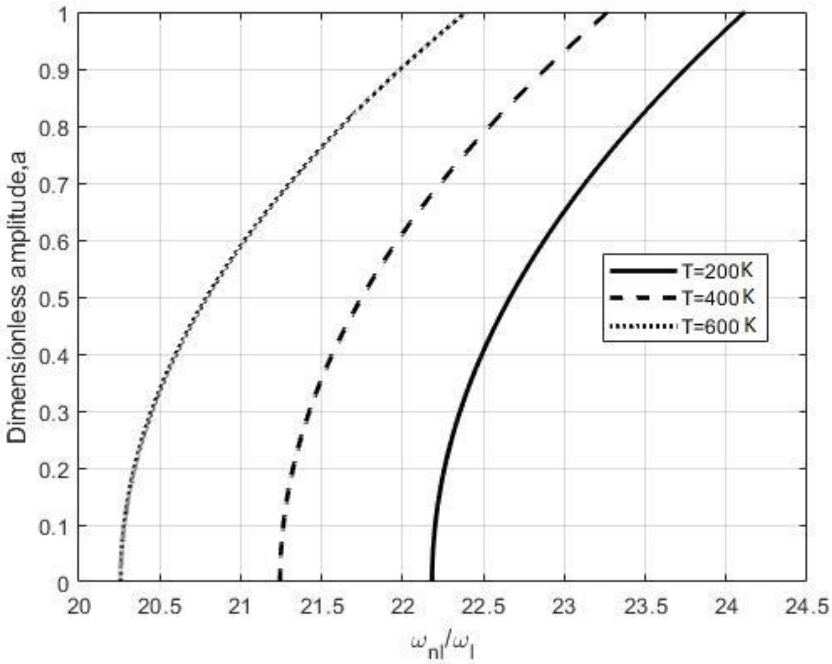

Figure 5.34 Amplitude and Nonlinear natural frequency change of C-C nanobeams for different High Temperature values, the first mode and (***γ***=0.1, $K_{nl} = 10,\ K_p = 5\ and\ K_w = 10$)

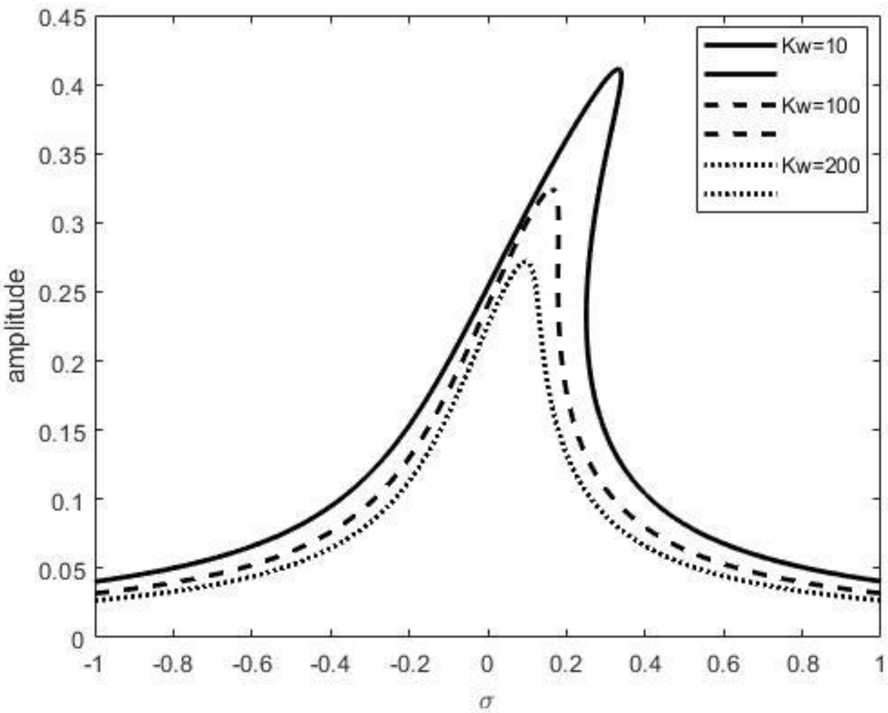

Figure 5.35. Frequency-response curves of S-S nanobeams for different Winkler parameter Kw=10, Kw=10 and Kw=20, the first mode and (***γ***=0.1, $K_{nl} = 10,\ K_p = 5\ and\ T = 0K$)

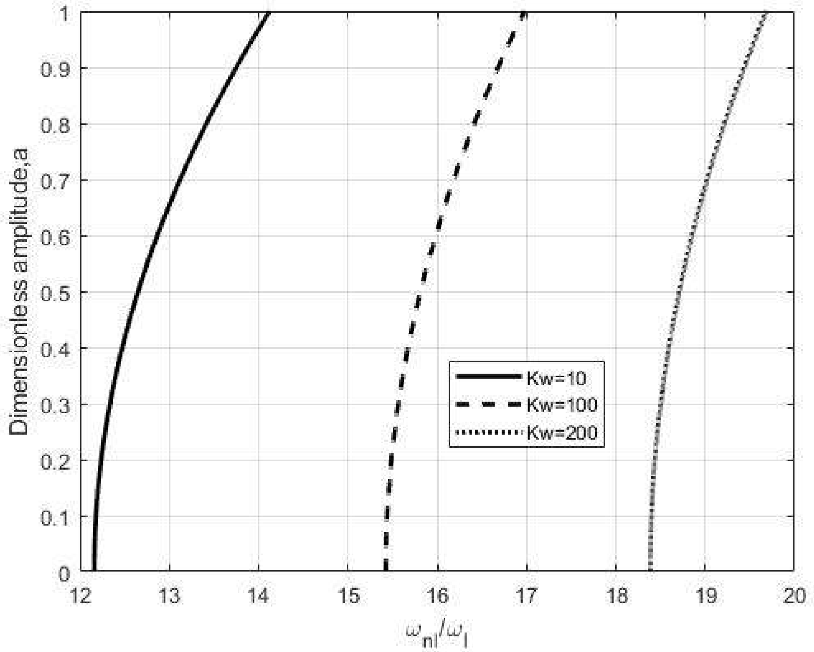

Figure 5.36. Amplitude and Nonlinear natural frequency change of SS nanobeams for different Winkler parameter Kw=0, Kw=100 and Kw=200, the first mode and (***γ***=0.1, $K_{nl} = 10,\ K_p = 5\ \ and\ \ T = 0K$)

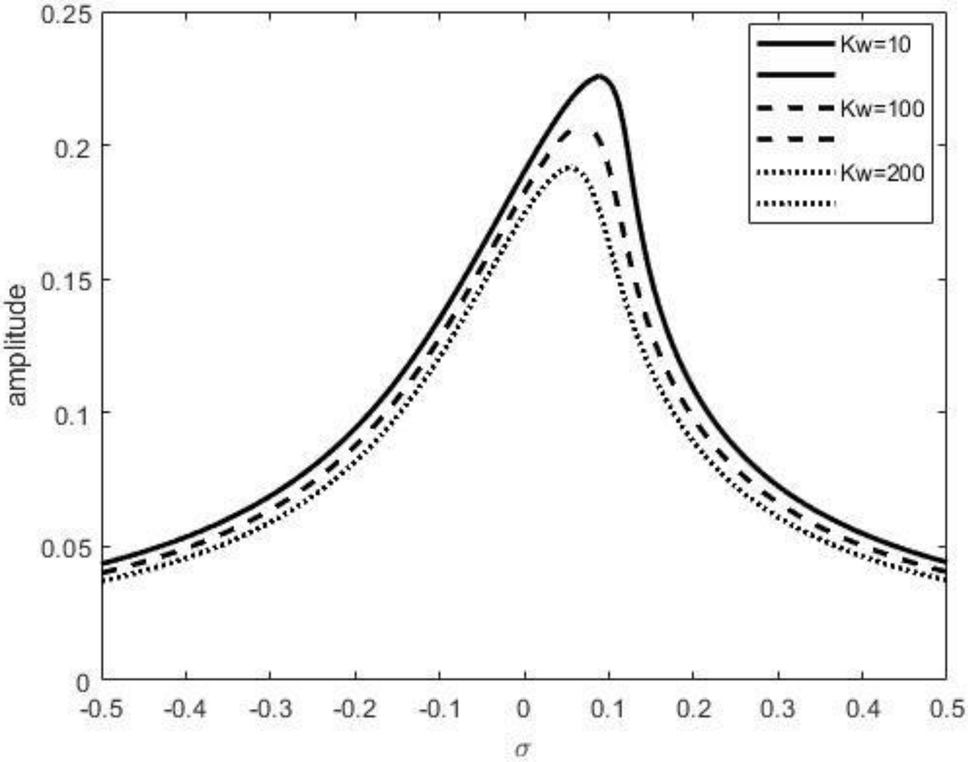

Figure 5.37. Frequency-response curves of CC nanobeams for different Winkler parameters Kw=10, Kw=10 and Kw=20, the first mode and (***γ***=0.1, $K_{nl} = 10,\ K_p = 5\ \ and\ \ T = 0K$)

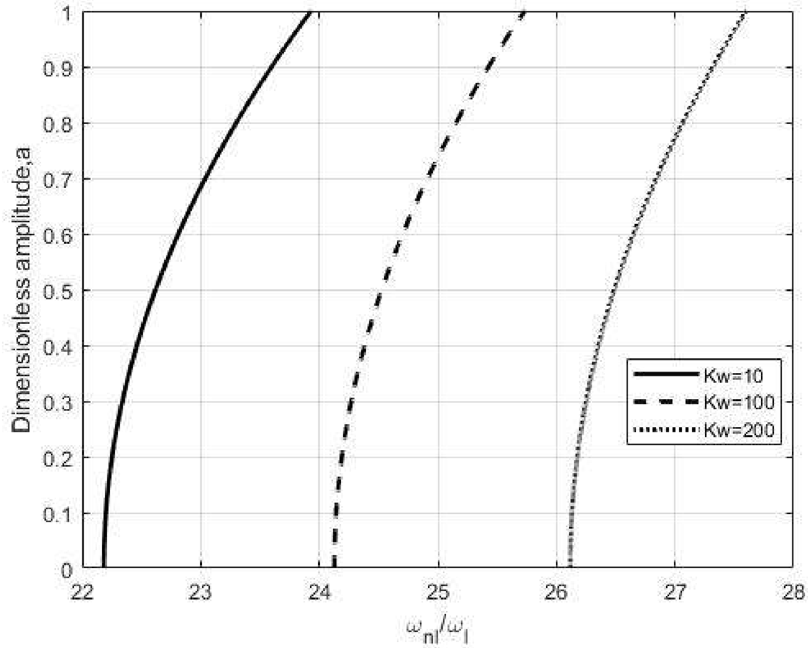

Figure 5.38. Amplitude and Nonlinear natural frequency change of CC nanobeams for different Winkler parameter Kw=0, Kw=100 and Kw=200, the first mode and (***γ***=0.1, $K_{nl} = 10,\ K_p = 5\ and\ T = 0K$)

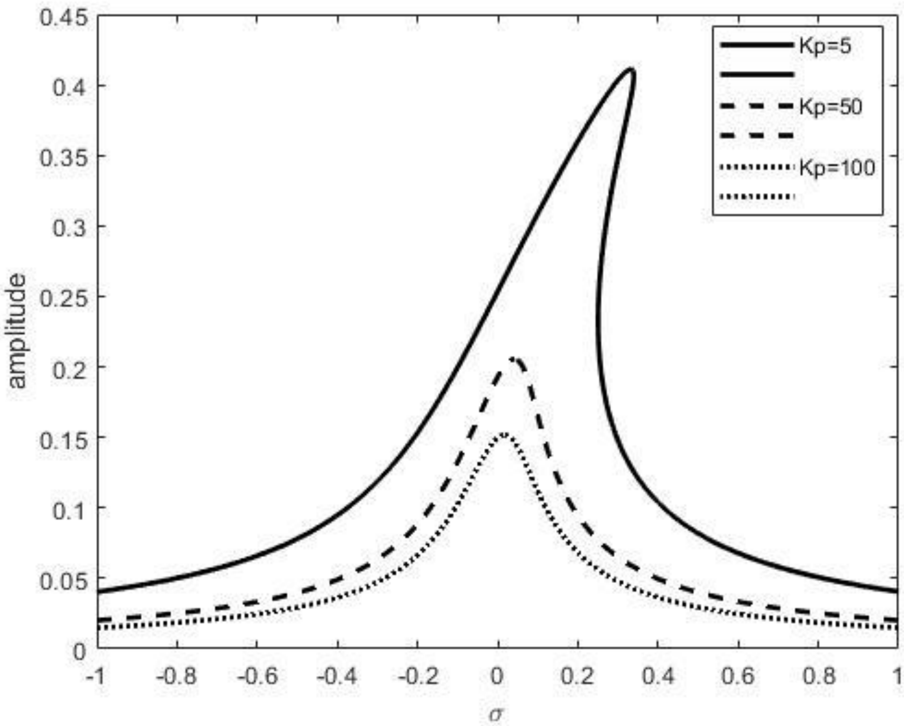

Figure 5.39. Frequency-response curves of SS nanobeams for different Pasternak parameters Kp=5, Kp=50 and Kp=100, the first mode and (***γ***=0.1, $K_{nl} = 10,\ K_w = 10\ and\ T = 0K$)

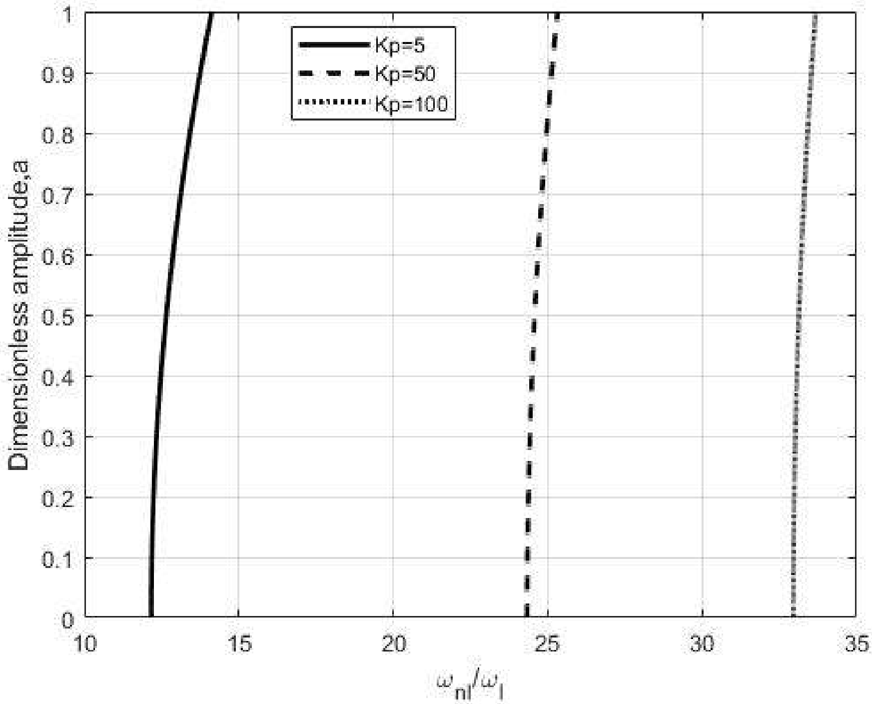

Figure 5.40. Amplitude and Nonlinear natural frequency change of SS nanobeams for different Pasternak parameters Kp=5, Kp=50 and Kp=100, the first mode and ($\boldsymbol{\gamma}$=0.1, $K_{nl} = 10,\ K_w = 10\ \ and\ \ T = 0K$)

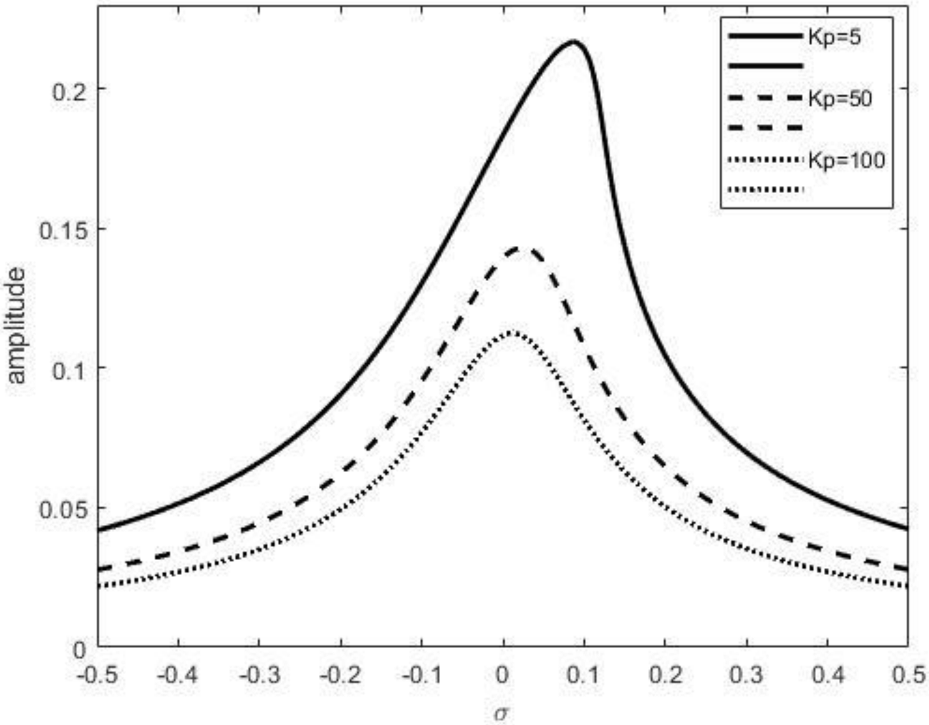

Figure 5.41. Frequency-response curves of CC nanobeams for different Pasternak parameters Kp=5, Kp=50 and Kp=100, the first mode and ($\boldsymbol{\gamma}$=0.1, $K_{nl} = 10,\ K_w = 10\ \ and\ \ T = 0K$)

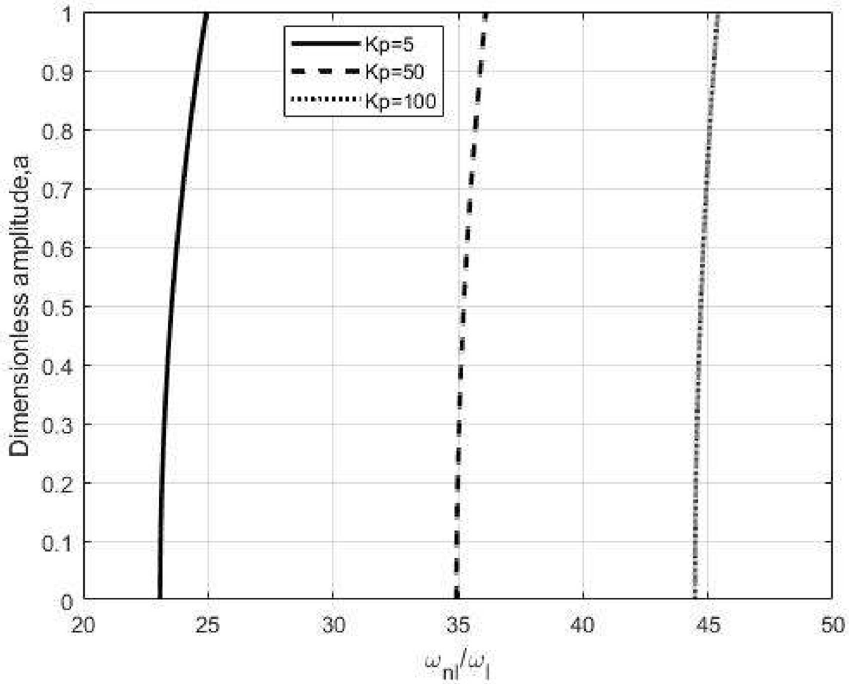

Figure 5.42. Amplitude and Nonlinear natural frequency change of CC nanobeams for different Pasternak parameters Kp=5, Kp=50 and Kp=100, the first mode and ($\boldsymbol{\gamma}$=0.1, $K_{nl} = 10,\ K_w = 10\ \ and\ \ T = 0K$)

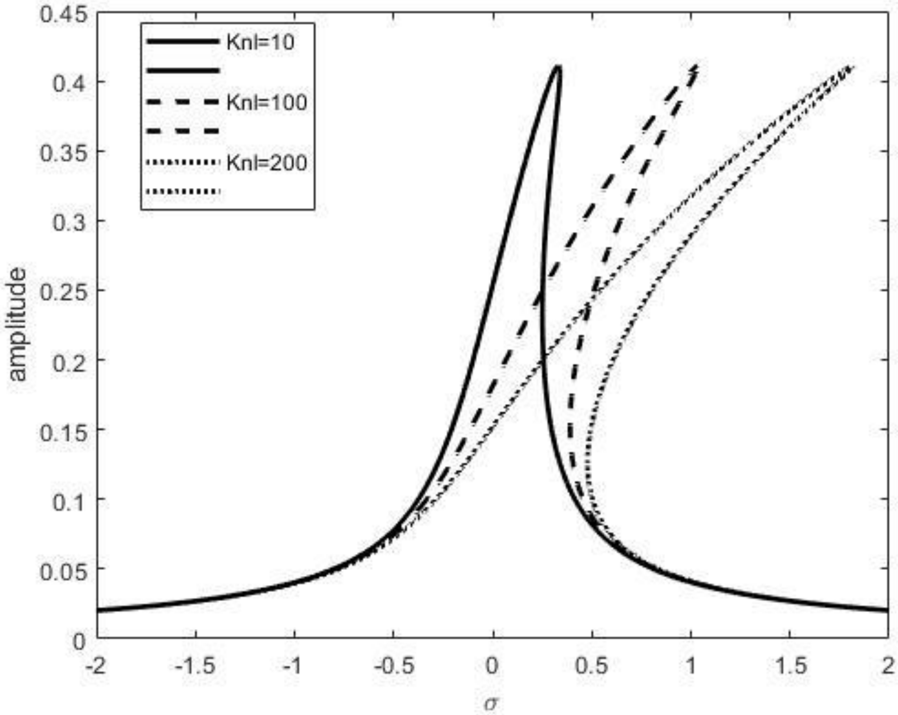

Figure 5.43. Frequency-response curves of SS nanobeams for different Nonlinear foundation parameters Knl=10, Knl=100 and Knl=200, the first mode and ($\boldsymbol{\gamma}$=0.1, $K_p = 5,\ K_w = 10\ \ and\ \ T = 0K$)

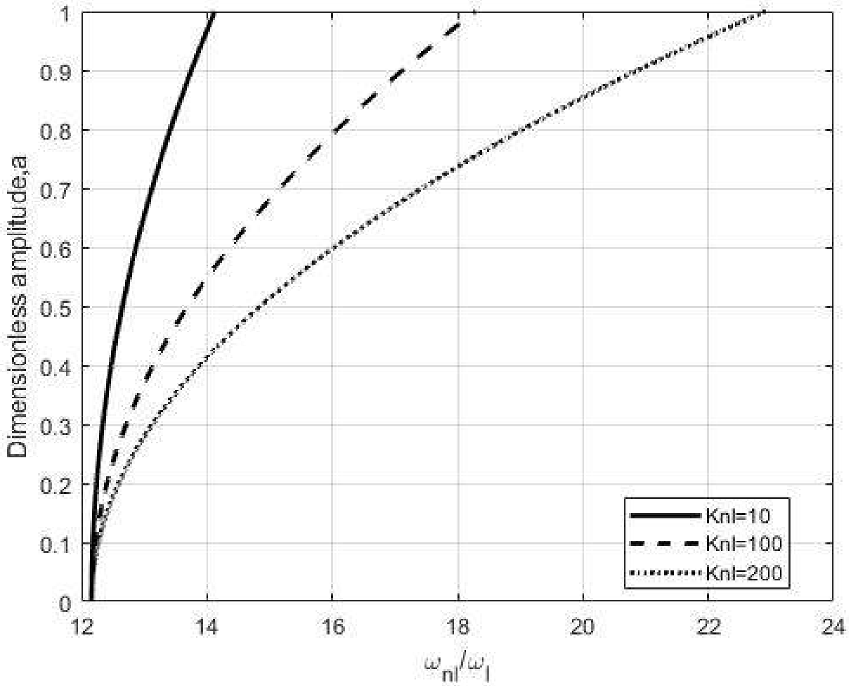

Figure 5.44. Amplitude and Nonlinear natural frequency change of S-S nanobeams for different nonlinear foundation parameters Knl=10, Knl=100 and Kw=200, the first mode and (***γ***=0.1, $K_w = 10,\ K_p = 5\ \ and\ \ T = 0K$)

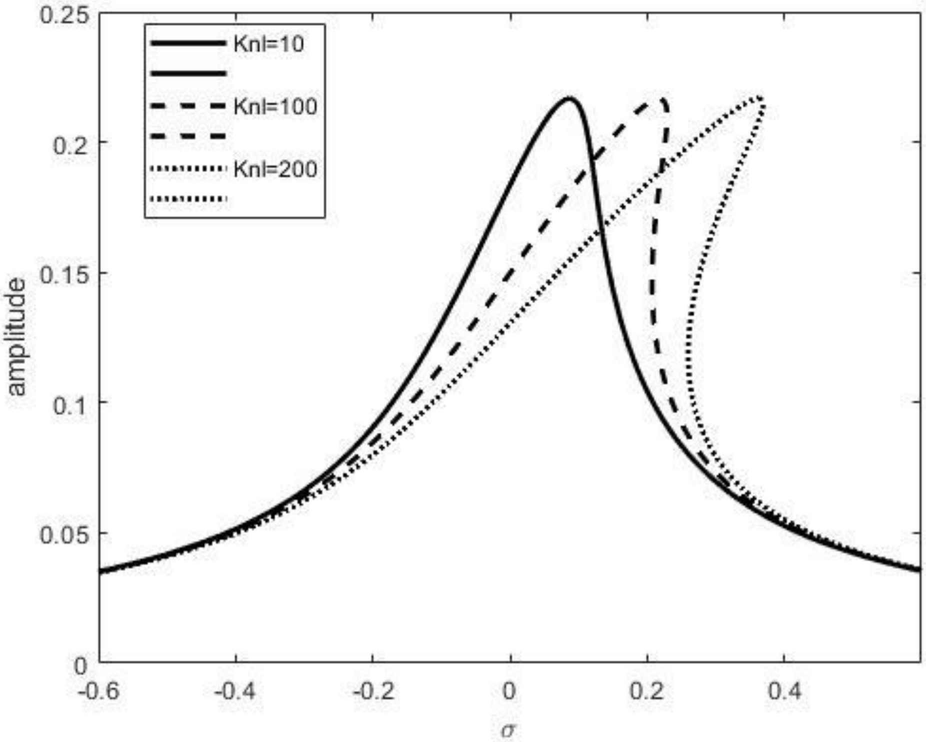

Figure 5.45. Frequency-response curves of CC nanobeams for different Nonlinear foundation parameters Knl=10, Knl=100 and Knl=200, the first mode and (***γ***=0.1, $K_p = 5,\ K_w = 10\ \ and\ \ T = 0K$)

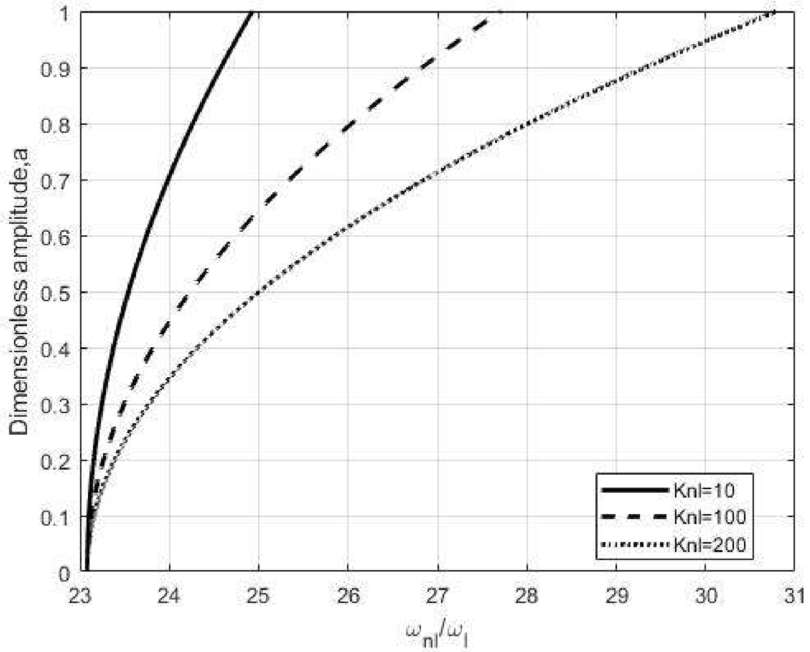

Figure 5.46. Amplitude and Nonlinear natural frequency change of CC nanobeams for different nonlinear foundation parameters Knl=10, Knl=100 and Kw=200, the first mode and ($\boldsymbol{\gamma}$=0.1, $K_w = 10,\ K_p = 5\ and\ T = 0K$)

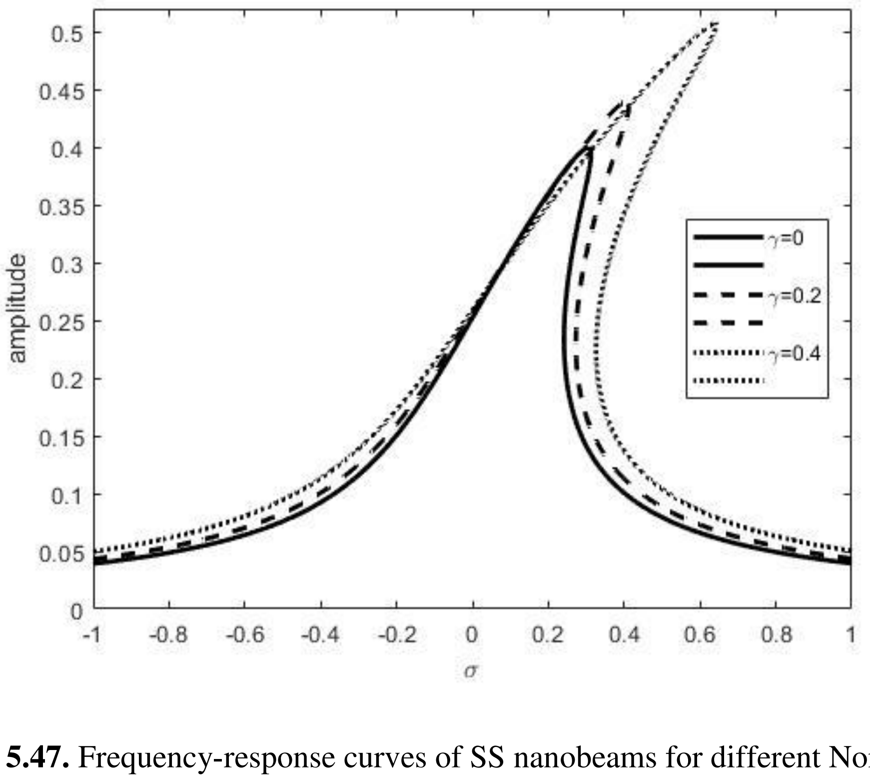

Figure 5.47. Frequency-response curves of SS nanobeams for different Nonlocal parameters $\boldsymbol{\gamma}$=0 and $\boldsymbol{\gamma}$=0.2 and $\boldsymbol{\gamma}$=0.4, the first mode and (K_{nl}= 10, $K_p = 5,\ K_w = 10\ and\ T = 0K$)

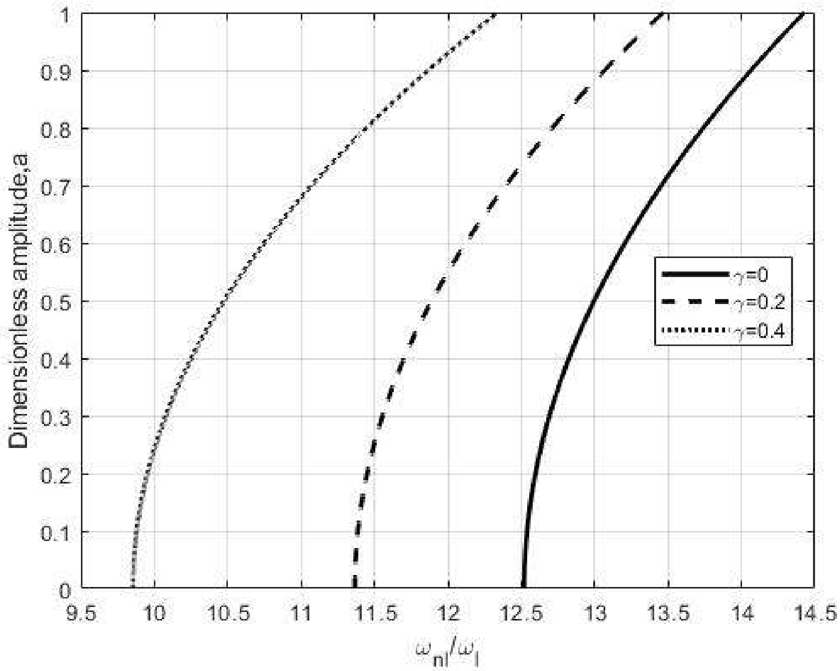

Figure 5.48. Amplitude and Nonlinear natural frequency change of S-S nanobeams for different nonlocal parameters ***γ***=0, ***γ***=0.2 and ***γ***=0.4, the first mode and (K_{nl}= 10, $K_w = 10,\ K_p = 5\ and\ T = 0K$)

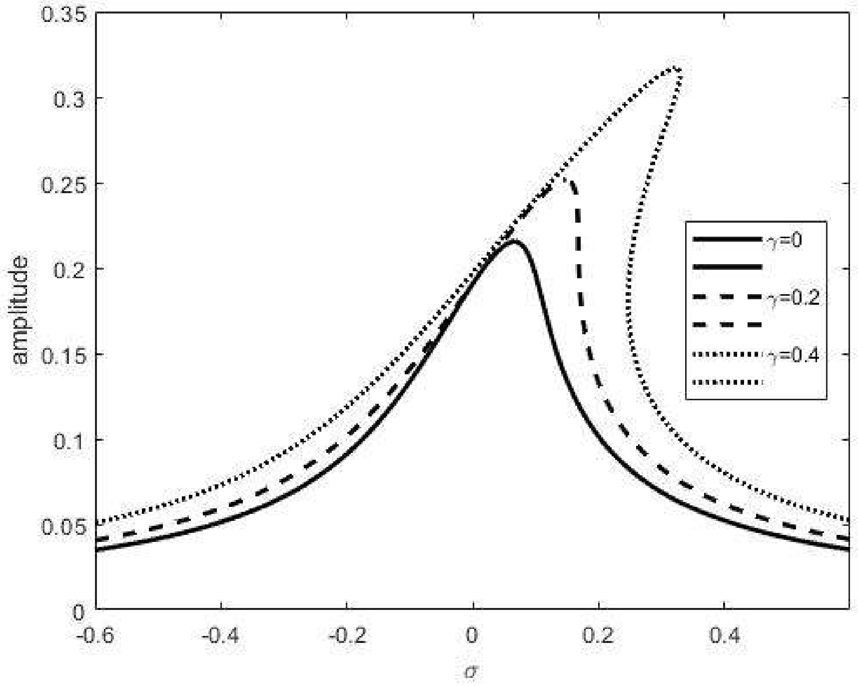

Figure 5.49. Frequency-response curves of C-C nanobeams for different Nonlocal parameters ***γ***=0 and ***γ***=0.2 and ***γ***=0.4, the first mode and (K_{nl}= 10, $K_p = 5,\ K_w = 10\ and\ T = 0K$)

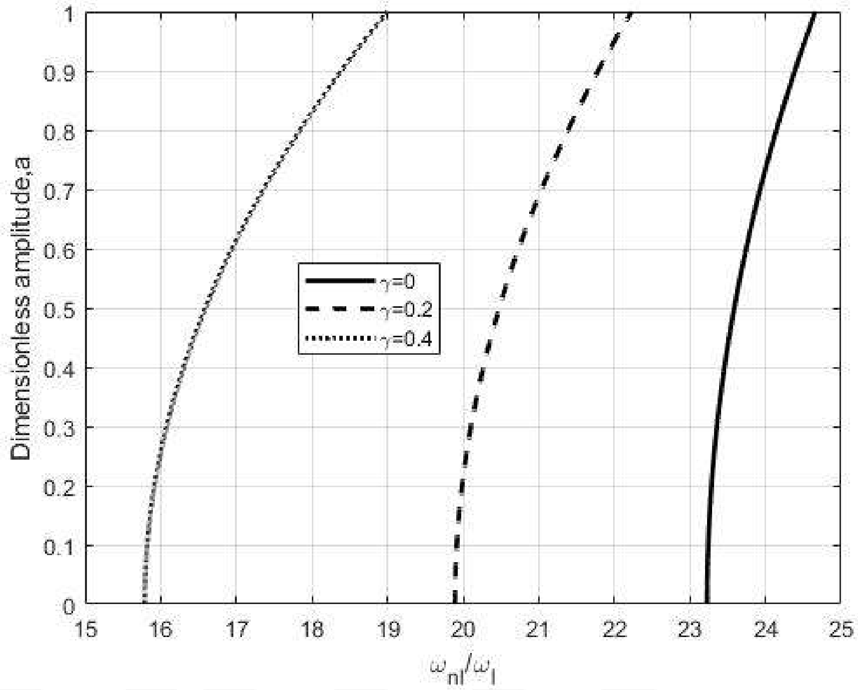

Figure 5.50. Amplitude and Nonlinear natural frequency change of C-C nanobeams for different nonlocal parameters $\boldsymbol{\gamma}$=0, $\boldsymbol{\gamma}$=0.2 and $\boldsymbol{\gamma}$=0.4, the first mode and (K_{nl}= 10, $K_w = 10,\ K_p = 5\ and\ T = 0K$)

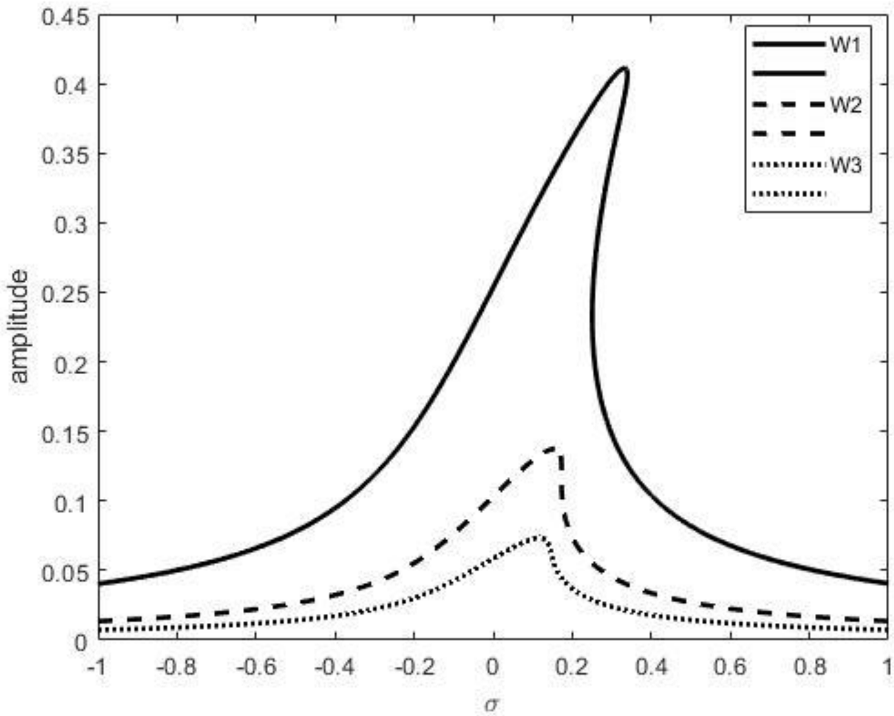

Figure 5.51. 1st mode (ω_1), 2nd mode (ω_2) and 3rd mode ($\omega_{3)}$ frequency-response curves of SS nanobeams for ($\boldsymbol{\gamma}$=0.1, K_{nl}= 10, $K_p = 5,\ K_w = 10\ and\ T = 0K$)

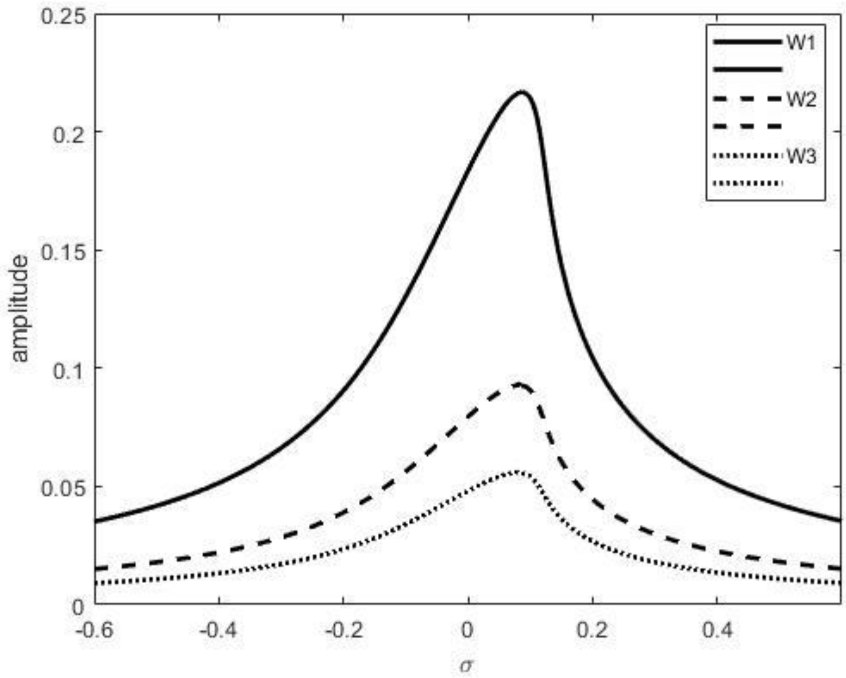

Figure 5.52. 1st mode (ω_1), 2nd mode (ω_2) and 3rd mode ($\omega_{3)}$ frequency-response of C-C nanobeams for ($\boldsymbol{\gamma}$=0.1, K_{nl}= 10, $K_p = 5$, $K_w = 10$ and $T = 0K$)

The Pasternak foundation assumes that the nanobeam is resting on a completely rigid surface. The Pasternak foundation takes into account the stiffness and deformation of the substrate on which the nanobeam is Placed. This can be important for predicting the behavior of nanobeam structures under different loading conditions such as Temperature. The inclusion of the Pasternak foundation allows for a more accurate analysis of the vibration behavior of nanobeams. The Pasternak foundation is an important consideration in the vibration analysis of nanobeams in thermal environments. When a nanobeam is subjected to thermal fluctuations, its vibrational behavior can be affected due to changes in the material properties and the boundary conditions. The Pasternak foundation can help to account for the thermal expansion and contraction of the substrate on which the nanobeam is put on, and its effect on the vibrational behavior of the nanobeam. It's also used to model the stiffness and deformation of the substrate in response to changes in temperature. This can be important in predicting the vibrational modes and frequencies of the nanobeam, as well as its response to external excitations or thermal fluctuations. By incorporating the Pasternak foundation into the analysis, we can obtain more accurate predictions of the vibrational behavior of nanobeams in thermal environments. From our tabulated numerical results, and graphs using the modified couple stress theory, we can observe that as K_p increases from 5 -100(5, 50, and 100) the amplitudes drop for both simple-simple and clamped-clamped boundary conditions. The dimensional amplitude versus nonlinear frequency ratio changes drop as K_p increases for both boundary conditions but it's seen that clamped-clamped boundary condition ratio changes are relatively higher compared to Simple-Simple boundary condition. The results obtained using Nonlocal Elasticity theory for $K_p = 5{,}50\ and\ 100$ shows the same pattern.

Another type of foundation is a Winkler foundation. Its structure is assumed to be resting on an elastic foundation that is modeled as a series of discrete, linear springs. Each spring represents a small area of the foundation, and the stiffness of the spring is proportional to the stiffness of the foundation in that area. By integrating the Winkler foundation into the analysis, we can see how this affects the vibrational behavior of the nanobeam due to a change in temperature. It is important for predicting the vibrational modes and frequencies of the nanobeam undergoing thermal changes. We can clearly see form the results we obtained using Nonlocal Elasticity theory that as K_w rises from 10-200 (10, 100, and 200) the amplitudes drop for both simple-simple and clamped-clamped boundary conditions. The dimensional amplitude versus nonlinear frequency ratio changes drop as K_w increases for both boundary conditions but it's seen that clamped-clamped boundary condition ratio changes are relatively higher compared to Simple-Simple boundary condition. The results obtained using modified couple stress theory for $K_w = 10{,}100\ and\ 200$ shows the same form.

The Study also includes a nonlinear foundation. In contrast to linear foundation models, which assume that the foundation is perfectly elastic and obeys Hooke's law, nonlinear foundation models take into account the nonlinear behavior of the foundation material. By analyzing the increments in the foundation stiffness and deformation, we can gain insights into the behavior of the foundation material under different temperature changes. The use of a nonlinear foundation model with incremental analysis can help to improve the accuracy of predictions of the vibrational behavior of nanobeams in thermal environments. We can clearly see form the results we obtained using Nonlocal Elasticity theory that as K_{nl} rises from 10-200 (10, 100, and 200) the amplitudes remains the same for both boundary conditions but the frequency response curves differences are observed clearly. The dimensional amplitude versus nonlinear frequency ratio changes are all similar at the beginning and later starts to deviate from each other and the ratio changes of clamped-clamped boundary condition nanobeams are relatively higher compared to Simple-Simple boundary condition. The results obtained using modified couple stress theory for $K_{nl} = 10, 100, and\ 200$ shows the same Pattern.

The material length parameter also affects the amplitude. The graphs show that as material length scale parameters increases from 1-5(1, 2, 3, 4 and 5), the amplitude shows increment at the same time having a different frequency response curves each time.

The nonlocal parameter for nonlocal elasticity theory increases from 0 to 0.5(0, 0.1, 0.2, 0.3, 0.4, 0.5) the amplitude also rises showing a different frequency response curves each time for C-C and S-S boundary condition. The dimensional amplitude versus nonlinear frequency ratio changes drop as length scale parameter and nonlocal parameter increases and the ratio changes of clamped-clamped boundary condition nanobeams are relatively higher compared to Simple-Simple boundary condition.

As the temperature increases, the nanobeam and its foundation may expand, which can change the stiffness of the system and affect the natural frequencies of the beam. This can cause the mode shapes of the nanobeam to change, leading to a shift in its resonance frequencies. The damping characteristics of the beam can also be affected by temperature variations, leading to changes in the amount of energy dissipated during vibration. The magnitude of these effects on the vibration of the nanobeam will depend on several factors, including the material properties of the beam and its supporting foundation, the level and rate of temperature change. For nonlocal Elasticity theory, amplitude drops as temperature increases (low temperature 0,100 and 200) and the dimensional amplitude versus nonlinear frequency ratio changes rise as temperature increase. Whereas for high temperature (400k and 600k) the amplitude rises as temperature increases. The dimensional amplitude versus nonlinear frequency ratio changes drop as temperature increases for both boundary condition. Using modified couple stress theory, the graphs show that amplitude drops as temperature increases. The dimensional amplitude versus nonlinear frequency ratio changes are higher for low temperature compared to higher temperatures.

5.3 Validation Study

In this section, comparisons are made with previous studies in order to verify the validity of the theory presented in the article. The numerical values obtained is compared with the studies of Şimşek [59] and Azrar et al. [60]. Comparative values are given in Table 5.9 for SS and CC cases. Comparison study is made for different values of dimensionless vibration amplitude(a=1,2,3,4) in Table 3. There is a good agreement with the results reported by Şimşek [59] and Azrar et al. [60]. Table 3 displays that as increasing the dimensionless amplitude, the frequency ratio of the macrobeams increases, as it was reported by Şimşek [59] and Azrar et al. [60]. If we accept the material length scale parameter as zero, we get a macrobeam.

Table 5.9. Comparison of the nonlinear frequency ratios obtained by the classical theory for various values of dimensionless amplitude for SS and CC macrobeam.

Dimensionless amplitude (a)	Simple-Simple (SS)			Clamped-Clamped (CC)		
	Present	Şimşek [59]	Azrar et al.[60]	Present	Şimşek [59]	Azrar et al.[60]
1	1.0895	1.0897	1.0891	1.0229	1.0231	1.0221
2	1.3207	1.3228	1.3177	1.0879	1.0897	1.0856
3	1.6348	1.6393	1.6256	1.18874	1.1924	1.1831
4	1.9918	2.0000	-----	1.31383	1.3228	1.3064

In this study, nonlinear vibration analysis is performed on a nanobeam resting on a nonlinear elastic foundation using the modified couple stress theory. However, there are not many studies available on this specific subject. As a result, a comparative analysis was conducted to check the reliability of the present formula and present solutions. For this purposes, second verification is performed for nano beam frequencies are compared with literature assuming elastic foundation is zero in Table 5.10. After that third verification is performed with a previous work which is used different theories and solution methods for modeling elastic foundation effects in Table 5.11. As it is seen that good harmony is observed for verification studies.

Table 5.10. Comparison of the nondimensional first mode natural frequencies of a beam (SS) with ν=0.38, K_L=K_P= K_{NL}=0

l/h	Present	Togun and Bagdatli (2016)	Wang et al. (2013)	Reddy (2011)

0.25	11.1309	11.1301	11.1187	11.1187
0.5	14.2579	14.2579	14.2433	14.2433
1	22.8238	22.8238	22.8004	22.8004

Table 5.11. Comparison of the nondimensional first mode natural frequencies of a beam with ν=0.38, l/h=1, K_P=5, K_{NL}=10..

	S-S		C-C	
K_L	Present	Simsek (2014)	Present	Simsek (2014)
10	24.0888	24.0889	23.9142	24.399
100	25.8896	25.8897	25.7272	26.1785
200	27.7538	27.7538	27.6024	28.0234

By comparing the non-dimensional frequency obtained from the analytical solutions in the presented study with the numerical results from Togun and Bagdatli(2016), Wang et al.(2013) and Reddy(2010) is given in Table 5.10 and Simsek(2014) in Table 5.11. Researchers can assess the accuracy and validity of the proposed analytical model. Consistent agreement in numerical results would indicate that the model is capable of accurately predicting the behavior of the nanobeam resting on nonlinear elastic foundation. By using different analytical methods in each study, the Navier solution procedure by Reddy(2010), the shooting method by Wang et al.(2013), the variational method by Simsek (2014) and multiple scale method (MSM) in the presented study, researchers can explore various approaches to solving the vibration problem.

Table 5.12. Model validation: estimates of the fundamental natural frequency for a beam with K_P=25, K_w=25, K_{NL} =0 and T=0

Boundry Cond.	Present Study	Reference[61]	Reference[62]
S-S	19.2133	19.2178	19.21
	50.7002	50.7804	50.71
C-C	28.7961	-------	------
	70.5261	-------	------

CHAPTER 6

CONCLUSION AND RECOMMENDATION

6.1. Conclusion and Recommendations for Future Work

In conclusion, the study on the vibration analysis of the nanobeam resting on nonlinear Winkler-Pasternak parameter in thermal environment reveals that several factors affect the dimensional amplitude and nonlinear frequency changes of the beam. Specifically, the study found that as Pasternak parameter increases, the dimensional amplitude versus nonlinear ratio changes drop, and Winkler parameter increases causes the dimensional amplitude versus nonlinear frequency changes to drop for both boundary conditions. Furthermore, the nonlinear foundation parameter causes the dimensional amplitude versus nonlinear frequency changes to deviate from each other at later changes, despite being similar at the beginning. Additionally the study found that the dimensional amplitude versus nonlinear frequency changes drop as the material length parameter and nonlocal parameter increases. Finally, the effect of temperature on the dimensional amplitude and nonlinear frequency changes depend on the temperature ranges, with the amplitude dropping and ratio changes rising at low temperatures, and amplitude rising and ratio changes dropping at high temperatures.

The study can also be very useful for future works in several ways. Firstly, the study can provide a better understanding of the dynamic behavior of nanobeams under thermal conditions, which is essential for the design and development of Nano scale devices. By analyzing the vibration characteristics of nanobeams under different thermal conditions, researchers can gain insights into how temperature affects the mechanical response of these structures, enabling them to optimize their designs for specific applications.

Secondly, the study can help to improve the accuracy of computational models used in nanoscale engineering. By incorporating the effects of thermal environment and nonlinear foundation into the models, researchers can better predict the behavior of nanobeams and other nanoscale structures, leading to more accurate simulations and designs that are more reliable.

Finally, the study can serve as a basis for further research in the field of nanomechanics. By identifying new research directions and areas of investigation, the study can inspire future works that build on its findings and expand our knowledge of the mechanical properties of nanoscale materials.

I would recommend that researchers in the field of nanotechnology consider conducting further studies on the vibration analysis of nanobeams under thermal conditions with Winkler-Pasternak and nonlinear foundations. Such studies can contribute significantly to the advancement of nanoscale engineering and help to address the challenges of designing and developing nanoscale devices.

REFERENCES

[1] F. Yang, A. C. M. Chong, D. C. C. Lam, P. Tong, Couple stress-based strain gradient theory for elasticity. Int. J. Solids Struct. 39 (2002), 2731–2743.

[2] S K Park and X-L Gao 2006 J. Micromech. Microeng. 16 2355

[3] Park, S.K., Gao, XL. Variational formulation of a modified couple stress theory and its application to a simple shear problem. Z. angew. Math. Phys. 59, 904–917 (2008).

[4] Mohandes, M.; Ghasemi, A. R. (2016). Modified couple stress theory and finite strain assumption for nonlinear free vibration and bending of micro/nanolaminated composite Euler-Bernoulli beam under thermal loading.

[5] Abouelregal, Ahmed E.; Marin, Marin (2020). The Response of Nanobeams with Temperature-Dependent Properties Using State-Space Method via Modified Couple Stress Theory

[6] Majid Ghadiri and Navvab Shafiei, Vibration analysis of rotating functionally graded Timoshenko microbeam based on modified couple stress theory under different temperature distributions, Acta Astronautica, http://dx.doi.org/10.1016/j.actaastro.2016.01.003

[7] Rahmani, S. Faroughi, M. Sari, A. Abdelkefi, Selection of size dependency theory effects on the wave's dispersions of magneto-electro-thermo-elastic nano-beam resting on visco-elastic foundation, European Journal of Mechanics - A/Solids, Volume 95, 2022, 104620, ISSN 0997-7538, https://doi.org/10.1016/j.euromechsol.2022.104620.

[8] Ola Ragb, Mokhtar Mohamed, M.S. Matbuly, Free vibration of a piezoelectric nanobeam resting on nonlinear Winkler-Pasternak foundation by quadrature methods, Heliyon, Volume 5, Issue 6, 2019, e01856, ISSN 2405-8440, https://doi.org/10.1016/j.heliyon.2019.e01856.

[9] Rahmani, A., Safaei, B. and Qin, Z., 2021. On wave propagation of rotating viscoelastic nanobeams with temperature effects by using modified couple stress-based nonlocal Eringen’s theory. Engineering with Computers, pp.1-21.

[10] Abouelregal, A.E. and Mohammed, W.W., 2020. Effects of nonlocal thermoelasticity on nanoscale beams based on couple stress theory. Mathematical Methods in the Applied Sciences.

[11] Qi, Z., Peng, W. and He, T., 2022. Investigation on the thermoelastic response of a nanobeam in modified couple stress theory considering size-dependent and memory-dependent effects. Journal of Thermal Stresses, 45(10), pp.773-792.

[12] Arash Rahmani, Shirko Faroughi, Michael I. Friswell & Alireza Babaei (2021): Eringen's nonlocal and modified couple stress theories applied to vibrating rotating nanobeams with temperature effects, Mechanics of Advanced Materials and Structures, DOI: 10.1080/15376494.2021.1939468

[13] Dashtaki, P.M. and Beni, Y.T., 2014. Effects of Casimir force and thermal stresses on the buckling of electrostatic nanobridges based on couple stress theory. Arabian Journal for Science and Engineering, 39(7), pp.5753-5763.

[14] Khorshidi, M.A., Shariati, M. and Emam, S.A., 2016. Postbuckling of functionally graded nanobeams based on modified couple stress theory under general beam theory. International Journal of Mechanical Sciences, 110, pp.160-169.

[15] Alibeigi, B., Tadi Beni, Y. and Mehralian, F., 2018. On the thermal buckling of magneto-electro-elastic piezoelectric nanobeams. The European Physical Journal Plus, 133(3), pp.1-18.

[16] Yahya, A.M., Abouelregal, A.E., Khalil, K.M. and Atta, D., 2021. Thermoelastic responses in rotating nanobeams with variable physical properties due to periodic pulse heating. Case Studies in Thermal Engineering, 28, p.101443.

[17] Kumar, H. and Mukhopadhyay, S., 2021. Response of deflection and thermal moment of Timoshenko microbeams considering modified couple stress theory and dual-phase-lag heat conduction model. Composite Structures, 263, p.113620.

[18] Attia, M.A. and Mohamed, S., 2020. Thermal vibration characteristics of pre/post-buckled bi-directional functionally graded tapered microbeams based on modified couple stress Reddy beam theory. Engineering with Computers, pp.1-27.

[19] Ebrahimi, F., Mahmoodi, F. and Barati, M.R., 2017. Thermo-mechanical vibration analysis of functionally graded micro/nanoscale beams with porosities based on modified couple stress theory. Advances in materials Research, 6(3), p.279.

[20] Babaei, A., Noorani, M.R.S. and Ghanbari, A., 2017. Temperature-dependent free vibration analysis of functionally graded micro-beams based on the modified couple stress theory. Microsystem technologies, 23(10), pp.4599-4610.

[21] Kutbi, M. A., & Zenkour, A. M. (2022). Modified couple stress model for thermoelastic microbeams due to temperature pulse heating. Journal of Computational Applied Mechanics, 53(1), 83-101.

[22] Rahmani, O., Hosseini, S. A. H., Ghoytasi, I., & Golmohammadi, H. (2018). Free vibration of deep curved FG nano-beam based on modified couple stress theory. Steel and Composite Structures, 26(5), 607-20.

[23] Sobhy, M., & Zenkour, A. M. (2020). The modified couple stress model for bending of normal deformable viscoelastic nanobeams resting on visco-Pasternak foundations. Mechanics of Advanced Materials and Structures, 27(7), 525-538.

[24] Jalali, M. H., Zargar, O., & Baghani, M. (2019). Size-dependent vibration analysis of FG microbeams in thermal environment based on modified couple stress theory. Iranian Journal of Science and Technology, Transactions of Mechanical Engineering, 43(1), 761-771.

[25] YAYLI, M. Ö., Küpeli, T., & ÇAVUŞ, Y. (2021). Weighted Residual Approach for Bending Analysis of Nanobeam Using by Modified Couple Stress Theory. International Journal of Engineering and Applied Sciences, 13(2), 43-55.

[26] Jia, X. L., Ke, L., Zhong, X. L., Sun, Y., Yang, J., & Kitipornchai, S. (2018). Thermal-mechanical-electrical buckling behavior of functionally graded micro-beams based on modified couple stress theory. Composite Structures, 202, 625-634.

[27] Shafiei, N., Hamisi, M., & Ghadiri, M. (2020). Vibration analysis of rotary tapered axially functionally graded Timoshenko nanobeam in thermal environment. Journal of Solid Mechanics, 12(1), 16-32.

[28] Attia, M. A., & Emam, S. A. (2018). Electrostatic nonlinear bending, buckling and free vibrations of viscoelastic microbeams based on the modified couple stress theory. Acta Mechanica, 229(8), 3235-3255.

[29] Abdullah, S. S., Hosseini-Hashemi, S., Hussein, N. A., & Nazemnezhad, R. (2020). Thermal stress and magnetic effects on nonlinear vibration of nanobeams embedded in nonlinear elastic medium. Journal of Thermal Stresses, 43(10), 1316-1332.

[30] Fang, J., Gu, J., & Wang, H. (2018). Size-dependent three-dimensional free vibration of rotating functionally graded microbeams based on a modified couple stress theory. International Journal of Mechanical Sciences, 136, 188-199.

[31] Akbarzadeh Khorshidi, M. (2021). Postbuckling of viscoelastic micro/nanobeams embedded in visco-Pasternak foundations based on the modified couple stress theory. Mechanics of Time-Dependent Materials, 25(2), 265-278.

[32] Karami, B., Shahsavari, D., Karami, M., & Li, L. (2019). Hygrothermal wave characteristic of nanobeam-type inhomogeneous materials with porosity under magnetic field. Proceedings of the Institution of Mechanical Engineers, Part C: Journal of Mechanical Engineering Science, 233(6), 2149-2169.

[33] Das, D. (2019). Nonlinear forced vibration analysis of higher order shear-deformable functionally graded microbeam resting on nonlinear elastic foundation based on modified couple stress theory. Proceedings of the Institution of Mechanical Engineers, Part L: Journal of Materials: Design and Applications, 233(9), 1773-1790.

[34] Akgöz, B., & Civalek, Ö. (2018). Vibrational characteristics of embedded microbeams lying on a two-parameter elastic foundation in thermal environment. Composites Part B: Engineering, 150, 68-77.

[35] Liu, H., Liu, H., & Yang, J. (2018). Vibration of FG magneto-electro-viscoelastic porous nanobeams on visco-Pasternak foundation. Composites Part B: Engineering, 155, 244-256.

[36] Nasr, M. E., Abouelregal, A. E., Soleiman, A., & Khalil, K. M. (2021). Thermoelastic Vibrations of Nonlocal Nanobeams Resting on aPasternak Foundation via DPL Model. Journal of Applied and Computational Mechanics, 7(1), 34-44.

[37] Jena, S. K., Chakraverty, S., Mahesh, V., & Harursampath, D. (2022). Wavelet-based techniques for Hygro-Magneto-Thermo vibration of nonlocal strain gradient nanobeam resting on Winkler-Pasternak elastic foundation. Engineering Analysis with Boundary Elements, 140, 494-506.

[38] Zarepour, M., & Hosseini, S. A. (2016). A semi analytical method for electro-thermo-mechanical nonlinear vibration analysis of nanobeam resting on the Winkler-Pasternak foundations with general elastic boundary conditions. Smart Materials and Structures, 25(8), 085005.

[39] Nayfeh, A. H. (2011). Introduction to perturbation techniques. John Wiley & Sons.

[40] Esen, I., Özarpa, C., & Eltaher, M. A. (2021). Free vibration of a cracked FG microbeam embedded in an elastic matrix and exposed to magnetic field in a thermal environment. Composite Structures, 261, 113552.

[41] Xiao, C., Zhang, G., Yu, Y., Mo, Y., & Mohammadi, R. (2022). Nonlinear vibration analysis of the nanobeams subjected to magneto-electro-thermal loading based on a novel HSDT. Waves in Random and Complex Media, 1-20.

[42] Toğun, N., & Bağdatlı, S. M. (2016). Nonlinear vibration of a nanobeam on a Pasternak elastic foundation based on non-local Euler-Bernoulli beam theory. Mathematical and Computational Applications, 21(1), 3.

[43] Mehrdad Pourkiaee, S., Khadem, S. E., & Shahgholi, M. (2017). Nonlinear vibration and stability analysis of an electrically actuated piezoelectric nanobeam considering surface effects and intermolecular interactions. *Journal of Vibration and Control*, *23*(12), 1873-1889.

[44] https://www.devdiscourse.com/article/technology/618643-new-insect-sized-robot-can-withstand-weight-of-a-human, 26.10.2022.

[45] https://industrywired.com/nanotechnology-and-cars-taking-automotive-to-next-level-of-development-2/

[46] https://www.dubizzle.com/blog/cars/nanotechnology-in-cars/

[47] https://www.100knots.com/how-nanotechnology-might-be-the-future-of-the-aerospace-industry/

[48] Abdullah, S. S., Hosseini-Hashemi, S., Hussein, N. A., & Nazemnezhad, R. (2020). Thermal stress and magnetic effects on nonlinear vibration of nanobeams embedded in nonlinear elastic medium. *Journal of Thermal Stresses*, *43*(10), 1316-1332.

[49] Hijaz Ahmad et al. (2022). Vibration analysis of nanobeams subjected to gradient-type heating due to a static magnetic field under the theory of nonlocal elasticity

[50] A.Cemal Eringen; D.G.B. Edelen (1972). *On nonlocal elasticity. , 10(3), 233–248.* doi:10.1016/0020-7225(72)90039-0

[51] Ebrahimi, Farzad; Salari, Erfan (2015). *Thermal buckling and free vibration analysis of size dependent Timoshenko FG nanobeams in thermal environments. Composite Structures, 128(), 363–380.* doi:10.1016/j.compstruct.2015.03.023

[52] Ebrahimi, Farzad; Barati, Mohammad Reza (2016). *A unified formulation for dynamic analysis of nonlocal heterogeneous nanobeams in hygro-thermal environment. Applied Physics A, 122(9), 792–.* doi:10.1007/s00339-016-0322-2

[53] Ebrahimi, F.; Barati, M. R. (2016). *Vibration analysis of smart piezoelectrically actuated nanobeams subjected to magneto-electrical field in thermal environment. Journal of Vibration and Control, (), 1077546316646239–.* doi:10.1177/1077546316646239

[54] Ebrahimi, Farzad; Barati, Mohammad Reza (2017). *Vibration analysis of viscoelastic inhomogeneous nanobeams resting on a viscoelastic foundation based on nonlocal strain gradient theory incorporating surface and thermal effects. Acta Mechanica, 228(3), 1197–1210.* doi:10.1007/s00707-016-1755-6

[55] Ismail Esen;Cevat Özarpa;Mohamed A. Eltaher; (2021). *Free vibration of a cracked FG microbeam embedded in an elastic matrix and exposed to magnetic field in a thermal environment . Composite Structures, (), –.* doi:10.1016/j.compstruct.2021.113552

[56] Ebrahimi, Farzad; Salari, Erfan (2015). *Thermo-mechanical vibration analysis of nonlocal temperature-dependent FG nanobeams with various boundary conditions. Composites Part B: Engineering, 78(), 272–290.* doi:10.1016/j.compositesb.2015.03.068

[57] Mohammadi, M.; Safarabadi, M.; Rastgoo, A.; Farajpour, A. (2016). *Hygro-mechanical vibration analysis of a rotating viscoelastic nanobeam embedded in a visco-Pasternak elastic medium and in a nonlinear thermal environment. Acta Mechanica, 227(8), 2207–2232.* doi:10.1007/s00707-016-1623-4

[58] Hamza-Cherif, Riad; Meradjah, Mustapha; Zidour, Mohamed; Tounsi, Abdelouahed; Belmahi, Samir; Bensattalah, Tayeb (2018). *Vibration Analysis of Nano Beam Using Differential Transform Method Including Thermal Effect. Journal of Nano Research, 54(), 1–14.* doi:10.4028/www.scientific.net/JNanoR.54.1

[59] Şimşek, M. Nonlinear static and free vibration analysis of microbeams based on the nonlinear elastic foundation using modified couple stress theory and He's variational method, Composite Structures, 2014, 112, 264-272.

[60] Azrar, A.; Ben Said, M.; Azrar, L.; Aljinaidi, A.A. (2019). Dynamic instability analysis of magneto-electro-elastic beams with uncertain parameters under

static and parametric electric and magnetic fields. Composite Structures, (), 111185–. doi:10.1016/j.compstruct.2019.111185

[61] Mustapha, K.B.; Zhong, Z.W. Free transverse vibration of an axially loaded non-prismatic single-walled carbon nanotube embedded in a two-parameter elastic medium. Comput. Mater. Sci. 2010, 50, 742–751.

[62] Yokoyama, T. Vibrations and transient responses of Timoshenko beams resting on elastic foundations. Arch. Appl. Mech. 1987, 57, 81–90.

CURRICULUM VITAE

Redwan Mohammed MAMU

EDUCATION

- Masters of Science (MSC), **Mechanical Engineering (Machine Theory and Dynamics),** *2019/2023 Gaziantep University (Gaün), Gaziantep, Türkiye*
- Bachelor of science (BSC), **Mechanical Engineering (Design), July** *2018 Addis Ababa Science and Technology University (AASTU), Addis Ababa, Ethiopia*

WORK EXPERIENCE

- Metals and Engineering Corporation, Practical experience in material treatment, precision, maintenance and machine building shops, internship, Addis Ababa, Ethiopia
- Middle school English Teacher and Translator, Gaziantep, Türkiye

TRAININGS (with certificate)

- Certification in Artificial Intelligence, BAU, Türkiye
- Certificate, Science and Technology in Today's World, YTB,Türkiye
- Certification in Leadership and Management, Türkiye
- Certification in Recycling Awareness Training, IOM, GaÜn and GETHAM
- Certified on international trade, Ethiopia
- Certificate in computer, Ethiopia
- Turkish Language(C1), Gaziantep, Türkiye

ADDITIONAL SKILLS

- *Proficiency in Microsoft applications (word, PowerPoint)*
- *Software Skills on Mat lab, ANSYS, solid Works and AutoCAD*
- *Machine operation skills- Lathe, Drilling, and Milling*
- *Ability to work independently or as part of a team*
- *Leadership, time management, Analytical, Organizational and Planning Skill*
- *Monitoring, Evaluation, Learning and Accountability*
- *Good Verbal and written communication skill*
- *Automobile driving license*

LANGUAGES

- *English (Spoken: fluent; Written: fluent)*
- *Two Ethiopian Languages (Amharic and Afaan Oromo)*

- *Turkish (Spoken: fluent; Written: fluent)*

REFERENCES

- Dr. *Necla Kara Toğun; Associate Professor, Gaün; Email: nkara@gantep.edu.tr, Thesis Advisor,Mobile Phone No. +905052914550*
- *Dr. Abdullah Akpolat; Associate Professor, Gaziantep University (Gaün); Email:akpolat@gantep.edu.tr , Mobile Phone No.+90 0342 317 2522*